Technische Universität München
Fakultät für Medizin

Vascular smooth muscle cell differentiation in patient-derived cells from stable versus ruptured plaques in carotid artery disease

Narcisse Sara Groß

Vollständiger Abdruck der von der Fakultät für Medizin der Technischen Universität München zur Erlangung des akademischen Grades einer Doktorin der Medizin (Dr. med.) genehmigten Dissertation.

Vorsitz: Prof. Dr. Wolfgang A. Weber

Prüfer der Dissertation:

1. Prof. Dr. Lars Mägdefessel
2. Priv.-Doz. Dr. Calogero D'Alessandria

Die Dissertation wurde am 14.06.2022 bei der Technischen Universität München eingereicht und durch die Fakultät für Medizin am 08.11.2022 angenommen.

Table of Contents

1. Abstract

Background: Atherosclerosis is the leading cause of vascular disease worldwide. Presently, vascular smooth muscle cells have been identified as a critical component in atherosclerosis by undergoing a phenotypic switch from a contractile to proliferative synthetic form and contributing to the thinning of the fibrous cap and vulnerable plaque formation. The study aimed to establish a vascular cell biobank to examine the plasticity of vascular smooth muscle cells (VSMCs) in carotid artery disease. We hypothesised that protein expression and phenotype would shift as the disease progresses from a stable to ruptured plaque.

Methods: Carotid artery stenosis samples were collected from symptomatic and asymptomatic patients (*n=18*) (age= 64-85 years) during carotid endarterectomy. Plaque stability was determined by measuring the fibrous cap thickness using haematoxylin and eosin (HE) and Elastica van Gieson (EvG) staining. VSMCs were isolated and cultured for 5-6 weeks. VSMC intima migration and phenotypical switch to an inflammatory cell type were confirmed with smooth muscle actin and CD68 immunohistochemistry staining. The current cell state was indirectly analysed by establishing a gene panel for contractile, inflammatory and synthetic genes via RT-qPCR. For direct phenotypical analysis, live-cell imaging for migration and proliferation behaviour was performed on stable, unstable and ruptured carotid samples and control cells (*n=4*) for 48 hours.

Results: Gene expression analysis showed a significant upregulation in versican mRNA in symptomatic vs asymptomatic patient plaque samples (*p=0.0477*). Platelet-derived growth factor B expression was significantly upregulated in asymptomatic patients (*p=0.0365*). Further, carotid samples from symptomatic patients revealed a higher expression of collagen type I than asymptomatic patients (*p=0.0103*). Moreover, a significant upregulation in versican expression in ruptured plaques was revealed compared to unstable plaques (*p=0.0300*). VSMCs from unstable lesions displayed a less effective migration activity than healthy VSMCs (p<*0.0001).* Stable and ruptured lesion VSMCs both, surprisingly, exhibited a higher migratory potency than those derived from unstable lesions (*p<0.0001* and *p=0.0026*, respectively). Proliferation behaviour analysis revealed that stable lesion-derived VSMCs arrived at

higher proliferation rates than healthy VSMCs and those from unstable and ruptured lesions. Additionally, significant differences were identified in proliferation activity between unstable lesion VSMCs vs control (*p=0.0182*) and between ruptured and unstable lesion VSMCs (*p=0.0152*).

Conclusion: Biobanking minimises the translational gap between experimental research and its clinical implementation. In addition, primary cell culture investigations enable a phenotypical analysis of VSMCs at different stages of CAD and provide the foundation for specific targeting of phasic expression levels in future research.

Keywords: atherosclerosis, carotid artery disease (CAD), cell culture, live-cell imaging, migration, phenotypic switch, proliferation, vascular smooth muscle cells (VSMCs).

2. Zusammenfassung

Hintergrund: Atherosklerose ist ein komplexer degenerativer Prozess in arteriellen Gefäßen und die weltweit führende Ursache vaskulärer Erkrankungen. Gegenwärtig wird glatten Gefäßmuskelzellen eine essenzielle Rolle in der Atherosklerose beigemessen, da sie die Plastizität besitzen ihren Phänotyp zu verändern: von einem kontraktilen zu einem inflammatorischen oder synthetischen Phänotyp. Damit tragen glatte Gefäßmuskelzellen zur Ausdünnung der fibrösen Kappe und zur Entstehung von vulnerablen Plaques bei. Zur Analyse der glatten Gefäßmuskelzellplastizität in Karotisstenosen wurde im Rahmen dieser Studie eine vaskuläre Zellbiobank etabliert. Wir erstellten die Hypothese, dass sich die Proteinexpression synchron mit dem Phänotyp im Krankheitsprogress verändern würde.

Methoden: Karotis Plaques wurden von symptomatischen und asymptomatischen Patienten nach Karotisendarteriektomie gesammelt (*n=18*) (Alter= 64-85 Jahre). Die Plaquestabilität wurde mittels Dickemessung der fibrösen Kappe in Hämatoxylin-Eosin und Elastika van Gieson Gewebefärbungen bestimmt. Aus diesen Proben wurden glatten Gefäßmuskelzellen isoliert und für 5-6 Wochen kultiviert. Neointima Migration und phänotypische Veränderungen zu inflammatorischen Zelltypen wurden durch Alpha Smooth Muscle Actin und CD68 immunhistochemische Färbungen bestätigt. Mit der Etablierung einer RT-qPCR Genexpressionsanalyse wurde der aktuelle Phänotyp indirekt anhand kontraktiler, synthetischer und inflammatorischer Gene bestimmt. Für eine direkte Analyse der Zellkonstitution, wurde eine Live Cell Imaging Analyse der Migrations- und Proliferationsaktivität der glatten Gefäßmuskelzellen aus stabilen, instabilen und rupturierten Plaques und einer gesunden Kontrolle (*n=4*) über 48 Stunden durchgeführt.

Ergebnisse: Genexpressionsanalysen zeichneten eine signifikante Hochregulierung der Versican mRNA in symptomatischen gegenüber asymptomatischen Patientenproben auf (*p=0.0477*). Die Expression des Wachstumsfaktors Platelet Derived Growth Factor B zeigte zusätzlich einen signifikanten Anstieg in asymptomatischen Patienten (*p=0.0365*). Karotis Proben von symptomatischen Patienten zeigten eine höhere Expression von Kollagen Typ I im Vergleich zu asymptomatischen Patienten (*p=0.0103*). Weiterhin zeichnete sich eine signifikante

Hochregulierung in der Versican Expression in rupturierten Plaques verglichen mit instabilen Plaques ab ($p=0.0300$). Glatte Gefäßmuskelzellen aus instabilen Läsionen wiesen eine geringere Migrationseffektivität auf als die gesunde Kontrolle ($p<0.0001$). Andererseits zeigten die Zellen aus stabilen und rupturierten Plaques beide eine verstärkte Migrationspotenz als instabilen Läsionen (jeweils $p<0.0001$ und $p=0.0026$). Die Proliferationsverhaltensanalyse offenbarte eine höhere Proliferationsrate in stabilen Plaques als die gesunde Kontrolle. Zusätzlich wurden signifikante Unterschiede in der Aktivität der glatten Gefäßmuskelzellen aus instabilen Plaques gegenüber der Kontrolle identifiziert ($p=0.0182$). Das gleiche gilt für den Vergleich der glatten Gefäßmuskelzellen aus rupturierten und instabilen Plaques ($p=0.0152$).

Fazit: Als translationale Forschung vernetzen Biobanken experimentelle und klinische Wissenschaft miteinander und ermöglichen die phänotypische Analyse auf Expressionsebene von glatten Gefäßmuskelzellen in unterschiedlichen Stadien der Atherosklerose und dessen Beziehung zu klinischer Symptomatik.

Stichwörter: Atherosklerose, Karotisstenose, Zellkultur, Live Cell Imaging, Migration, Phänotyp, Proliferation, glatte Gefäßmuskelzellen.

3. List of Abbreviations

Abbreviation	Definition
AAA	Abdominal aortic aneurysm
ASS	Acetylsalicylic acid
ATP	Adenosine triphosphate
bFGF	Basic fibroblast growth factor
BSA	Bovine serum albumin
CAD	Carotid artery disease
CAS	Carotid arterial angioplasty and stenting
CD 31	Cluster of differentiation 31
CD 68	Cluster of differentiation 68
cDNA	Complementary desoxyribonucleic acid
CEA	Carotid artery endarterectomy
CREST	Carotid Revascularization Endarterectomy versus Stenting Trial
DAMP	Damage-associated molecular patterns
DAPI	4´,6-diamidino-2-phenylindole
DEPC	Diethylpyrocarbonate
DIT	Diffuse intimal thickening
DNA	Desoxyribonucleic acid
DNase	Desoxyribonuclease
EC	Endothelial cell
ECM	Extracellular matrix
ECST	European Carotid Surgery Trial
EDRF	Endothelium-derived relaxing factor
EDTA	Ethylenediaminetetraacetic acid

EGF	Epidermal growth factor
ESC	European Society of Cardiology
EvG	Elastica van Gieson
FBS	Fetal bovine serum
FCS	Fetal calf serum
g	Gram
h	Hours
HDL	High-density lipoprotein
ICA	Internal carotid artery
ICAM1	Intercellular adhesion molecule 1
IL-1	Interleukin 1
kg	Kilogram
KLF4	Kruppel-like factor 4
LDL	Low-density lipoprotein
LP	Lipoprotein
MCP	Monocyte chemotactic protein
MCS-F	Macrophage colony-stimulating factor
mg	Milligram
min	Minutes
miRNA	Micro ribonucleic acid
ml	Millilitre
MMP	Matrix metalloprotease
mRNA	Messenger ribonucleic acid
MYOCD	Myocardin
NASCET	North American Symptomatic Carotid Endarterectomy Trial
NF-kappa B	Nuclear factor-kappa B
NO	Nitric oxide

PBS	Phosphate buffered saline
PDGF-β	Platelet-derived growth factor-β
PFA	Paraformaldehyde
qPCR	Quantitative polymerase-chain-reaction
RNA	Ribonucleic acid
RNase	Ribonuclease
rpm	Rounds per minute
RT	Reverse transcriptase
RT-qPCR	Real-time quantitative polymerase chain reaction
s	Seconds
SD	Standard deviation
SMC	Smooth muscle cell
SPSS	Statistical package for the social sciences
SRF	Serum response factor
TGF-β	Transforming growth factor-β
TNFα	Tumour necrosis factor-alpha
TRIS	Tris (hydroxymethyl)-aminomethane
VA	Veterans Affairs Trial 309
VCAM1	Vascular cell adhesion molecule 1
VSMC	Vascular smooth muscle cell
xg	The gravity of the earth
α-SMA	Smooth muscle actin
µl	Microliter

4. Introduction

4.1. Atherosclerosis

4.1.1. Definition

Atherosclerosis is the leading cause of vascular disease worldwide, manifesting as angina, myocardial infarction and stroke, with an advancing incidence caused by the global spread of diabetes mellitus type 2 and obesity (World Health Organisation, 2020). It is defined as the process of plaque formation on the intima of arterial walls: containing lipids, cells, cell debris and scar tissue (Jonasson et al., 1986).

4.1.2. Anatomical structure of arteries

Human arteries have three layers: the tunica intima, media and adventitia. The tunica intima consists of single-layered endothelial cells (ECs) linked via tight junctions (Palade, 1953). The media is formed by vascular smooth muscle cells (VSMCs) and extracellular matrix (ECM). The adventitia contains mast cells, microvessels, nerve endings and ECM.

4.1.3. Risk factors

Modifiable and non-modifiable factors heighten the risk of atherosclerosis development. Non-modifiable risk factors include male gender, age and genetic disposition: a family history of cardiovascular diseases, familial hypercholesteremia, reduced HDL levels, geographic origin and elevated lipoprotein (a) levels (Assmann et al., 1999; Goldbourt et al., 1986; D. J. Gordon et al., 1989; Kronenberg et al., 1999; Nathan et al., 1997). Modifiable factors are tobacco consumption, increased calorie intake, lack of physical activity, a high fat, raw meat and high natrium diet (Assmann et al., 1999). Moreover, arterial hypertension, chronic systemic inflammatory and metabolic diseases, including adiposity, diabetes mellitus, hypercholesterolaemia, hyperhomocysteinaemia, hyperphosphataemia and hyperfibrinogenaemia are associated with atherosclerosis (Assmann et al., 1999; Gerhard et al., 1999; Kugiyama

et al., 1999; Luft, 1998). Therefore, reducing these risk factors is vital in preventing cardiovascular diseases by atherosclerosis.

4.1.4. Location of atherosclerotic lesions

Haemodynamic forces predominantly regulate the location of atherosclerotic plaque formation. Focal atherosclerotic lesions are inclined to develop in so-called lesion-prone regions in the arterial tree, most commonly in large and medium-sized arteries with branches, bifurcations or curvatures, for example, the carotid sinus (Cunningham et al., 2005; Ross, 1999; K. J. Williams et al., 1995). Mechanical measurements have conveyed that these regions are characterised by low shear stress, turbulent blood flow and a high oscillatory shear index (Caro et al., 1971; Chatzizisis et al., 2007; Cornhill et al., 1976). In comparison, unbranched arteries with laminar flow and high shear stress, markers of athero-protective flow, are distinguished by an absence of lesion development (Abe et al., 2014; Mattsson et al., 1997). Athero-prone flow acts as a stimulus for ECs, contributing to endothelial dysfunction; a phenotypic switch to pro-inflammatory and pro-thrombotic ECs with impaired inflammatory barrier function occurs (Atkins et al., 2013; P. F. Davies et al., 2013; Hajra et al., 2000). Contrastingly, athero-protective flow activates anti-inflammatory and anti-thrombotic pathways (Nigro et al., 2011). The development of the atherosclerotic lesion further elevates the disturbed flow by constricting the arterial lumen (P. F. Davies, 2009).

4.1.5. Pathogenesis

In 1856, Virchow established a theory in *Cellular pathology as based upon physiological and pathological histology*, in which he described atherosclerosis as a form of vascular inflammation resulting from intimal injury by mechanical factors (Virchow, 1989). A century later, Ross et al. (1977) coined this hypothesis the `response to injury´ hypothesis (Ross et al., 1976; Ross et al., 1977). However, current studies denounce Ross et al. (1977) hypothesis' and suggest that endothelial injury is not imperative for atheroma development; endothelial denudation is instead the result of advanced complicated lesions (Constantinides, 1966; Falk, 1989; Katsuda et al., 1992; Richardson et al., 1989; Stary et al., 1995). Moreover, researchers suggest that an intact endothelial layer is essential for atherogenesis initiation (Minick et al., 1977).

Present known triggers of atherogenesis are endothelial dysfunction, arterial hypertension, dyslipidaemia and pro-inflammatory mediators (Tabas et al., 2015; K. J. Williams et al., 1995). Potential risk factors for endothelial dysfunction are elevated and modified low-density lipoproteins (LDL), diabetes mellitus, elevated plasma homocysteine concentrations, non-laminar flow and free radicals (Gimbrone et al., 2013; Ross, 1999). Cell types involved in atherogenesis are ECs, VSMCs, monocyte-derived macrophages and T-lymphocytes (Jonasson et al., 1986).

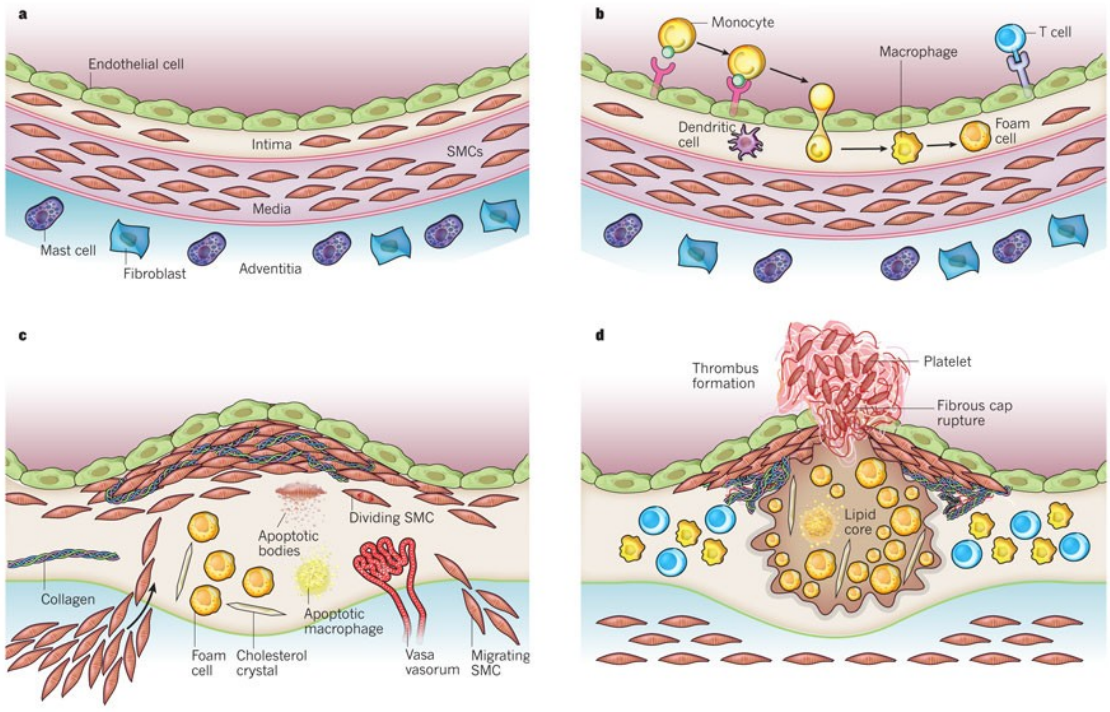

Figure 1: Illustration of the atherosclerotic plaque development (Libby et al., 2011).
(a) The vessel wall can be divided into the tunica intima (ECs), the media (VSMCs, ECM), and the adventitia (ECM, fibroblasts, mast cells, nerve endings, microvessels). (b) Blood monocytes are chemoattracted to the lesion site by cytokines and attach to receptors on ECs. Next, they transmigrate into the intima by diapedesis, where they differentiate into macrophages. The macrophages consequently engulf lipids, initiating the transformation into foam cells. (c) A lipid core develops by foam cell accumulation; this sparks the development of the fibrous cap, constructed of ECM by migrating and proliferating VSMCs. (d) The growth of the lipid core and thinning of the fibrous cap trigger lesion rupture. Pro-thrombotic factors are exposed to the bloodstream, resulting in thrombus formation.

The phases of atherosclerotic plaque development are illustrated in Figure 1. In healthy vessels, the endothelium, as an endocrine, autocrine and paracrine organ, is vital in maintaining vascular homeostasis and acts as a barrier between the arterial vessel and bloodstream (Brenner et al., 1989; Gimbrone, 1987; Rubanyi, 1991). It

regulates vascular tone, selective permeability, and leukocyte and platelet activation (Karnovsky, 1967; Muller, 2002; Rubanyi, 1991; Stary et al., 1992). Systemic release of acetylcholine induces endothelial vasodilation (Furchgott et al., 1980). Locally, the ECs counteract platelet adhesion and aggregation by luminal secretion of nitric oxide (NO) and endothelium-derived relaxing factor (EDRF) (Forstermann et al., 1989; Palmer et al., 1988; Yao et al., 1992). Furthermore, the endothelial release of NO results in local vasodilation and attenuation of leukocyte adhesion (Hickey et al., 1997; Kubes et al., 1993; Kubes et al., 1991; Quyyumi et al., 1995).

Atherosclerosis is marked by endothelial dysfunction: resulting in diminished vascular relaxation and the formation of a pro-coagulatory and pro-inflammatory environment (Bonetti et al., 2002). Studies have demonstrated the augmented tissue factor expression in dysregulated ECs contributes to the pro-thrombotic milieu in atheromas (Wilcox et al., 1989). Furthermore, research has provided evidence of reduced endothelium-regulated vasodilation in response to acetylcholine by decreased expression of NO and increased expression of endothelium-derived contracting factors such as endothelin-1 (Lerman et al., 1992; Yanagisawa et al., 1988; Zeiher et al., 1991). The endothelial dysregulation also results in a modified permeability and ECM composition (McGill et al., 1957; Skalen et al., 2002). Matrix transformation is a result of the VSMC phenotypical switch to a synthetic cell form: producing an atherogenic, lipid-retentive ECM composed of mostly proteoglycans (versican, biglycan and perlecan) and glycosaminoglycans (hyaluronan) (Chang et al., 2000; Little et al., 2002).

The endothelial imbalance initiates an attachment and retention of cholesterol-lipoproteins (LPs) in the vessel walls (Skalen et al., 2002). According to Williams et al. (1995) latest `response-to-retention´ theory of atherosclerosis, the subendothelial retention of apolipoprotein B LPs is the core culprit and initiating event for the lesion development (Tabas et al., 2007; K. J. Williams et al., 1995, 2005). Several studies have substantiated this hypothesis, supplying evidence of LP retention in atherosclerotic-susceptible regions preceding atheroma development (Schwenke et al., 1989a, 1989b; Spring et al., 1989). Moreover, the extravasation of cholesterol-LPs is encouraged by the interaction between the positively charged LPs and negatively charged side chains of the proteoglycans (Camejo et al., 1980; Iverius, 1972).

In hypercholesteraemic animal models, exposure to LPs resulted in an upregulation of inflammatory cell adhesion molecule expression in activated ECs and VSMCs: selectins, monocyte chemoattractant cytokines, intracellular adhesion molecule 1 (ICAM1), CD31 and vascular cell-adhesion molecule 1 (VCAM1) (Berliner et al., 1990; Cushing et al., 1990; Cybulsky et al., 1991; Kume et al., 1992; Quinn et al., 1987). Likewise, studies have emphasised the augmentation of leukocyte adhesion molecule expression in ECs by exposure to athero-prone flow (Dai et al., 2004). Kubes et al. (1991,1993) suggested an indirect correlation between NO synthesis in dysfunctional ECs and leukocyte attachment (Kubes et al., 1993; Kubes et al., 1991).

These mechanisms initiate a tethering and rolling of blood monocytes on the vessel wall; the primary adhesion is strengthened by positive feedback via cytokines and P-, E- and L-selectin interaction, inducing leukocyte activation and diapedesis through the semipermeable endothelium (Butcher, 1991; Dutrochet, 1824; Schenkel et al., 2004). The leukocyte retention triggers their proliferation and differentiation into tissue macrophages (Lusis, 2000). Within the vessel wall, the previously retained LPs, mostly LDL, are modified by oxidation, lipolysis and proteolysis (Steinberg, 2009). As a result of scavenger receptor expression, the monocyte-derived macrophages and VSMCs engulf the modified LP particles for phagocytosis (Mietus-Snyder et al., 2000; Yan et al., 2011).

Phagocytosis of LDL prompts the intracellular accumulation of cholesterol and the development of foam cells (Klouche et al., 2000; Stary et al., 1994). The LDL-induced diminished lipid metabolism capacity generates foam cell transformation via inhibition of cholesterol efflux mechanisms, for example, the ATP binding cassette transporter (ABCA1) (Allahverdian et al., 2014; Nagao et al., 2006). The foam cells undergo apoptosis and are subsequently degraded by secondary necrosis (Okura et al., 2000). A specific plaque milieu develops, inhibiting the process of efferocytosis (Clarke et al., 2010; Schrijvers et al., 2005). The accumulation of foam cells, lipids and apoptotic cells advances the necrotic core formation in atherosclerotic lesions.

Late-atherogenesis is marked by the generation of a fibrous cap comprised of both VSMCs and ECM. Studies suggest that VSMCs are the main contributors to the fibrous cap ECM (Bennett et al., 2016). The ECM is partly supplied by VSMCs, which have migrated from the tunica media to the intima, as well as by a few pre-existing intimal VSMCs (Barrett et al., 1988; Dardik et al., 2005; Libby et al., 2011). The fibrous

cap poses a protective barrier between the bloodstream and the pro-thrombotic material within the necrotic core; its formation supports the outward and presumed positive remodelling of the arterial wall. While luminal blood flow is preserved, studies have detected a higher macrophage and foam cell lesion content in lesions with positive remodelling, resulting in vulnerable plaque formation (Varnava et al., 2002).

4.1.6. Atherosclerotic lesion stability

Clinical complications of atherosclerosis are not merely caused by the advancement of lesions within the arteries and restriction of blood flow by stenosis. According to post-mortem examinations, the formation of the so-called `vulnerable plaque´ is a more significant precursor to the development of acute neurological and coronary events than the degree of stenosis (Libby, 2000). The main contributors to the vulnerable plaque formation are a thin fibrous cap, large necrotic core, high levels of inflammatory cells and a defective efferocytosis, as demonstrated in Figure 2 (Bennett et al., 2016). Other frequent findings in advanced plaques are calcification and neovascularisation (Nicoll et al., 2014).

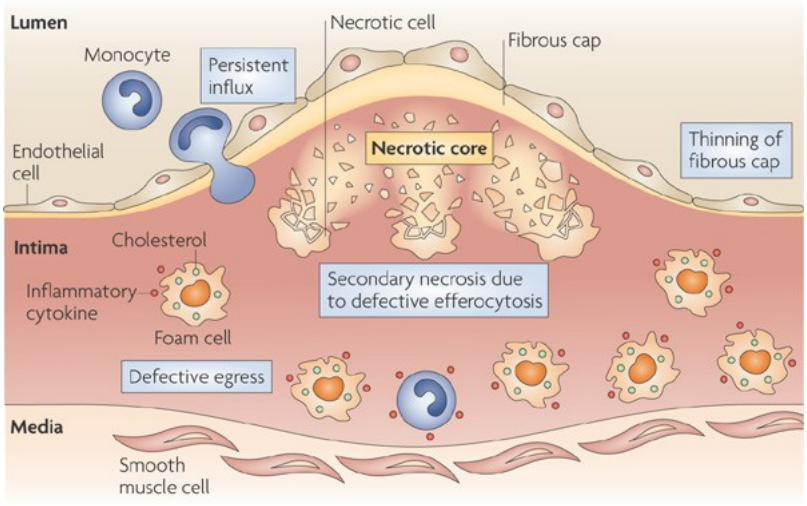

Figure 2: Illustration of vulnerable atherosclerotic plaque formation (Tabas, 2010).
Elements contributing to vulnerable plaque formation are a large necrotic core, thin VSMC-depleted fibrous cap, persistent influx of inflammatory cells and defective efferocytosis.

The first mechanism promoting vulnerable plaque formation is the thinning of the fibrous cap. A fibrous cap thickness reduction results from both VMSC depletion and low proliferation activity (Bauriedel et al., 1999; D. Gordon et al., 1990). Accordingly, a surge in VSMC apoptosis rate further reduces lesion stability (Bauriedel et al., 1999;

Clarke et al., 2006). Likewise, the loss of VSMCs instigates a reduced ECM quantity (Clarke et al., 2006; Clarke et al., 2008). Prior research has demonstrated a weakening of the fibrous cap by collagen degradation (P. K. Shah et al., 1995). These findings correlate with the cytokine-induced amplification of matrix metalloproteinase (MMP) expression in VSMCs and lipid-laden macrophages in vulnerable plaques (Andreeva et al., 1997a; Galis et al., 1995; Galis et al., 1994b; Molloy et al., 2004). The highest MMP expression was present in sections of foam cell accumulation and in the shoulder region of the plaque, where the fibrous cap merges with the normal intima of the vessel (Galis et al., 1994a; Galis et al., 1994b). A thinning of the fibrous cap can also be initiated by low or oscillatory shear stress (C. Cheng et al., 2006).

The quantity of inflammatory cells indirectly correlates with lesion stability. By positive feedback, ingested LDL particles upregulate the expression of pro-inflammatory cytokines in macrophages, such as tumour necrosis factor-alpha (TNFα), macrophage colony-stimulating factor (MCS-F), monocyte chemotactic protein (MCP) and interleukin-1 (IL-1), initiating a vicious cycle of continuous macrophage recruitment (Quinn et al., 1987; Rajavashisth et al., 1990). Histological investigations have established a direct link between the primary point of monocyte lesion entry and the region most susceptible to rupture: the shoulder of the plaque (Libby et al., 2010; Richardson et al., 1989). Angiogenesis in the tunica adventitia further advances the leukocyte migration into the necrotic core (Libby et al., 2010). Additionally, computer calculations of circumferential intimal stress have identified parallels between the site of maximum tension, plaque rupture and location of foam cell accumulation (Richardson et al., 1989).

The necrotic core, consisting of lipids, foam cells and apoptotic cells, is the centre of inflammation. The continuous monocyte recruitment and phagocytosis of LDL particles stimulate a steady foam cell influx and expedite cellular necrosis and inflammation; this generates insufficient efferocytosis and necrotic core growth (Back et al., 2019; Yurdagul et al., 2017). The secretion of matrix metalloproteinases by macrophages and VSMCs further promotes the necrotic core development (Galis et al., 1994b; Loftus et al., 2000; Molloy et al., 2004). Simultaneous to fibrous cap thinning, the growth of the necrotic core into the vessel lumen increases the possibility of plaque rupture by surface area expansion and elevation of plaque stress (G. C. Cheng et al., 1993; Li et al., 2006; van der Wal et al., 1993).

The last crucial mechanism in vulnerable plaque formation is angiogenesis. Animal models exposed to a high-cholesterol diet have revealed the dominant role of neovessels originating from the adventitial vasa vasorum in early atherosclerosis (Hayden et al., 2004; Herrmann et al., 2001; Kumamoto et al., 1995). In histological investigations, ruptured plaques presented with increased neovascularisation and local intraplaque haemorrhage, with significant microvessel density in the shoulder and fibrous cap region (Jeziorska et al., 1999). In accordance with these observations, plaque destabilisation is speculated to be contingent upon rupture of defect neovessels (Langheinrich et al., 2006; McCarthy et al., 1999; Mofidi et al., 2001; Moreno et al., 2004). Furthermore, the abundance of neovascularisation positively correlates with the extent of inflammation and luminal stenosis (Kamat et al., 1987).

4.1.7. Clinical manifestation of atherosclerosis

The clinical presentation of atherosclerosis depends on its anatomical location in the vascular system. For instance, atherosclerosis in coronary arteries causes angina and myocardial infarction; in the extremities, it presents as peripheral artery disease. In this study, atherosclerosis will be examined as carotid artery disease (CAD), manifesting as stroke or transient ischemic attack (TIA).

Clinical manifestation most frequently occurs because of thrombus formation. Thrombus formation can either present locally as flow-limiting stenosis and tissue ischaemia or distantly as emboli. As stated by Davies et al. (1984), 60-70% of thrombosis occurs due to the rupture of the fibrous cap following unstable lesion formation (M. J. Davies et al., 1984). The tearing exposes pro-thrombotic factors to the bloodstream, triggering the activation of coagulation proteins and platelets, resulting in thrombosis (Libby, 2008). Clinical manifestation resulting from plaque erosion and consequent thrombus formation without rupture is less common than with rupture (M. J. Davies et al., 1984; van der Wal et al., 1993). Prior studies have highlighted the relevance of the lesion structure and vulnerability in atherosclerosis compared to the stenosis severity (Falk, 1983; Hackett et al., 1988). Consistent with these observations, patients with neurological symptoms showed higher frequencies of thin fibrous caps, fibrous cap foam cell infiltration and plaque rupture than asymptomatic patients (Carr et al., 1996).

Additionally, post-mortem analyses have yielded evidence of subclinical plaque ruptures in lesions (Mann et al., 1999). These lesions disclosed processes of reparation and reorganisation by VSMCs (Burke et al., 2001). Consequently, this outlines the importance of VSMC proliferation, migration and ECM synthesis in late atherosclerosis and may represent an essential process of plaque progression (Burke et al., 2001; Mann et al., 1996).

4.2. Vascular smooth muscle cells

In the past, the significance of VSMCs in atherogenesis was severely underestimated. Meanwhile, the current understanding considers VSMCs crucial for maintaining the fibrous cap and plaque stability in late atherosclerosis. However, the VSMCs' ability for de-differentiation and apoptosis suggests a different role: advancing and destabilising atherosclerotic lesions.

4.2.1. Function

In healthy vessels, VSMCs have a low proliferation index and regulate arterial compliance in response to biomechanical condition changes (D. Gordon et al., 1990). VSMCs are recognised as quiescent and contractile cells with high expression rates of contractile marker genes, such as smooth muscle actin (α-SMA), smooth muscle myosin heavy chain (MYH11), transgelin (TAGLN) and smoothelin (SMTN) (Shanahan et al., 1998; van der Loop et al., 1996; Weissberg et al., 1995). Healthy VSMCs morphologically display a spindle-shaped form. VSMCs are critical in maintaining vessel stability by secretion of ECM: elastin, collagen and proteoglycans.

4.2.2. VSMC phenotypes

VSMCs, as functional and differentiated cells, maintain remarkable plasticity in atherosclerosis (as seen in Figure 3). Past researchers have demonstrated the reversibility of phenotypes, for instance, in cells which have undergone less than five population doublings (Aikawa et al., 1997). While healthy VSMCs regulate vascular contraction, de-differentiated VSMCs are involved in vascular reconstruction.

A synthetic phenotype distinguishes de-differentiated VSMCs from other smooth muscle cells (SMCs) in the human body. Prior investigations discovered a reduced expression of contractile genes and an enhanced expression of ECM-remodelling enzymes and ECM elements in synthetic VSMCs (Andreeva et al., 1997a; Rensen et al., 2007). These discoveries were reinforced by an upregulated expression of collagen types I and III in atherosclerotic VSMCs: the predominant vessel collagen types (Amento et al., 1991; Ang et al., 1990; Rekhter et al., 1993). Morphologically, the VSMCs transform from their spindle shape to epithelioid cells (Chamley-Campbell

et al., 1979). Moreover, studies have observed the loss of myofilaments and increased synthetic organelles: ribosomes, mitochondria and rough endoplasmic reticulum (Mosse et al., 1985; Rensen et al., 2007). Chappell et al. (2016) highlighted behavioural changes with augmented proliferation and migration rates in synthetic VSMCs (Chappell et al., 2016).

VSMCs retain the capacity to develop an inflammatory phenotype: VSMC-derived macrophage-like cells (Feil et al., 2014). Additionally, lineage-tracing studies in mice have demonstrated that inflammatory VSMCs acquire the ability to engulf LPs and subsequently transform into foam cells; this was substantiated by the expression of the macrophage markers galectin 3 (MAC2 in mice, LGALS3 in humans) and CD68 (Allahverdian et al., 2014; Andreeva et al., 1997b; Rong et al., 2003).

Recent investigations have suggested that VSMCs switch to osteochondrogenic cells and thus contribute to calcification processes (Chellan et al., 2018). Accordingly, VSMCs have exhibited the capacity to synthesise calcifying vesicles, produce a calcification-prone matrix and express decreased mineralisation inhibitory molecule genes (Durham et al., 2018).

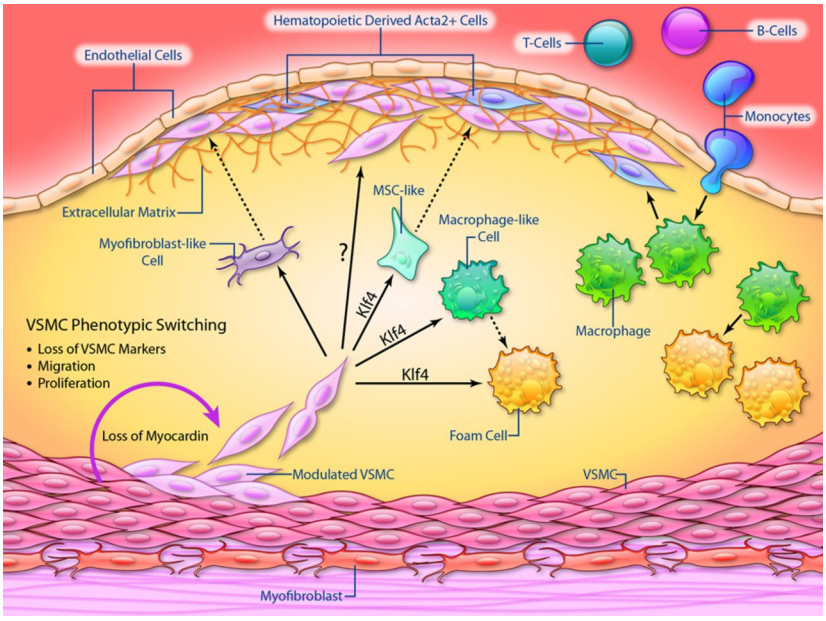

Figure 3: Illustration of the influence of KLF4 on possible VSMC phenotypes (Bennett et al., 2016).

Phenotypic switching of contractile media VSMCs is hypothesised to be KLF4-dependent (Kruppel-like factor 4). The solid lines represent experimentally validated paths; the dotted lines show mechanisms not yet verified. VSMCs have demonstrated the capability of assuming a myofibroblast-like cell type,

macrophage-like cell type and foam cell type. Simultaneously, macrophages can acquire SMC features, for example, by expression of α-SMA.

4.2.3. Phenotypic switch regulation

The phenotypical switch of VSMCs is regulated by environmental factors, transcription factors, extracellular stimuli, cell interactions and epigenetics.

The main transcription factors involved are myocardin (MYOCD) and Kruppel-like factor 4 (KLF4). The molecular mechanisms of MYOCD and KLF4 are illustrated in Figure 4. The transcriptional coactivator MYOCD activates a contractile phenotype in VSMCs (Pipes et al., 2006). MYOCD forms a complex with serum response factor (SRF); this enables the binding to CArG-box elements in the promotor area of contractile and cytoskeletal genes and, consequently, their expression upregulation (Parmacek, 2008; Pipes et al., 2006; Wang et al., 2001). An increased expression of MYOCD *in vitro* resulted in reduced inflammatory behaviour in VSMCs (Ackers-Johnson et al., 2015). Contrary to this, KLF4 is a promoter of atherogenesis and is not expressed in healthy VSMCs (Ghaleb et al., 2017; Yoshida et al., 2008b). KLF4 binds to G/C repressor elements and decreases the expression of contractile genes by inhibiting MYOCD attachment to CArG-boxes (Liu et al., 2005). Likewise, phenotypical switching has been declared KLF4-contingent (Shankman et al., 2015).

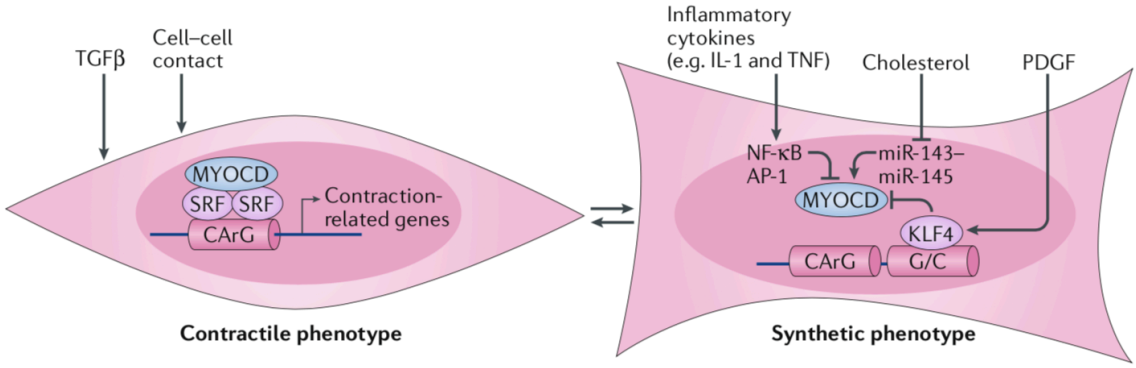

Figure 4: Illustration of the molecular mechanisms behind the phenotypical de-differentiation of VSMCs (Basatemur et al., 2019).

TGF-β and cell-cell contact stimulate a contractile phenotype via MYOCD and SRF interaction, permitting the attachment of MYOCD to CArG-box units in the promoter area of VSMC contractile genes. Inflammatory cytokines regulate the phenotypic switching via the transcription factors NF-kB

and AP-1: by inhibiting MYOCD. PDGF obstructs MYOCD via the transcription factor KLF4. Cholesterol advances a synthetic phenotype by inhibiting miR-143 and miR-145.

Similarly, extracellular stimuli, such as growth factors, inflammatory cytokines and cholesterol-LPs, play a prominent part in the phenotypical switch regulation. The macrophage-derived transforming growth factor-β (TGF-β) promotes the expression of α-SMA and smooth muscle myosin heavy chain (Chen et al., 2004; Hautmann et al., 1997; N. M. Shah et al., 1996). Furthermore, it activates collagen type I (COL1A1) and thus produces more stable fibrous caps (Mallat et al., 2001). Platelet-derived growth factor (PDGF) promotes a synthetic phenotype and encourages proliferation and migration activity via KLF4 stimulation (Deaton et al., 2009; Holycross et al., 1992; Sano et al., 2001). Inflammatory cytokines induce de-differentiation to a macrophage phenotype via nuclear factor-kB (NF-kB) and inhibition of MYOCD expression (Atkins et al., 2013; Yoshida et al., 2013). Correspondingly, lipid-loading of VSMCs *in vitro* encourages a macrophage phenotype development by inflammatory gene expression and elevation of phagocytic activity via KLF4 (Pidkovka et al., 2007; Vengrenyuk et al., 2015; Yoshida et al., 2008a). In addition to influencing inflammatory pathways, oxidised LPs enhance VSMC proliferation and migration behaviour and initiate the transformation into an osteoblast-like cell (Chellan et al., 2018; Heery et al., 1995; Klouche et al., 2000).

Further research has implied the relevance of the ECM environment and hemodynamical forces on the VSMC phenotype, migration and proliferation behaviour (Lee et al., 2001; Opitz et al., 2007; Raines, 2000).

4.2.4. VSMCs' role in atherosclerosis

The VSMC plasticity enables the alteration of their function as the disease progresses from early to late atherosclerosis. Whilst VSMCs are predominantly perceived to play a valuable part in the remodelling of the artery by contributing to the production of a fibrous cap, its function changes with each stage of atherosclerosis. The following section portrays the importance and role of VSMCs at each stage.

4.2.4.1. Pre-atherosclerosis

Pre-atherosclerotic lesions, such as diffuse intimal thickenings (DITs) and intimal xanthomas, can be observed in children and may represent a physiological adaptation of the tunica intima in response to blood flow (Stary et al., 1994; Velican et al., 1975, 1984). DITs are found in atheroprone regions of the vascular system, consisting of solely VSMCs, proteoglycans and elastin (Nakashima et al., 2002; Nakashima et al., 2008; Velican et al., 1975; Virmani et al., 2000). Intimal xanthomas contain additional monocyte-derived macrophages and T-lymphocytes; they form in various regions of the arterial tree (Velican, 1981). Investigations have depicted a de-differentiated synthetic state of VSMCs in DITs with a significant increase in synthetic organelles (Mosse et al., 1985). Similarly, a reduced contractile gene expression and increased ECM production were detected (Aikawa et al., 1993; Andreeva et al., 1997a).

4.2.4.2. Early atherosclerosis

DITs have the potential of progressing into pathological intimal thickenings (PITs): the first stage of atherosclerosis (Kim et al., 1985). In contrast to DITs, PITs contain an intimal extracellular lipid pool beneath the layers of VSMCs and VSMC-synthesised ECM (Kolodgie et al., 2007; Virmani et al., 2000). The lipid pools are composed of proteoglycans (versican, biglycan and perlecan), glycosaminoglycans, lipids and free cholesterol (Tran-Lundmark et al., 2008). By induction of ingested LDL, the synthetic VSMCs transform into foam cells (Allahverdian et al., 2014; Campbell et al., 1983; Campbell et al., 1985). A further phenotypic switch is substantiated by a decrease of α-SMA-positive cells, perhaps by VSMC de-differentiation and LDL-induced apoptosis induction, as well as a co-expression of α-SMA and CD68 (Andreeva et al., 1997b; Kockx et al., 1998; Okura et al., 2000). Furthermore, previous research has identified evidence of microcalcification in late PITs, potentially derived from apoptotic VSMCs (Bobryshev, 2005; Clarke et al., 2008).

4.2.4.3. Late atherosclerosis

Fibroatheroma formation is a crucial feature of late-stage atherosclerosis, marked by the existence of a fibrotic layer with an underlying necrotic core. The lipid pool

advances to a necrotic core by further lipid retention and macrophage- and VSMC-apoptosis (Basatemur et al., 2019). As a reaction to cell damage, the necrotic tissue liberates molecules such as damage-associated molecular patterns (DAMPs) into the extracellular space, promoting an inflammatory response; thereby, a positive feedback mechanism necessary for a non-resolving inflammation is sustained (Back et al., 2019).

Following the necrotic core formation, VSMCs attempt to strengthen the lesion by constructing a fibrous cap (Rekhter et al., 1993). VSMCs transmigrate from the tunica media to the intima, stimulated by growth factors and cytokines such as PDGF (Barrett et al., 1988; Sano et al., 2001). In the early stages, the fibrous cap is thick and rich in α-SMA positive VSMCs (Chappell et al., 2016). In late atherosclerosis, synthetic VSMCs generate modified ECM to strengthen the fibrous cap: decreased proteoglycan and increased collagen concentrations (Basatemur et al., 2019; Lee et al., 2001). Fibrous cap stability directly correlates with VSMC number: an observation which supports the hypothesis that VSMCs have a favourable effect on early lesions (M. J. Davies et al., 1993). Lipid phagocytosis contributes to the phenomenon of VSMC-derived macrophage-like cells (Campbell et al., 1983). However, compared to monocyte-derived macrophages, they display impaired phagocytic abilities, thus contributing to the inefficient apoptotic cell clearance and enlargement of the necrotic core (Allahverdian et al., 2014). In late atherogenesis, prior studies have also highlighted the role of VSMCs in fortifying calcification (Proudfoot et al., 2000).

4.3. Carotid artery disease

4.3.1. Definition

Carotid artery disease (CAD) is caused by the formation of atherosclerotic plaques in the extracranial internal carotid artery (ICA).

4.3.2. Epidemiology

Stroke is the second leading cause of death worldwide; it affects 1.1 million people and is accountable for 440 000 deaths in Europe annually (Naylor et al., 2018; Wafa et al., 2020). Stroke can be subdivided into ischaemic (89.1%) and haemorrhagic (10.1%) stroke; it is mainly induced by arterio-arterial embolisation (Andersen et al., 2009; Rothwell et al., 2000). Extracranial internal CAD accounts for 15-20% of ischemic stroke events (Petty et al., 1999). Supported by systematic meta-analyses, the prevalence of extracranial ICA stenosis ≥50% in the global population was estimated at 4.2% (de Weerd et al., 2009). Investigations have disclosed that 1% of women and 3% of men aged >80 years are diagnosed with severe CAD (≥70% stenosis), while 5% and 12%, respectively, are diagnosed with mild CAD (50-70% stenosis) (de Weerd et al., 2010). Besides stroke, CAD correlates with TIA and cognitive deterioration by chronic hypoperfusion and microemboli (Balestrini et al., 2013; Buratti et al., 2014; Jayasooriya et al., 2011).

4.3.3. Aetiology

The risk factors for CAD correspond with those previously discussed for atherosclerosis.

4.3.4. Diagnostics

Currently, CAD is clinically diagnosed using imaging analysis. The most frequent technologies are ultrasonography and magnetic resonance tomography imaging (Meschia et al., 2017). Secondary to imaging are laboratory diagnostics involving the patient lipid status: LDL-, HDL-, triglyceride- and apo-E-levels. The primary

determinant for clinical disease severity is the degree of lumen stenosis calculated by ultrasonography.

Other plaque quality factors correlating with high stroke risk include ulceration, echolucency, intraplaque haemorrhage, lipid content, fibrous cap thickness, necrotic core size and overall plaque thickness (Gupta et al., 2013; Kolodgie et al., 2003). Past research has also outlined the clinical relevance of quantifying lesions in terms of flow velocity criteria by doppler sonography: peak systolic velocity and end-diastolic velocity (Grant et al., 2003; Oates et al., 2009). Further imaging technologies involve digital subtraction angiography, computer tomography and catheter angiography (Naylor et al., 2018). Whereas ultrasonography is used most frequently for CAD diagnosis and stenosis grading, catheter angiography remains the gold standard. Nevertheless, the Carotid Revascularization Endarterectomy versus Stenting Trial (CREST) recommends angiography only if inconsistencies arise during non-invasive diagnostics (Mantese et al., 2010). In accordance with the guidelines of the Deutsche Gesellschaft für Gefäßchirurgie und Gefäßmedizin, a general population CAD screening is not recommended (Eckstein et al., 2020).

4.3.5. Symptoms

Patients diagnosed with CAD can be divided into symptomatic and asymptomatic patients. Manifestation occurs when the blood flow to the brain is disrupted, whereby the exact neurological symptoms depend upon the area affected. Common symptoms are loss of vision, facial numbness, difficulty in verbal expression and balance or one-sided weakness in extremities (Sobieszczyk et al., 2006). The National Institute of Health Stroke Scale (NIHSS) is frequently used to objectify clinical neurological symptoms (Brott et al., 1989). This study depicts patients as symptomatic if neurological symptoms occur within six months prior to intervention (Eckstein et al., 2020; Wendorff et al., 2015).

4.4. Treatment of carotid artery disease

4.4.1. Lifestyle management

Lifestyle management plays a critical role in the treatment and prevention of CAD. For example, abdominal adiposity and blood-triglyceride levels are positively associated with stroke incidence (Sarwar et al., 2007; Winter et al., 2008). Similarly, nicotine abstinence has proven crucial; the relative risk of stroke via smoking increases by 25-50% (Wolf et al., 1988). Additionally, European Society of Cardiology (ESC) guidelines recommend a moderated salt intake (<5-6g/day), resulting in arterial hypertension reduction (Aboyans et al., 2018). Furthermore, the Northern Manhattan Stroke Study has illustrated the protective effects of physical activity on stroke event rates (Sacco et al., 1998).

4.4.2. Medical treatment

Medical therapy for CAD mainly involves antiplatelet therapy and treatment of hypertension, diabetes mellitus and hyperlipidaemia.

ESC guidelines advise antiplatelet treatment in all CAD patients, regardless of clinical symptoms or revascularisation therapy. The risk of stroke in patients with TIA was significantly reduced when treated with antiplatelet medication (Goldstein et al., 2006). Antiplatelet therapy includes 100 mg/day acetylsalicylic acid (ASS) or clopidogrel 75 mg/day, an ADP-receptor antagonist (Eckstein et al., 2020). After carotid angioplasty and stenting intervention (CAS), dual antiplatelet treatment (ASS and clopidogrel) is recommended for ≥1 month (Aboyans et al., 2018; Eckstein et al., 2020). Furthermore, long-term single antiplatelet treatment with ASS or clopidogrel is advised for symptomatic patients (Aboyans et al., 2018). For asymptomatic patients with >50% stenosis, long-term single antiplatelet therapy is recommended when the risk for bleeding is considered low (Aboyans et al., 2018; Eckstein et al., 2020).

Hypertension is presently treated by dual drug therapy with diuretics, beta-blockers, angiotensin-converting enzyme inhibitors, calcium antagonists or angiotensin-receptor blockers. For every 10 mmHg decrease in systolic blood pressure, prior research has highlighted a 33% stroke risk reduction (Lawes et al., 2004). Therefore,

current guidelines recommend a goal blood pressure of <140/90 mmHg (Aboyans et al., 2018).

Hyperlipidaemia treatment by lowering LDL levels is advocated in CAD patients with ≥50% stenosis irrespective of symptoms, as studies have accentuated a positive correlation between blood cholesterol levels and risk of cardiovascular diseases or stroke (Eckstein et al., 2020; O'Leary et al., 1996; Sharrett et al., 1994). A target LDL-level of 70 mg/dl or a reduction of LDL levels by ≥50%, if initial levels were between 70-135 mg/dl, was associated with a reduced stroke incidence (Aboyans et al., 2018; Amarenco et al., 2020; Baigent et al., 2005). HMG-CoA reductase inhibitors, also known as statins, are currently recommended for hyperlipidaemia treatment (Amarenco et al., 2004). Additionally, statin-treated patients exhibited a 0.73% per year reduction of intima-media thickness per 10% reduction in LDL concentration (Amarenco et al., 2004). Ezetimibe monotherapy is an alternative to statins, in case of non-tolerance, reducing LDL levels by inhibiting the intestinal cholesterol absorption (Eckstein et al., 2020; Sudhop et al., 2002). Ezetimibe and statin combination therapy is employed if adequate LDL levels are not attained by statin monotherapy (Eckstein et al., 2020). Endeavours to treat hyperlipidaemia by increasing HDL levels have been made with CETP-Inhibitors (dalcetrapib, anacetrapib), apolipoprotein-A-I-transcription modifiers and nicotinic acid, up-to-date resulting in minor to no cardiovascular event reduction (Brown et al., 2008; Cannon et al., 2010; Frick et al., 1987; Robins et al., 2001).

4.4.3. Interventional treatment

Interventional revascularisation of CAD involves two methods: carotid endarterectomy (CEA) and carotid angioplasty and stenting (CAS). Contraindications for interventional treatment include disabling stroke, high probability of periprocedural complications, stenosis degree <50% or total carotid artery obstruction (Ooi et al., 2015; Rothwell et al., 2003a).

During CEA, the atherosclerotic plaque containing the intima and media is removed via an ICA incision. Depending on the local clinic standard, a temporary shunt can be implemented during carotid clamping to maintain brain blood flow. After plaque removal, the ICA incision is either closed with direct stitches or patch plastic. According

to the North American Symptomatic Carotid Endarterectomy Trial (NASCET), European Carotid Surgery Trial (ECST), and the Veterans Affairs Trial 309 (VA), CEA is recommended in symptomatic patients with a stenosis degree of 70-99% and should be considered in corresponding patients with a 50-69% stenosis (Barnett et al., 1998; Group, 1998; Rothwell et al., 2003a; Rothwell et al., 2003b). Consistent with current guidelines, CEA is advised in asymptomatic patients with a 60-99% stenosis presenting with clinical or imaging characteristics related to increased stroke risk: contralateral TIA or stroke, lipid-rich necrotic cores, stenosis progression, intraplaque haemorrhage, ipsilateral silent infarction and large or echolucent plaques (Gupta et al., 2013; Gupta et al., 2015; Kakkos et al., 2014; Kakkos et al., 2009; Nicolaides et al., 2005; Nicolaides et al., 2010). CEA should be performed within 3-14 days of stroke or TIA event (Eckstein et al., 2020). CEA, compared to CAS, is recommended in patients aged 70-74 years, with high periprocedural stroke risk, long-section stenosis >10 mm or difficult catheter access due to aortic arch calcification (Eckstein et al., 2020; Howard et al., 2016; Rantner et al., 2017). Investigations by Brott et al. (2010) yielded no significant difference in the risk of myocardial infarction, stroke and death between symptomatic or asymptomatic patients following CEA or CAS (Brott et al., 2010).

CAS is a minimal invasive endovascular revascularisation technique for the treatment of CAD. A catheter is advanced into the extracranial ICA via the femoral artery, followed by balloon inflation and stent placement. Current guidelines recommend a dual antiplatelet treatment during CAS and for ≥1 month following revascularisation (Eckstein et al., 2020). The therapy is considered an alternative to CEA in symptomatic patients with 50-99% stenosis and disadvantageous surgical anatomy, high perioperative risks, contralateral recurrent laryngeal nerve paresis or restenosis (Aboyans et al., 2018). Similarly, CAS may be advised in asymptomatic patients with a ≥50% stenosis (Aboyans et al., 2018).

5. Aim of this study

This study aimed to examine the changes in VSMC plasticity as the lesions transition from early- to late-stage atherosclerosis by establishing and streamlining a vascular cell biobank of patients diagnosed with CAD. Biobanking is a method gaining significance in modern medicine. It bridges the gap between experimental and clinical research and provides the opportunity for personalised medicine. As the leading source of cardiovascular disease worldwide, atherosclerosis involves a complex interaction of inflammatory, immunological, and mechanical processes, whereby many see VSMCs as the focal point of atherogenesis. The following list represents the main objectives of this doctoral thesis:

1. To establish a method for VSMC isolation and culture from patient-derived carotid lesions sampled during CEA
2. To set up a vascular cell biobank
3. To study the phasic gene expression in VSMCs derived from stable, unstable and ruptured carotid lesions *in vitro*
4. To compare the changes in gene expression of atherosclerotic VSMCs to healthy VSMCs *in vitro*
5. To study the changes in proliferation and migration behaviour of VSMCs derived from stable, unstable and ruptured carotid lesions by live-cell imaging *in vitro*
6. To provide a basis for potential novel therapeutic targets in the treatment of CAD at different stages of the disease

6. Materials

6.1. Chemicals and reagents

Materials	Manufacturer	Charge/ Reference Nr.
Antibody Diluent DAKO Real	Dako Denmark A/S	20042092
Bovine serum albumin	Thermofisher	Ref: 15561-020
Citric acid monohydrate	Merck KGaA Darmstadt	5949-29-1
Collagenase A	Sigma-Aldrich Chemie GmbH D-89555 Steinheim	
DEPC Diethyl Pyrocarbonate	Sigma-Aldrich Chemie GmbH D-89555 Steinheim	D5758
Dimethyl sulfoxide	Sigma-Aldrich Chemie GmbH D-89555 Steinheim	Lot: SHBG7041 V
Distilled water	B. Braun Meisungen AG Meisungen Germany	Lot: 164478001
Dulbecco's Modified Eagle's Medium/ Nutrient Mixture F-12 Ham	Sigma-Aldrich Chemie GmbH D-89555 Steinheim	Lot: RNBG6717
Dulbecco's Phosphate Buffered Saline	Sigma-Aldrich Chemie GmbH D-89555 Steinheim	Lot: RNBG8372
Eosin 1%	Morphisto GmbH Weißmüllerstraße 45 60314 Frankfurt a. Main	Lot: 19307-8 Ref: 11503 01000
Ethanol 70%	Carl Roth GmbH + Co KG Karlsruhe D-76185	Charge: 3036247495
Ethanol absolute	VWR Chemicals International Fontenot-Sous-Bois, France	Lot: 18D264013
Ethylenediaminetetraacetic acid (EDTA)	Sigma-Aldrich Chemie GmbH D-89555 Steinheim	Lot: BCBR6991V
Eukitt Quick-hardening mounting medium	Sigma-Aldrich Chemie GmbH D-89555 Steinheim	BCBV4833
Fetal bovine serum	Gibco by Life Technologies	Lot: 42G9150K Ref: 10270-106

Formaldehyde solution	Sigma-Aldrich Chemie GmbH D-89555 Steinheim	Lot: BCBT3790
Hämalaun Lösung Sauer nach Mayer	Carl Roth GmbH + Co KG Karlsruhe D-76185	Charge: 467265140
Hydrochloric acid 25%	Klinikum rechts der Isar, Krankenhausapotheke	
Hydrogen peroxidase 30%	Merck KGaA Darmstadt	1.085.971.000
Isopropanol 99,5%	Klinikum rechts der Isar, Krankenhausapotheke	Charge: 3-164
Milk powder	Carl Roth GmbH + Co. KG Karlsruhe D-76185	T145.2
Natronlauge (2N) 2mol/l – 2 N Maßlösung	Carl Roth GmbH + Co. KG Karlsruhe D-76185	T135.1
Paraffin	Klinikum rechts der Isar, Krankenhausapotheke	
Paraformaldehyde	Klinikum rechts der Isar, Krankenhausapotheke	
Penicillin streptomycin glutamine (100x)	Gibco by Life Technologies	Lot: 1786395 Ref: 10378-016
Phalloidin 488 (green) Alexa Fluor	Life Technologies Corporation	Ref.: A12379
Picrofuchsin solution	Klinikum rechts der Isar, Krankenhausapotheke	Charge: 300617
Poly-l-lysine solution	Sigma-Aldrich Chemie GmbH D-89555 Steinheim	P8920
Prolong Gold antifade reagent with DAPI	Life Technologies Corporation	Lot: 1796982 Ref: P36935
Resorcin-Fuchsin nach Weigert	Klinikum rechts der Isar, Krankenhausapotheke	Charge: 190318
RNase and DNase free H_2O	Thermofisher	AM9930
RNase Zap	Sigma Life Science	Lot: SLBX5613
Sodium chloride >99,8%	Carl Roth GmbH + Co. KG Karlsruhe D-76185	9265.1
TRIS base molecular biology grade	EMD Chemicals	D00137505

Triton™ X-100	Sigma-Aldrich Chemie GmbH D-89555 Steinheim	Lot: 1945359 CAS: 9002-93-1
Trypsin-EDTA 0,25%	Gibco by Life Technologies	Lot: STBG3972V CAS: 9002-93-1
Weigert'sche Lösung I	Klinikum rechts der Isar, Krankenhausapotheke	Lot: 1945359 Ref: 25200-056
Weigert'sche Lösung II	Klinikum rechts der Isar, Krankenhausapotheke	Charge: 030717
Xylene	Carl Roth GmbH + Co KG Karlsruhe D-76185	Charge: 216243494

6.2. Primers

Materials	**Manufacturer**	**Charge/ Reference Nr.**
α-SMA primer assay	Thermofisher	Hs00426835_G1 Lot: P200214-002H09
CD68 primer assay	Thermofisher	Hs02836816_G1 Lot: P170619-012H09
COL1A1 primer assay	Thermofisher	Hs00164004-M1 Lot: 1834841
COL3A1 primer assay	Thermofisher	Hs00943809_M1 Lot: 1835843
GAPDH primer assay	Thermofisher	Hs02758991_g1 1535886 B8 Lot: 1535865
KLF4 primer assay	Thermofisher	Hs00358836 1666432 C2 Lot: 1666428
LGALS3 primer assay	Thermofisher	Hs00173587_M1 Lot: 1748781
MYOCD primer assay	Thermofisher	Hs00538076_m1 1779697 E10 Lot: 1779686
PDGFB primer assay	Thermofisher	Hs00234042_M1 Lot: 1714797

RPLPO primer assay	Thermofisher	Hs00420895gH PN4351370 Lot: P190904-002 H10
SMTN primer assay	Thermofisher	Hs01022255_g1 PN4351370 Lot: P190723-003 G08
TAGLN primer assay	Thermofisher	Hs01038777_g1 1809558 G1 Lot: 1809549

6.3. Antibodies

Materials	Manufacturer	Charge/ Reference Nr.
Monoclonal Mouse Anti-Human CD68 Clone KP1	Dako Denmark A/S	20053851
Mouse Anti-Human Monoclonal Muscle Actin	Dako Denmark A/S	M0635

6.4. Laboratory equipment

Materials	Manufacturer	Charge/ Reference Nr.
96-pin IncuCyte WoundMaker Tool	Essen BioScience Cat	4563
Balance	Kern & Sohn	T8028
Centrifuge multifuge X3R	Thermofisher Scientific	Inv. Nr. 47187
Centrifuge small 5415D	Eppendorf	Inv. Nr. 20357
Confocal microscope	Leica	
Cooling plate	Leica	EG1150C
Flow hood	Thermoscientific	Serial Nr. 41451124
Freezer -80°C	Thermoscientific	Serial Nr.: 118249001171013 Item Nr.: 162VE5C01M

Incubator Heratherm Oven	Thermoscientific	
IncuCyte® S3 Live-Cell Zoom Analysis System	Sartorius	Inv. Nr. 5204605 Serial: 41133
Mastercycler	Nexus gradient	Inv. Nr: 47198
Microscope	Leica	DM4000B
Microtome	Leica	RM2255
Mr. FrostyTM Freezing Container	Nalgene	Cat. No. 5100-001
Nanodrop 2000c Spektrophotometer	Thermoscientific Peqlab	Inv. Nr: 46595
pH meter	InoLab, WTW	T8028
Pressure cooker	Silitherm	
QuantStudio 3 Real-Time PCR Instrument	Life Technologies Holdings Pct. Ltd. Singapore 739256	Product Nr. A28131 Serial Nr. 272311593
Vortex mixer	VWR	Inv. Nr. 47114
Water bath	GFL	1952
WoundMaker Rinse Boats	Essen BioScience Cat	5025-0191-A00

6.5. Kits

Materials	**Manufacturer**	**Charge/ Reference Nr.**
Dako REAL Detection System Peroxidase/ DAB+, Rabbit/Mouse	Dako Denmark A/S	20000821
High-Capacity RNA-to-cDNA Kit™ (Applied Biosystems™)	Applied biosystems by Thermofisher Scientific	Lot: 00761806 Ref: 4387406
RNeasy® Plus Mini Kit (Qiagen)	Quiagen GmbH	Lot: 154045694 GTIN: 04053228006138

Smooth Muscle Cell Growth Medium Kit Classic	PELO Biotech	Lot: QC-05B17F11
Supplement Kit: Smooth Muscle Cell Growth Medium Classic: FCS, glutamine, antibiotics, EGF, insulin, bFGF	PELO Biotech	Lot: QC-05B17F11
TaqMan™ Gene Expression Master Mix	Applied biosystems by Thermofisher Scientific	Lot: 00794860 Ref: 4369016

6.6. Consumables

Materials	**Manufacturer**	**Charge/ Reference Nr.**
4-well chamber-plate	Corning Incorporated Corning, NY 14831 USA	
6-well plate (flat bottom with lid; tissue culture treated)	Corning Incorporated Corning, NY 14831 USA	Ref: 3516
96-well ImageLock plate	Essen BioScience Cat	4379
FastGene®Fast 96-Well qPCR plate	Genetics NIPPON Genetics Europe GmbH	Lot: B23287
96-well flat-bottom-plate	Corning Incorporated Corning, NY 14831 USA	Lot: 11415027
Cell culture flask 25 cm2 vent cap; cell bind surface	Corning Incorporated Corning, NY 14831 USA	Lot: 33817016 Ref: 3289
Cell culture flask 75 cm2 vent cap; cell bind surface	Corning Incorporated Corning, NY 14831 USA	Lot: 14118011 Ref: 3289
Cell strainer 100 µm	Corning Incorporated Corning; NY 14831 USA	Lot: 171124-299
Cryogenic vial (2,0 ml)	Corning Incorporated Corning, NY 14831 USA	Lot: 430659
Tubes 0,5 ml	Peqlab	472496
Eppendorf tubes 1,5 ml	Eppendorf	
Falcon tissue culture dish	Corning Incorporated Corning, NY 14831 USA	Lot: 6108087 Ref: 353003
Tubes 25 ml	Greiner bio-one	

Tubes, 50 ml	Greiner bio-one	Lot: E16093QJ
Feather disposable scalpel No. 10	Feather safety razor Co., LTD	Lot: 16120786 Ref: 02.001.30.010
Menzel Gläser Deckgläser 24x50 mm	Gerhard Menzel B.V. & Co. KG Braunschweig	521187
Menzel Gläser Superfrost	Gerhard Menzel B.V. & Co. KG Braunschweig	
Menzel Gläser Superfrost Plus	Gerhard Menzel B.V. & Co. KG Braunschweig	J1800AMNZ
C-Chip Neubauer counting chamber	NanoEntek	
Serological pipette sterile 10 ml in 1/10 ml	Greiner bio-one	Lot: F181034N
Serological pipette sterile 2 ml in 1/100 ml	Greiner bio-one	Lot: 15042071
Syringe 30 ml	Henke Sass Wolf	Lot: 18I188B Ref: 4830001000
Syringe 50 ml	Henke Sass Wolf	Lot: 18I188B Ref: 4830001000

7. Methods

7.1. Study design

The study design is an experimental study.

7.2. Ethics approval

The approval for patient carotid endarterectomy specimen collection was granted by the local hospital ethics committee (Ethikkommission der Fakultät für Medizin der Technischen Universität München, Munich, Germany). The experiments were performed according to the principles of the Declaration of Helsinki. Informed consent was obtained in written form from every patient enrolled in this study.

7.3 Munich Vascular Biobank

The Munich Vascular Biobank contains over 2000 formalin-fixed paraffin-embedded (FFPE) tissue samples of abdominal aortic aneurysms (AAA), carotid artery plaques and peripheral arterial disease, 300 fresh frozen tissue samples and 4400 serum samples. Consequently, it is one of the most substantial human vascular biobanks worldwide. As part of this study, we expanded the biobank by adding patient-derived isolated VSMCs from AAA and CAD samples. The biological material was collected from patients undergoing surgery at the Department of Vascular and Endovascular Surgery at the Klinikum rechts der Isar, Munich.

7.4. Study population and tissue sample collection

The study population consisted of 18 patients. The patients were diagnosed with high-grade CAD and underwent interventional treatment via CEA. CEA was performed according to the recommended European Society for Vascular Surgery guidelines on the management of atherosclerotic carotid and vertebral artery disease (Eckstein, 2018).

In addition to tissue sample collection, clinical data was accumulated regarding the patients' medical history: gender, age, degree of stenosis, absence or presence of

neurological symptoms and location of the stenosis (Wendorff et al., 2015). The patients were examined two days before and after surgery by experienced neurologists from the Department of Neurology at Klinikum rechts der Isar, Munich (Wendorff et al., 2015). The degree of stenosis was measured by doppler ultrasound; in unclear cases, computer tomography or magnetic resonance angiography were implemented to supplement carotid stenosis imaging (Wendorff et al., 2015). The complete experimental workflow is illustrated in Figure 5.

7.5. Tissue sample processing

The carotid artery samples were collected within 1 hour after CEA, transported in sterile Dulbecco's Modified Eagle's Medium/ Nutrient Mixture F-12 Ham (DMEM/F-12) and stored at 4°C. The specimen was cut into 3-5 equal 1 cm sized segments. The divided segments were designated for different purposes: histology, cell isolation, or to be snap-frozen and stored at -80°C for future molecular analyses. The pieces selected for histological analysis were fixed overnight in 4% formaldehyde followed by decalcification by ethylenediaminetetraacetic acid (EDTA) for 24-72 h, dehydrated and then embedded in paraffin (Pelisek et al., 2019). The segments for cell isolation were immediately processed in the Laboratory for Vascular Biology and Experimental Vascular Medicine at the Biederstein campus or stored overnight in sterile Dulbecco's Modified Eagle's Medium/ Nutrient Mixture F-12 Ham (DMEM/F-12) at 4°C and processed the following day.

7.6. Preparation of collagenase A

1.4 mg of collagenase A powder was prepared per 1 ml DMEM/F-12 with 5% FBS and 1% penicillin and streptomycin (Pen-Strep) for the enzymatic digestion of human carotid artery samples.

7.7. Isolation of vascular smooth muscle cells

To expand the Munich Vascular Biobank and set up a patient-derived cell biobank, a method was established to isolate vascular smooth muscle cells from human carotid plaque samples collected by CEA.

Under a laminar flow hood and sterile conditions, forceps were used to remove the carotid tissue sample from the falcon tube and place it in a tissue culture dish. The samples were washed 1-2 times with Dulbecco's Phosphate Buffered Saline (PBS) to remove excess blood and then placed into a new tissue culture dish containing 10 ml of previously at 37°C incubated 1.4 mg/ml collagenase A solution. The tissue was cut into 0.1 mm sized pieces using a scalpel to aid digestion via collagenase A enzyme and remove calcifications. The tissue culture dish containing the tissue fragments was incubated at 37°C, 5% CO_2 for 4-6 hours, depending on the size of the specimen.

After incubation, the digested cell collagenase suspension was strained under the flow hood using a 100 µm cell strainer to remove calcification and debris. The remaining cell solution was centrifuged at 1000 rpm, 400 xg for 5 min. The cell pellet was then resuspended in 15 ml of complete DMEM/F-12 (DMEM/F12 + 5% FBS + 1% Pen-Strep). The cells were washed twice with 15 ml complete DMEM/F-12 each and then resuspended in 7 ml of complete DMEM/F-12 and subsequently pipetted into a 25 cm^2 cell culture flask. The cells remained in culture for 5-6 weeks.

7.8. Cell culture

7.8.1. Medium change

The VSMCs were incubated at 37°C, 5% CO_2 for 72 hours until the first medium change. Then every 48-72 hours, the cells were washed with PBS, and the old medium was replaced with fresh complete DMEM/F-12. At 40-50% cell confluency in the 25 cm^2 flasks, the medium was switched to a specific smooth muscle cell medium: SMC Growth Medium Kit Classic supplemented with FCS, glutamine, antibiotics, EGF, insulin and bFGF provided by PELO Biotech.

7.8.2. Passaging cells

At 80-90% cell confluency, the cultured VSMCs were passaged into two 75 cm^2 cell culture flasks. After washing the cells with PBS, 1-2 ml of previously warmed trypsin enzyme solution was added to the flask. Next, the flask was incubated at 37°C, 5% CO_2 for 2-5 min. Cell detachment was verified under the microscope, and trypsin was neutralised using 5-10 ml SMC Growth Medium. Afterwards, the cell suspension was

centrifuged at 1000 rpm, 400 xg for 5 min. Finally, the cell pellet was resuspended in 24 ml SMC Growth Medium, transferred into two 75 cm^2 cell culture flasks and incubated at 37°C, 5% CO_2.

7.8.3. Freezing cells

At 90-100% cell confluency in the 75 cm^2 cell culture flasks, the VSMCs were passaged and frozen for storage at -80°C. The cells were washed, detached with trypsin and suspended in 10 ml SMC medium. The cell suspension was centrifuged at 1000 rpm, 400 xg for 5 min. The cell pellet was then resuspended in 3 ml freezing medium (10% Dimethyl sulfoxide, 20% SMC medium, 70% FBS) per 75 cm^2 flask and transferred to three cryovials. The cryovials were placed into a Mr. Frosty™ freezing container at -80°C. After one week, the frozen VSMCs were transferred to a liquid nitrogen container.

7.8.4. Thawing cells

For the thawing of cells, the cryovials were removed from the liquid nitrogen, transported on dry ice and immediately placed into a 37°C water bath for 30 seconds. Meanwhile, cell culture flasks were prepared with the pre-warmed medium. The cell solution was then added to the cell culture flask. The thawed cells were plated at high confluency to enhance cell attachment and survival. After 4-5 hours, the medium was changed to remove DMSO and necrotic cells from the attached cells. The cells were incubated at 37°C, 5% CO2.

7.8.5. Cell counting

For the following experiments using VSMCs, the cells were counted using a Neubauer chamber. 10µl of cell suspension was pipetted under the cover glass on each side of the chamber. The grid is 3 mm x 3 mm in size and consists of four 4x4 squares. Under the microscope, the cells in one 4x4 square of the upper area and one square of the lower area are counted, and the cell numbers are averaged.

The equation for calculation of the cell-concentration:

$$Concentration\ (cell/ml) = \frac{Number\ of\ Cells}{Volume\ (ml)}$$

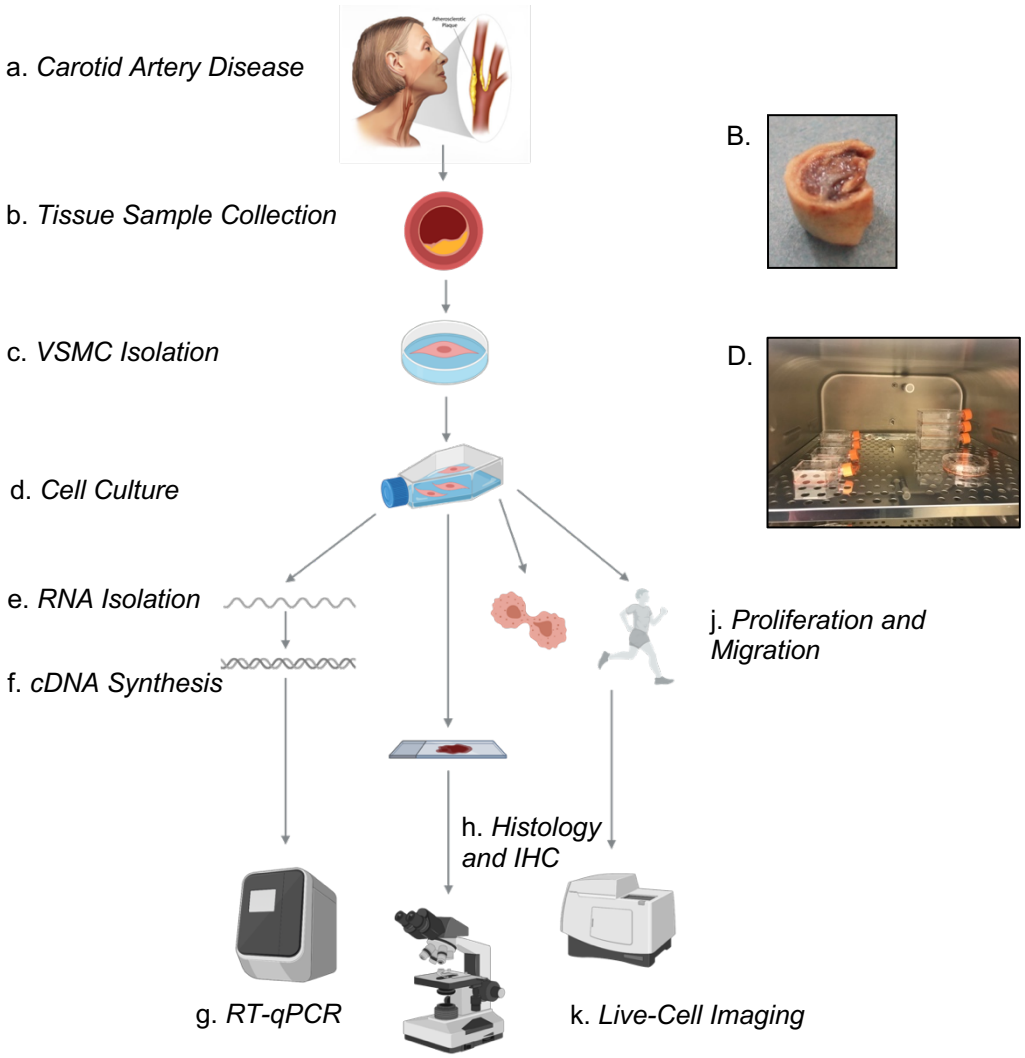

Figure 5: Schematic experimental workflow of the Munich Vascular Biobank.
(a.-b.) Carotid endarterectomy samples were collected from patients diagnosed with CAD. (B.) displays an example of the carotid samples. (c.) VSMCs were isolated from the specimen and (d) remained in culture for 5-6 weeks. (D.) shows the VSMCs in culture flasks in the incubator during cultivation. (e.) RNA was isolated from the primary VSMCs and (f.) used for cDNA synthesis. (g.) The cDNA was used to examine gene expression using RT-qPCR. (h.) The carotid samples were stained using HE, EvG and IHC and then (i.) classified. (j.) Migration and proliferation activity of the primary VSMCs was examined using (k.) live-cell imaging.

7.9. RNA isolation

To examine the plasticity of VSMCs derived from carotid artery lesions and establish a gene panel, RNA was extracted from patient VSMC specimens (*n=18*) and healthy human carotid artery VSMCs (*n=1*).

At 90-100% confluency, 2 ml of trypsin enzyme were used to detach the VSMCs from the cell culture flasks. The cells were centrifuged, and the cell pellet was resuspended in medium. The cell number was counted using the Neubauer chamber. Afterwards, the cell suspension was diluted to a concentration of 120 000 cells/ ml and seeded into a 6-well plate with 1 ml cell suspension and 1 ml medium added to each well. The 6-well plate was incubated at 37°C, 5% CO_2 for 2-3 days.

Table 1: Chemical materials for RNA isolation

Materials	Components	Final Volume
RNAse Zap		-
RNAse-free H_2O		90 µl
RNeasy® Plus Mini Kit (Qiagen)	RTL Buffer Plus	2.1 ml
	Buffer RW1	2.1 ml
	Buffer RPE	3.0 ml
70% Ethanol		2.1 ml

RNA extraction was performed using the RNeasy® Plus Mini Kit in accordance with the manufacturer's protocol, as seen in Table 2, using the chemical reagents in Table 1. RNA quantity and quality were assessed using a NanoDrop 2000c Spectrophotometer previously tared to 0 ng/µl with RNAse-free H_2O.

Table 2: RNA isolation protocol

RNeasy® Plus Mini Kit Protocol
1. Aspiration of the medium from every well of a 6-well plate containing previously seeded cells
2. Washing of cells with PBS and aspiration of PBS
3. Addition of 350 µl RTL Buffer Plus to each well for cell-lysis

4. Aspiration of the cell-buffer suspension and transferring of the contents of 2 wells into one 1,5 ml Eppendorf tube
5. Each Eppendorf tube now contains 700 µl of cell-lysis suspension
6. Spray everything with RNAse Zap to avoid RNA degradation
7. Addition of 700 µl 70% EtOH to each Eppendorf tube and generate an adequate mixture by pipetting up and down several times
8. Transferring of 700 µl cell suspension to a pink spin column and centrifugation for 1 min at 8000 xg
9. Discarding of the flow through
10. Transferring of the other 700 µl to the spin column and centrifugation for 1 min at 8000 xg
11. Discarding of flow through
12. Addition of 700 µl Buffer RW1 to each spin column
13. Centrifugation for 1 min at 8000 xg
14. Discarding of flow through
15. Addition of 500 µl Buffer RPE to each spin column
16. Centrifugation for 1 min at 8000 xg
17. Discarding of flow through
18. Addition of 500 µl Buffer RPE to each spin column
19. Centrifugation for 2 min at 8000 xg
20. Discarding of flow through
21. Centrifugation for 1 min at full speed to dry the membranes
22. Placement of the column on a new 1,5 ml Eppendorf tube
23. Addition of 30 µl RNAse-free H_2O
24. Centrifugation for 1 min at 8000 g
25. Placement of Eppendorf tubes containing the isolated RNA on ice
26. Storage of the isolated RNA at -80°C

7.10. cDNA synthesis

After RNA extraction from the isolated patient-derived VSMCs, cDNA was synthesised using the High-Capacity RNA-to-cDNA™ Kit (Applied Biosystems™) consistent with

the manufacturer's protocol and materials in Table 3. During this protocol, every step was performed on ice and with materials previously sprayed with RNAse Zap to avoid RNA degradation. First, the formerly isolated RNA was diluted down to a concentration of 1000 ng in 9 µl. Then, 10 µl of the cDNA synthesis buffer mix and 1 µl of the reverse transcriptase enzyme from the kit were added to the RNA. Each Eppendorf tube containing the reaction solution was placed into the thermal cycler, where the "cDNA Program" was run following the temperatures and times listed in Table 4. Finally, the cDNA samples were diluted with 180 µl RNAse-free water and stored at -20°C.

Table 3: Chemical materials for cDNA synthesis

Materials	Components	Final Volume (per reaction solution)
High-Capacity RNA-to-cDNA™ Kit	Buffer Mix RT-Enzyme	10 µl 1 µl
RNAse-free H_2O		180 µl
RNAse Zap		-

Table 4: cDNA Program: Reverse transcription reaction

Step	Temperature (°C)	Time (min)
1	37	60
2	95	5
Preservation	4	Unlimited

7.11. Real-time quantitative polymerase chain reaction

The TaqMan™ Assay Primers and TaqMan™ Fast Advanced Master Mix were used for real-time quantitative polymerase chain reaction (RT-qPCR) to compare the gene expression patterns of VSMCs derived from stable, unstable and ruptured carotid artery plaques to one healthy control donor cell. 17 carotid VSMC patient samples and 1 healthy carotid VSMC donor sample were included in this experiment (*n=18*). For each specimen, the expression patterns of 13 genes were examined, including 2 housekeeping genes: glyceraldehyde 3-phosphate dehydrogenase (GAPDH) and

ribosomal protein lateral stalk subunit P0 (RPLP0). Details of the primers are outlined in Table 19. A 20 µl reaction, including 2 µl of VSMC-derived cDNA, was mixed with components shown in Table 5. The RT-qPCR was performed on the QuantStudio™ 3 Real-Time PCR Instrument using the QuantStudio™ Design and Analysis Software version 1.4.3. for Windows with standard settings.

Table 5: qPCR reaction system components

Components	Volume in each reaction (µl)
TaqMan™ Fast Advanced Master Mix	10
RNAse-free H_2O	7
TaqMan™ Assay Primer	1
VSMC-derived cDNA	2
Total	20

The reactions were prepared in duplicates for each corresponding cDNA and gene pair on a 96-well plate. The cycling settings used in the experiment are displayed in Table 6. For each reaction sample, a baseline level was automatically calculated by the software. Consequently, a threshold level was determined, which mirrored a statistically significant increase in the PCR reaction over the measured baseline signal. The threshold level allows for discrimination between relevant and irrelevant amplification signals. The threshold cycle (C_t) values were calculated for each patient-derived cDNA and gene pair, corresponding to the amplification cycle number during the RT-qPCR when the fluorescent signal intersects with the previously determined threshold level.

Table 6: qPCR cycles

Segment	Cycle	Temperature (°C)	Duration (s)
Denaturation	1	95	20
Annealing		95	1
Elongation	40	60	20

The mean and standard deviation of the C_t value duplicates were calculated for data analysis. The following equations were used to examine the RT-qPCR data.

$$\Delta CT = CT_{Target\ Gene} - CT_{Housekeeping\ Gene}$$

$$\Delta\Delta CT = \Delta CT_{Patient-derived\ Cells} - \Delta CT_{Control-Donor\ Cells}$$

$$Fold\ Change\ (F.C) = 2^{-\Delta\Delta CT}$$

7.12. Histology staining

Histology staining was performed on the patient-derived tissue samples for plaque classification using haematoxylin and eosin (HE), Elastica van Gieson (EvG) staining and immunohistochemistry (IHC) staining.

The carotid plaques were classified according to the American Heart Association (AHA) classification of atherosclerotic lesions (Stary et al., 1995). Furthermore, the plaque stability was determined by measuring the fibrous cap thickness over the necrotic or lipid core following the Redgrave and Rothwell criteria (Redgrave et al., 2008). Per this criteria, carotid plaques with a fibrous cap thickness of <200 µm were depicted as unstable; lesions with a discontinuous fibrous cap were characterised as ruptured (Redgrave et al., 2008). On the other hand, lesions with either a thick fibrous cap measured >200 µm or lesions without a lipid or necrotic core were classified as stable plaques (Redgrave et al., 2008). The fibrous cap thickness was quantified with the Aperio ImageScope software version 12.3.3.5048 for Windows.

Additional elements examined during the plaque classification were stage and extent of calcification, the degree of inflammation, cellularity, the content of elastin and collagen fibres and neovascularisation. A semiquantitative scoring system was established for characterising carotid lesion features: absent (-) to strongly present (+++). These components were examined using a Leica bright light microscope. Each characterisation was performed separately and blinded for the corresponding clinical and study data by two investigators and reviewed by one experienced senior pathologist.

7.12.1. Preparation of tissue slices

The FFPE tissue samples were cut consecutively in 2-3 µm sections with a Leica microtome and brought onto Superfrost slides. The sections were dried overnight in a 56°C oven.

7.12.2. Haematoxylin and eosin staining

Each tissue sample slide was stained for haematoxylin and eosin according to protocol, as disclosed in Table 7. Before HE staining, the tissue slides were incubated at 56°C for 20 minutes. The stained slides were then sealed with Eukitt Quick-hardening mounting medium and a coverslip and stored at room temperature.

Table 7: Haematoxylin and eosin staining protocol

Chemical Reagent	Incubation period
Xylene	2 x 10 min
Isopropanol	2 x 5 min
Ethanol 96%	2 x 5 min
Ethanol 70%	2 x 5 min
Distilled water	1 min
Haematoxylin	10 min
Water wash	2 min
Eosin	2 min
Ethanol 96%	1 s
Isopropanol	2 x 30 s
Xylene	2 x 2 min

7.12.3. Elastica van Gieson staining

Each tissue sample slide was stained with Elastica van Gieson according to protocol, as shown in Table 8. Before the EvG staining, the tissue slides were incubated at 56°C for 20 minutes. Afterwards, the stained slides were sealed with Eukitt Quick-hardening mounting medium and a coverslip and stored at room temperature.

Table 8: Elastica van Gieson staining protocol

Chemical Reagent	Incubation period
Xylene	2 x 10 min
Isopropanol	2 x 5 min
Ethanol 96%	2 x 5 min
Ethanol 70%	2 x 5 min
Distilled water	1 min
Resorcin fuchsin	25 min
Ethanol 96%	2 x 1,5 min
1:1 Mixture: Weigert'sche Lösung I and Weigert'sche Lösung II	15 min
Water wash	2 min
Picrofuchsin	2 min
Ethanol 96%	30 s
Isopropanol	2 x 30 s
Xylene	2 x 2 min

7.12.4. Immunohistochemistry staining

7.12.4.1. Coating microscope slides with poly-l-lysine

Before IHC staining, the Superfrost Plus microscope slides were coated with poly-l-lysine to ensure proper tissue adhesion to the slide. Poly-l-lysine was diluted at 1:10 using distilled water; the thereby resulting working solution was stored in the fridge. Before coating the slides, the working solution was warmed to 22°C (room temperature). The microscope Superfrost Plus slides were then immersed in the poly-l-lysine-distilled water solution for 5 minutes and incubated for 1 hour at 54°C to dry.

7.12.4.2. Preparation of TRIS buffer

10x TRIS buffer stock was prepared for IHC staining using the chemical reagents listed in Table 9. 60.5 g TRIS base was added to 700 ml of distilled water. A pH of 7.6 was calibrated by a pH meter using hydrochloric acid. 90 g of NaCl was added to the

solution. Afterwards, the solution was replenished to 1 L with distilled water. The 10x TRIS buffer stock was further diluted to 1x TRIS using distilled water.

Table 9: Chemical reagents for TRIS buffer

Chemicals	Quantity
TRIS Base	60.5 g
Distilled water	1.7 l
NaCl	90 g
Hydrochloric acid	Until a pH = 7.6 is reached

7.12.4.3. CD68 and SMA IHC staining

Each tissue sample slide was stained for the antigens CD68 and α-SMA according to protocol, illustrated in Table 10. The antibody dilutions are presented in Table 11. Prior to IHC staining, the tissue slides were incubated at 56°C for 20 minutes. Afterwards, the stained slides were sealed with Eukitt Quick-hardening mounting medium and a coverslip and stored at room temperature.

Table 10: IHC CD68 and SMA staining protocol

Method	Incubation period
1. Incubation of slides at 56°C	20 min
2. Deparaffination:	
Xylene	2 x 10 min
Isopropanol	2 x 5 min
Ethanol 96%	1 x 5 min
Ethanol 70%	1 x 5 min
Distilled water	5 min
3. Preparation of citrate buffer: Addition of 4.2 g citric acid monohydrate to 2 l of distilled water and calibration of pH = 6.0 with a pH meter using NaOH	
4. Cooking of slides in the pressure cooker with citrate buffer	7 min
5. Washing with 1x TRIS buffer	1 x 2 min

6. Blocking: 50 ml distilled water and 1.5 ml hydrogen peroxidase 30%	15 min
7. Washing with 1x TRIS buffer	3 x 2 min
8. Preparation of blocking solution: 5 % milk (0.25 g milk powder per 5 ml antibody-diluent)	
9. Pipetting of 100 µl of blocking solution on each microscope slide	1 h
10. Washing with 1x TRIS buffer	1 x 1 min
11. Dilution of the primary antibody with antibody-diluent	
12. Pipetting of 100 µl primary antibody-dilution per microscope slide	25 min
13. Washing with 1x TRIS buffer	3 x 2 min
14. Addition of 2-3 drops of secondary biotinylated antibody per microscope slide	25 min
15. Washing with 1x TRIS buffer	3 x 2 min
16. Addition 2-3 drops of streptavidin peroxidase per microscope slide	25 min
17. Washing with 1x TRIS buffer	3 x 2 min
18. Preparation of 1:50 mixture of DAB and HRP substrate buffer and addition of 100 µl per microscope slide	5 min
19. Washing with 1x TRIS buffer	3 x 2 min
20. Haematoxylin staining	20 s
21. Washing with distilled water	1 min
22. Dehydration:	
Ethanol 70%	3 min
Ethanol 96%	3 min
Isopropanol	3 min
Xylene	3 min
23. Mounting and sealing with a coverslip	

Table 11: IHC antibody dilutions

Primary Antibody	Dilution with Antibody Diluent
Monoclonal Mouse Anti-Human CD68 Clone KP1	1: 1000
Monoclonal Mouse Anti-Human Muscle Actin	1: 500

7.13. Phalloidin VSMC staining

For immunofluorescence VSMC staining, the VSMCs were washed with PBS and detached from the cell culture flasks using 2 ml of trypsin enzyme previously warmed to 37°C. Trypsin was neutralised, and the cells were resuspended in 5-10 ml SMC growth medium. The proceeding cell suspension was centrifuged at 1000 rpm, 400 xg for 5 min. Subsequently, the cell pellet was resuspended in SMC growth medium; the cells were counted using a Neubauer chamber. The suspension was diluted to a concentration of 50 000 cells/ ml and seeded into a 4-well-chamber plate, where 1 ml cell suspension and 1 ml medium were added to each well. The 4-well plate was incubated at 37°C, 5% CO_2 for 1 day. After 24 hours, the medium was aspirated from the wells, and the cells were washed twice with PBS. For fixation, 1 ml of PBS with 4% paraformaldehyde (PFA) was added to each well for 15 minutes. After aspirating the fixating medium and 3 washes with PBS, the VSMCs were stained according to the protocol in Table 12.

Table 12: Phalloidin VSMC staining protocol

Phalloidin VSMC Staining Protocol
1. Preparation of blocking solution: 5% bovine serum albumin (BSA) and 0,3% Triton X 100 in PBS
2. Addition of 400 µl of the blocking solution to each chamber
3. Incubation of 4-well plate at 22°C (room temperature) for 30 min
4. Washing with PBS for 5 min
5. Preparation of antibody solution: 1% BSA and 0,3% Triton X 100 in PBS
6. Preparation of 1:80 green phalloidin dilution with antibody solution: 10 µl green phalloidin + 800 µl antibody solution
7. Addition of 200 µl per chamber

8. Incubation of 4-well plate at 22°C (room temperature) for 30 min in the dark
9. Washing with PBS for 3 x 5 min: 400 µl PBS per well
10. Mounting with Prolong Gold antifade reagent with DAPI
11. Sealing of coverslip with clear lacquer and storage at 4°C

7.14. Histology image processing

The histology image processing and measuring of fibrous cap thickness were performed using the Aperio ImageScope software version 12.3.3.5048 for Windows.

7.15. Live-cell imaging

Live-cell imaging is a technique for the direct visualisation of cell morphology and function, previously only determined indirectly through gene expression patterns. The study population consisted of the following VSMC samples: patient-derived VSMCs from stable, unstable and ruptured carotid artery plaques and VSMCs from healthy donor human carotid arteries (*n=4*). These groups were established to assess cell behaviour in early and end-stage atherosclerosis. Using two different experiments, VSMC migration and proliferation activity were analysed separately for 48 hours each. Real-time image analysis and kinetic measurements were completed using the IncuCyte® Software.

7.15.1. Migration assay

IncuCyte® Scratch Wound Assay analyses the invasion and migration behaviour of cells. For this experiment, a 96-well ImageLock EssenBioscience plate was used. Before cell seeding, the plate was coated with a layer of biomatrix (50 µl/ well).

On day 0, a cell-stock solution of 120 000 cells/ ml was generated. Then, 100 µl of the solution was pipetted in each well, creating a concentration of 12 000 cells/ well, correlating to a 90-100% cell confluency. Six technical replicate wells were seeded for each group of VSMCs. The plate was placed inside the incubator at 25°C, 5% CO_2 for 15 min to ensure equal cell settling and incubated overnight at 37°C, 5% CO_2.

On day 1, the IncuCyte® WoundMaker was used to construct identical wound scratches in each well. Empty wells were filled with PBS not to damage the WoundMaker pins. After creating the wound, the medium was immediately aspirated from each well, and the cells were washed twice using 100 µl/ well PBS. Subsequently, 100 µl of SMC growth medium was added to each well. After microscopically ensuring scratch success, the 96-well ImageLock plate was placed inside the IncuCyte® live-cell analysis system. The experiment was terminated after 48 hrs (day 2). The system settings are presented in Table 13.

Table 13: IncuCyte® live-cell analysis system settings for scratch-wound assay

Settings	Conditions
Objective	10x
Channel selection	Phase-contrast
Scan type	Scratch Wound
Scan interval	Every 2 hours
Photos per well	2
Total time observed	48 hours

7.15.2. Proliferation assay

To explore cell proliferation behaviour, the IncuCyte® Cell Proliferation Assay was implemented. On day 0, a 20 000 cells/ ml cell-stock solution was created. Next, 100 µl of the cell solution was pipetted in each well of a 96-well flat-bottom-plate, generating a concentration of 2 000 cells/ well. This concentration coincides with a cell confluency of 10-20%. Six technical replicate wells were seeded for each group of VSMCs. Following cell seeding, the plate was placed inside the incubator at 25°C, 5% CO_2 for 15 min to ensure equal cell settling and incubated overnight at 37°C, 5% CO_2.

On day 1, the plate was placed inside the IncuCyte®. Then, using the IncuCyte® Software, the “proliferation assay” program was run for 48 hours. The system settings are displayed in Table 14. During this time, the data was collected for analysis using the integrated confluence algorithm.

Table 14: IncuCyte® live-cell analysis system settings for proliferation assay

Settings	Conditions
Objective	10x
Channel selection	Phase-contrast
Scan type	Standard
Scan interval	Every 2 hours
Photos per well	2
Total time observed	48 hours

7.16. Statistical analysis

Statistical analysis was performed using SPSS for macOS Version 26.0 (SPSS Inc., Chicago, IL, USA). GraphPad Prism Version 8.3.1 (332) for macOS was used to generate statistical figures. The differences between delta CT, delta-delta CT and fold change values of gene expression between VSMCs from stable, unstable, ruptured or healthy control carotid arteries were evaluated using non-parametric tests for non-normal distributed data: Mann-Whitney-U- and Kruskal-Wallis-Tests. VSMC migration behaviour was analysed by relative wound density calculation (in per cent) per hour registered. The comparison of relative wound density between the four groups of VSMCs was interpreted using a Two-Way-ANOVA analysis for significant differences in the groups. Furthermore, proliferation behaviour was defined by the phase object confluence; significant differences in the four groups were determined using a Two-Way-ANOVA test. A p-value of <0.05 was identified as statistically significant. The level of statistical significance was displayed using the asterisks notation in Table 15.

Table 15: Notation of statistical significance

P-Value	Implication	Notation
< 0.0001	Extremely significant	****
0.0001 - 0.001	Extremely significant	***
0.001 - 0.01	Very significant	**

0.01 – 0.05	Significant	*
≥ 0.05	Not significant	ns

8. Results

8.1. Study population

Human carotid endarterectomy specimens were collected from 18 patients from September 2018 until June 2019. The patient collective consisted of 6 female and 12 male patients aged 64-85. The degree of stenosis ranged from 50-70%. The collected clinical patient data is summarised in Table 16.

Table 16: Clinical characteristics of the patient collective

Patient Number	Gender	Age (years)	Neurological Symptoms	Degree of Stenosis	Location of stenosis (Internal carotid artery)
1	Female	75	Asymptomatic	70%	Right
2	Female	68	Symptomatic	80%	Right
3	Male	78	Asymptomatic	80%	Right
4	Male	72	Symptomatic	80%	Right
5	Female	78	Asymptomatic	90%	Left
6	Male	74	Symptomatic	80%	Right
7	Male	78	Asymptomatic	80%	Right
8	Female	69	Asymptomatic	75%	Right
9	Male	74	Asymptomatic	80%	Right
10	Male	76	Asymptomatic	70%	Right
11	Male	76	Asymptomatic	85%	Right
12	Male	78	Asymptomatic	90%	Right
13	Male	80	Asymptomatic	90%	Right
14	Male	68	Symptomatic	90%	Right

15	Female	85	Symptomatic	80%	Right
16	Male	78	Asymptomatic	90%	Right
17	Male	74	Symptomatic	70%	Left
18	Female	80	Symptomatic	50%	Left

8.2. Histological carotid lesion classification

For patient sample classification, plaque stability was assessed. By inspection of fibrous cap thickness and presence of intimal rupture, the atherosclerotic lesions were divided into stable, unstable or ruptured carotid plaques (Redgrave et al., 2008). Additionally, the lesions were categorised in agreement with the American Heart Association (AHA) classification of atherosclerotic lesions illustrated in Figure 6 (Stary et al., 1995).

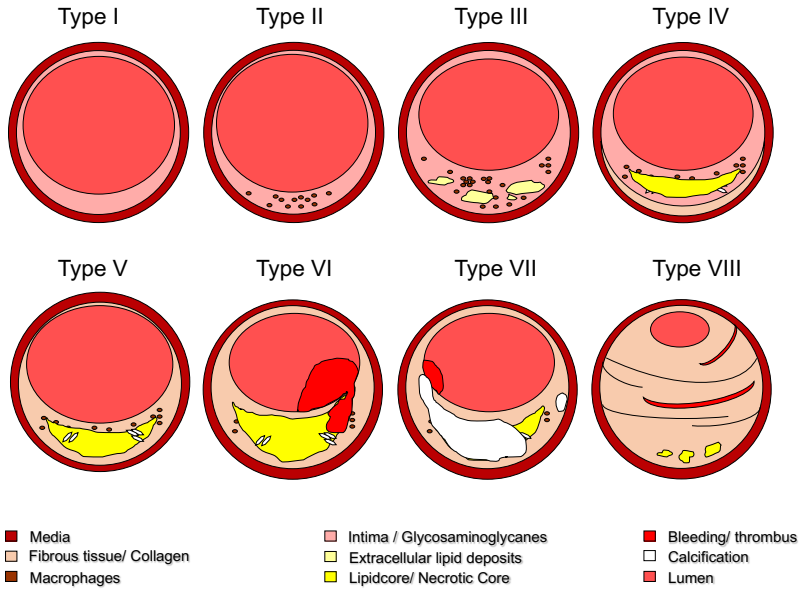

Figure 6: Schematic representation of the American Heart Association (AHA) classification of atherosclerotic lesions (modified from Pelisek et al., 2019).

Type I lesions or initial lesions contain isolated macrophage foam cells. Type II lesions or fatty streaks are composed of an accumulation of foam cells and intracellular lipids. Type III lesions are called intermediate lesions or pre-atheroma, which, in addition to type II plaques, contain extracellular lipid accumulations. Type IV lesions are atheromas marked by an absent fibrotic layer and an extracellular lipid core. Type V lesions are called fibroatheromas, characterised by a lipid core and fibrotic layer: the fibrous cap. From type VI onwards, the lesions are classified as complex lesions. Type VI lesions

additionally exhibit thrombus formation with or without intraplaque haemorrhage. Type VII lesions are type V lesions with the addition of calcified tissue. Lastly, type VIII lesions are fibrotic lesions with a small lumen and no lipid core. (Stary, 2000; Stary et al., 1995; Stary et al., 1994)

The carotid lesions were histologically classified using HE and EvG staining. Figure 7 presents samples of stable, unstable and ruptured carotid lesion EvG staining, with a focus on the rupture-prone shoulder region of the lesion and the fibrous cap thickness.

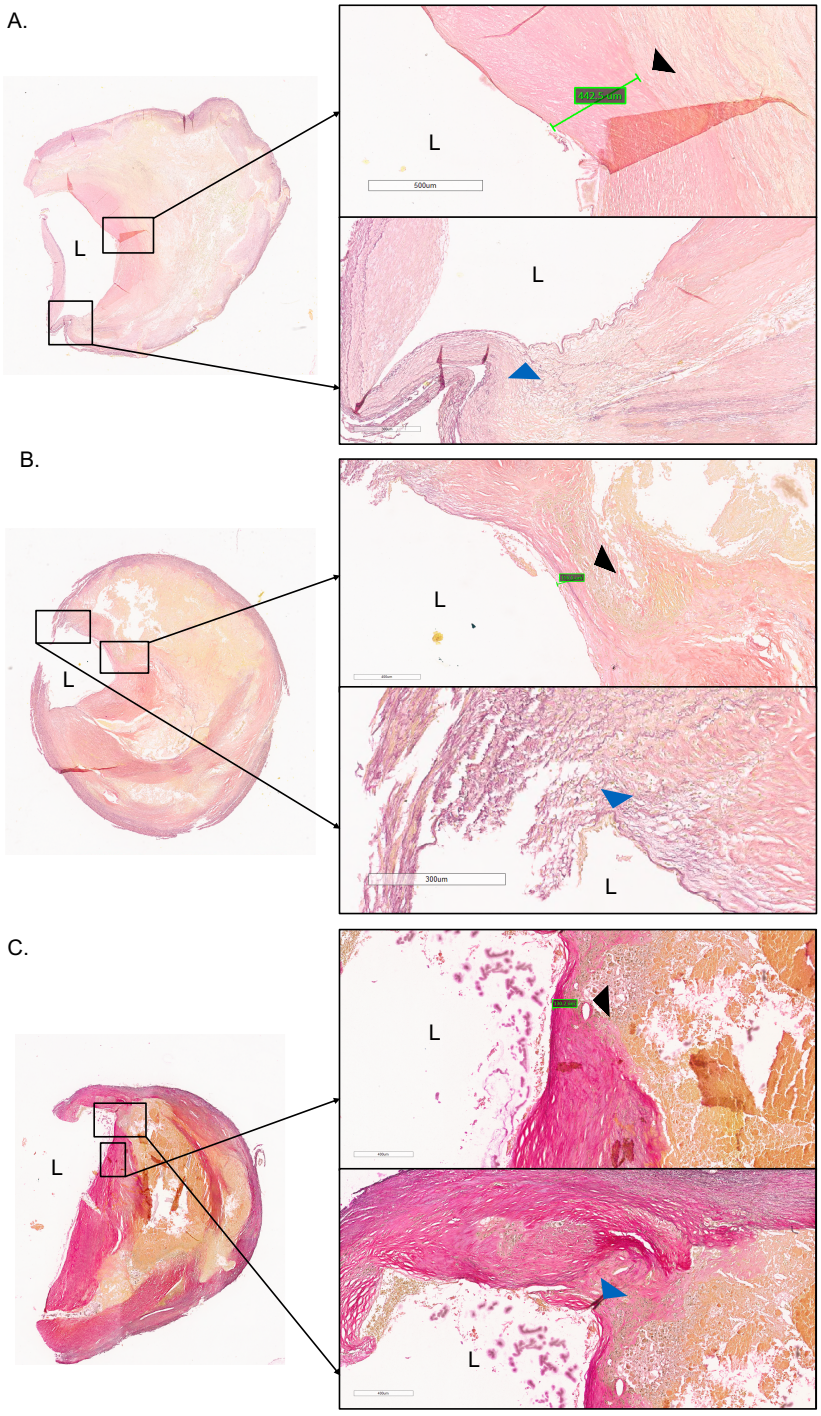

Figure 7: Histological characterisation of carotid lesions by Elastica van Gieson staining.

These images represent examples of the histological characterisation of the carotid lesion samples. The black indicator (►) displays the fibrous cap thickness measurement using Aperio Image Scope; the blue indicator (►) highlights the rupture-prone plaque shoulder region. (L) shows the area of the arterial lumen. (A.) depicts a stable, (B.) an unstable, and (C.) a ruptured carotid lesion.

From the 18 collected patient samples, *n=5* lesions were classified as stable and *n=13* as unstable. Two unstable lesions presented with a ruptured intima, substantiating the hypothesis that unstable lesions are more rupture-prone than stable lesions. According to the AHA classification, the lesions ranged from type III to VII. The most abundant lesion type was type VII (*n=9*), followed by type VI (*n=7*). Table 17 outlines the results of the histological classification.

Table 17: Patient sample histological classification

Patient Number	Stability	Rupture	AHA Type	Lesion
1	unstable	no	III	
2	unstable	no	VII	
3	unstable	no	VI	
4	unstable	no	VI	
5	stable	no	VI	
6	unstable	yes	VI	
7	stable	no	V	
8	unstable	no	VII	
9	unstable	no	VII	
10	unstable	no	VI	
11	stable	no	VII	
12	unstable	no	VI	
13	stable	no	VII	
14	unstable	no	VII	

15	stable	no	VII
16	unstable	yes	VII
17	unstable	no	VII
18	unstable	no	VI

8.3. Immunohistochemistry

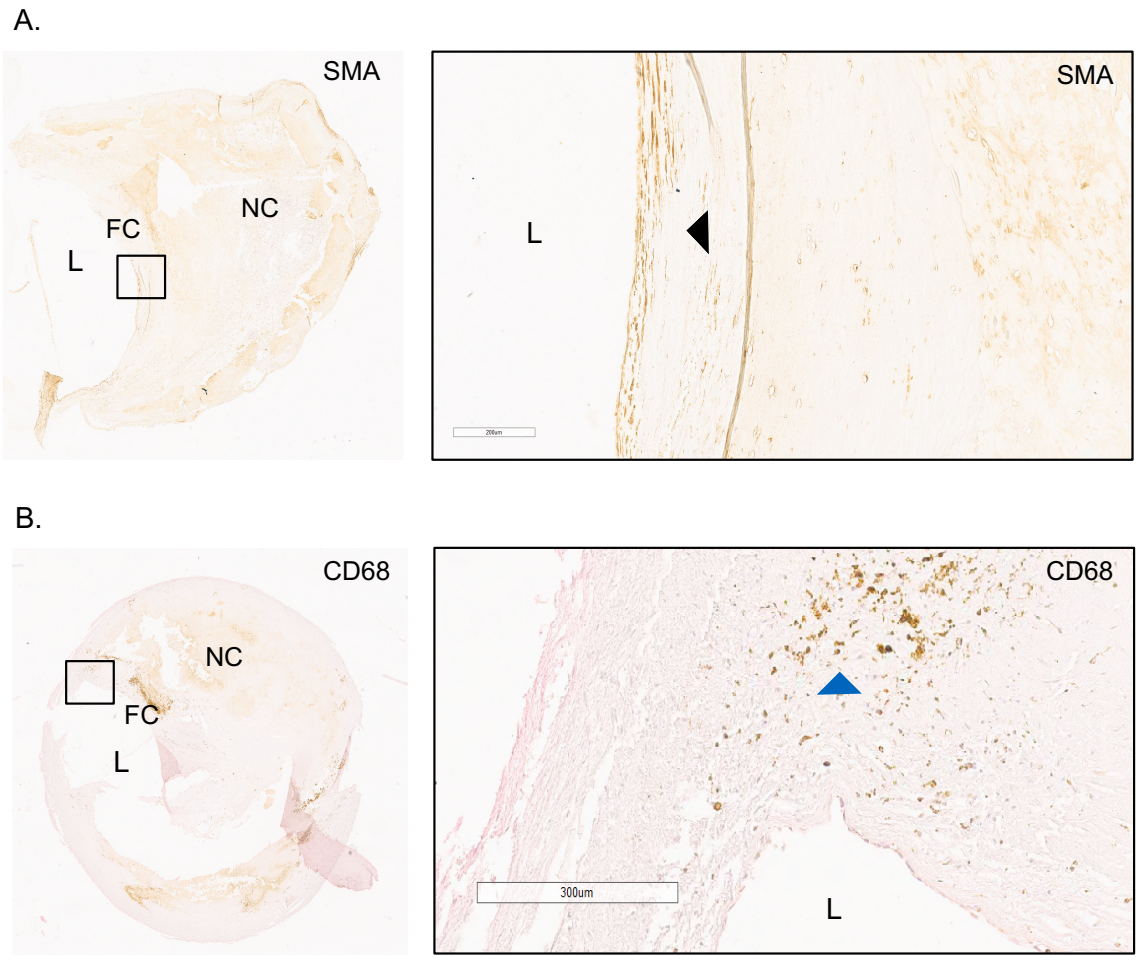

Figure 8: Immunohistochemistry: SMA and CD68 staining of carotid lesion samples.
(A.) α-SMA+ cells were present in the media and intima of the stained carotid lesion. The black indicator (►) points towards α-SMA+ cells. (B.) CD68+ cells were detected in the lesions' necrotic core and the shoulder region. The blue indicator (►) highlights the CD68+ cells. (L) Lumen, (NC) Necrotic core, (FC) Fibrous cap.

Anti-SMA and anti-CD68 immuno-expression was performed on the human carotid lesion samples. α-SMA is expressed by VSMCs, myofibroblasts and myoepithelial

cells (Frangogiannis et al., 2000; Skalli et al., 1986). Studies have further revealed α-SMA expression induction in monocyte-derived macrophages in atherosclerotic lesions (Martin et al., 2009; Stewart et al., 2009). The IHC staining displayed a presence of α-SMA+ cells in the media and neointima of the carotid lesions, as seen in Figure 8. Subsequently, α-SMA+ cells were presumed to be either of VSMC- or macrophage-origin.

CD68 is a transmembrane glycoprotein expressed by the monocyte and macrophage cell line (Holness et al., 1993). Prior research concluded that VSMCs in atherosclerosis acquire an inflammatory phenotype with simultaneous CD68 expression (Albarran-Juarez et al., 2016; Andreeva et al., 1997b). Therefore, the marker was employed to identify inflammatory active regions of the lesion. IHC staining in Figure 8 highlights the abundance of CD68+ cells in the necrotic core and the shoulder region of the plaque.

8.4. VSMC phalloidin staining

Using Phalloidin staining, we morphologically confirmed the isolation of primary VSMCs. Figure 9 illustrates the fluorescent green staining of the actin filaments in the cytoskeleton of the patient-derived VSMCs, with a blue DAPI co-stain of the nuclei. Consequently, we could substantiate that the experiments throughout this investigation involving gene expression and live-cell imaging were solely performed on VSMCs and not inflammatory cells.

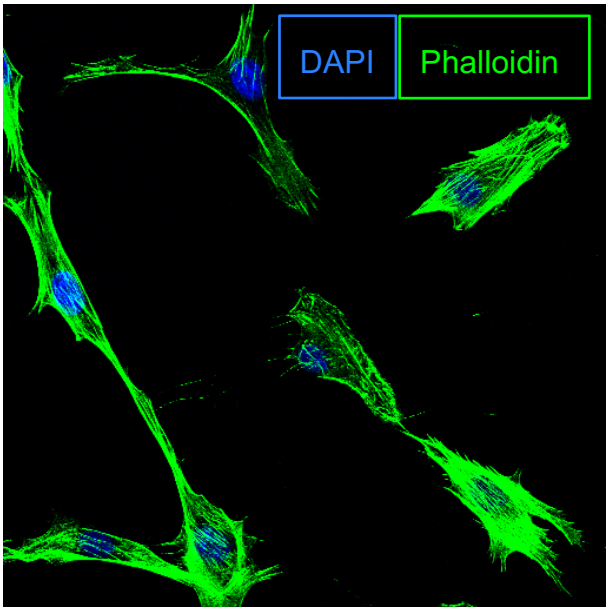

Figure 9: Fluorescence phalloidin and DAPI staining of isolated VSMCs using confocal microscopy.

Isolation confirmation of VSMCs with immunofluorescence staining was performed using a confocal microscope. The phalloidin (green) staining represents the actin filaments in the cytoskeleton of VSMCs, illuminating their fusiform structure. DAPI (blue) was used to stain DNA and display the cells' nuclei.

8.5. RNA isolation quantification

RNA was isolated from the cultured cells and the quantity was measured for each carotid specimen using a Nanodrop 2000x spectrophotometer previously tared to 0 ng/ µl with RNAse-free water. The results are presented in Table 18.

Table 18: Concentration and quantification of RNA samples using Nanodrop

Patient Number	RNA Concentration (ng/ µl)
1	247.3
2	255.0
3	389.1
4	48.1
5	128.7
6	297.3
7	53.3
8	236.3
9	185.1
10	306.8
11	271.6
12	114.5
13	135.9
14	332.1

15	377.1
16	156.6
17	212.7
18	296.0
Healthy human carotid VSMCs	335.6

8.6. Gene expression of VSMCs

RT-qPCR analysis on the cDNA was performed using the primers listed in Table 19. Apart from two housekeeping genes, the following primer pairs were chosen to identify contractile VSMCs: α-SMA, TAGLN and SMTN. Additionally, primer pairs for genes overly expressed in inflammatory cells, such as monocytes and macrophages, were selected: CD68 and LGALS3. To locate synthetic VSMCs, the primers VCAN, COL1A1 and COL3A1 were employed. As previously mentioned, MYOCD is a transcription factor which triggers the expression of contractile genes (Pipes et al., 2006). The transcription factor KLF4 was used to identify phenotypically switched VSMCs (Shankman et al., 2015). The growth factor PDGF-β is a marker for VSMC proliferation and migration (Dandre et al., 2004).

Table 19: Primers used for gene expression panel with known functions of the gene product

TaqMan™ Assay Primer	Gene Product	Marker/ Function
RPLP0	Ribosomal protein lateral stalk subunit P0	Housekeeping gene
GAPDH	Glycerinaldehyd-3-phosphate-dehydrogenase	Housekeeping gene
α-SMA	Smooth muscle alpha actin 2	Contractile phenotype, vascular blood pressure homeostasis
VCAN	Versican	Synthetic phenotype, proteoglycan

PDGF-β	Platelet-derived growth factor-β	Development of VSMCs, ECs and fibroblasts, growth factor influencing migration and proliferation
COL1A1	Pro-alpha 1 chain of collagen type I	Synthetic phenotype
COL3A1	Collagen type III	Synthetic phenotype
CD68	Cluster of differentiation 68	Inflammatory phenotype
LGALS3	Galectin-3	Inflammatory phenotype
TAGLN	Transgelin	Early VSMC differentiation marker
SMTN	Smoothelin	Contractile phenotype
MYOCD	Myocardin	Transcription factor, SMC lineage differentiation
KLF4	Kruppel-like factor 4	Transcription factor, marker for phenotypic switching

Consequently, the phenotypical state of the isolated VSMCs was assessed using the gene panel outlined in Table 19. The CT values calculated by the RT-qPCR were normalised to RPLP0 and compared to the values of healthy carotid VSMCs. The expression patterns in symptomatic to asymptomatic patients were compared by examining the fold change. Furthermore, the gene expression of VSMCs derived from carotid lesions histologically classified as either stable, unstable or ruptured was measured to explore the phenotype at different stages of atherosclerosis.

8.6.1. Asymptomatic vs symptomatic patients

Firstly, the gene expression differences between asymptomatic vs symptomatic patients were examined. The results are presented in Figure 10 and 11.

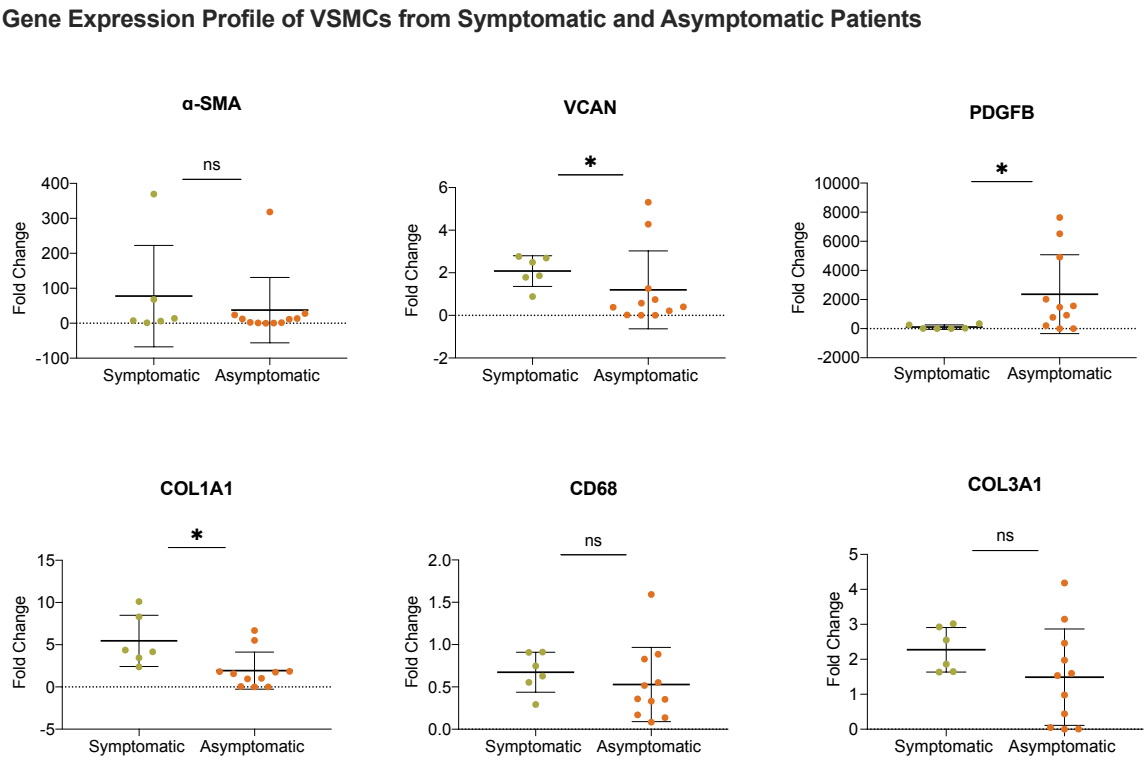

Figure 10: Gene expression panel of VSMCs derived from symptomatic vs asymptomatic patients, normalised to RPLP0, and compared to healthy carotid VSMCs.

Smooth muscle alpha actin 2 (α-SMA); Versican (VCAN); Platelet-derived growth factor-β (PDGFB); Collagen type I (COL1A1); Cluster of differentiation 68 (CD68); Collagen type III (COL3A1). Expression data is represented as mean ±SD. *$p<0.05$, **$p<0.01$, ***$p<0.001$, ****$p<0.0001$, ns: non-significant.

The expression of VCAN was significantly upregulated *(p=0.044)* in symptomatic vs asymptomatic patients, highlighting the augmented synthesis of versican in patients with neurological symptoms. Both patient groups displayed a 74-fold and 79-fold increase, respectively. Similarly, COL1A1 was expressed significantly higher *(p=0.012)* in symptomatic patients compared to asymptomatic patients, as was COL3A1, though not significantly *(p=0.132)*. These results concur with the increased expression of VCAN in symptomatic patients.

A significantly increased expression of PDGFB in asymptomatic patients *(p=0.035)* was detected, indicating a higher level of growth factors synthesised by VSMCs in asymptomatic patients. VSMCs of symptomatic patients showed a 33-fold expression increase, while those of asymptomatic patients displayed a 120-fold increase.

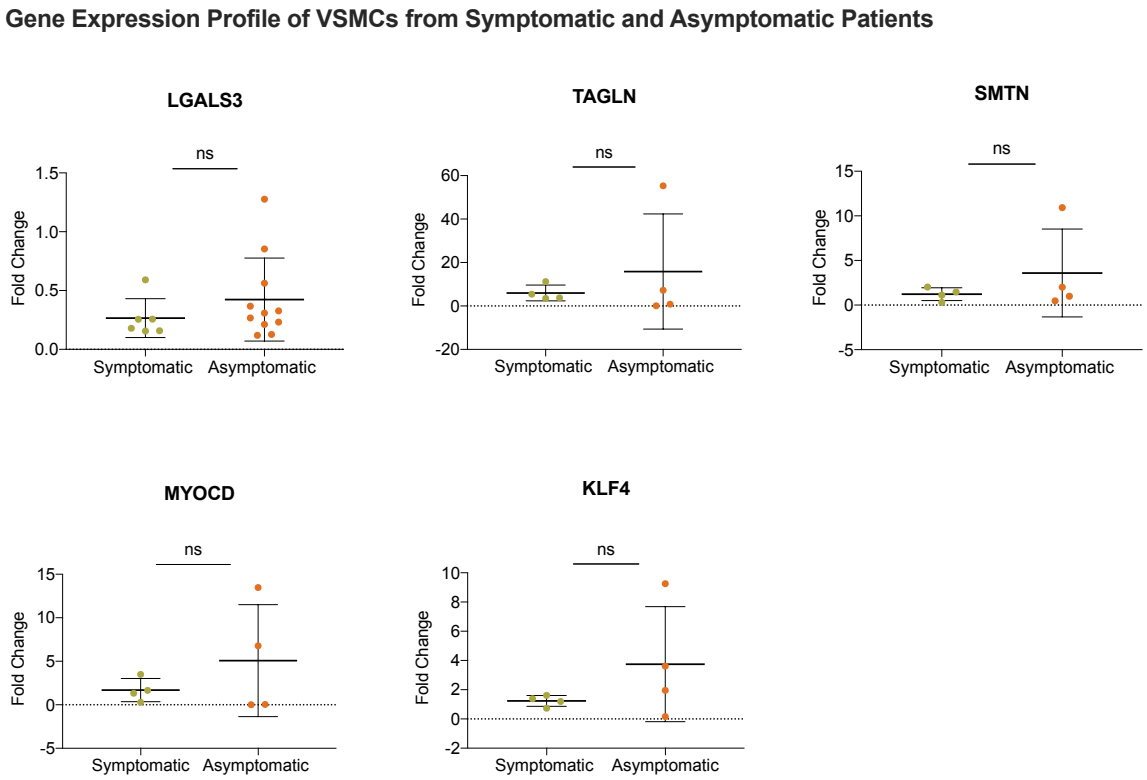

Figure 11: Gene expression panel of VSMCs derived from symptomatic vs asymptomatic patients, normalised to RPLP0, and compared to healthy carotid VSMCs.

Galectin-3 (LGALS3); Transgelin (TAGLN); Smoothelin (SMTN); Myocardin (MYOCD); Kruppel-like factor 4 (KLF4). Expression data is represented as mean ±SD. *$p<0.05$, **$p<0.01$, ***$p<0.001$, ****$p<0.0001$, ns: non-significant.

No significant difference in α-SMA expression was evident between the patient groups (*p=0.404*); the results depicted a 90-fold increase in symptomatic patients and a 63-fold increase in asymptomatic patients compared to normal healthy VSMCs. Moreover, symptomatic patient samples exhibited an increased CD68 expression, however non-significantly *(p=0.159).* Unfortunately, LGALS3, TAGLN, SMTN, MYOCD and KLF4 expression showed no significant differences between symptomatic and asymptomatic patients.

8.6.2. Stable vs unstable vs ruptured carotid lesions

Additionally, the gene expression of VSMCs derived from unstable, stable and ruptured carotid lesions was examined. The results of the RT-qPCR are featured in Figure 12 and 13.

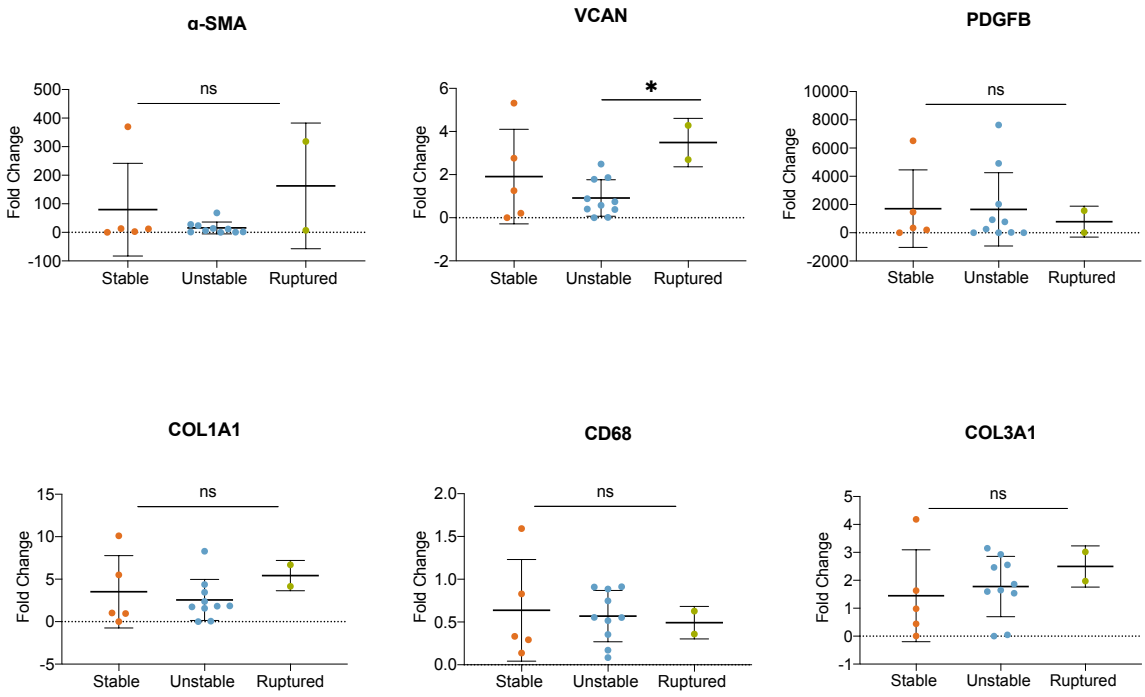

Figure 12: Gene expression panel of VSMCs derived from carotid lesions classified as stable, unstable or ruptured, normalised to RPLP0, and compared to healthy carotid VSMCs.

Smooth muscle alpha actin 2 (α-SMA); Versican (VCAN); Platelet-derived growth factor-β (PDGFB); Collagen type I (COL1A1); Cluster of differentiation 68 (CD68); Collagen type III (COL3A1). Expression data is represented as mean ±SD. *$p<0.05$, **$p<0.01$, ***$p<0.001$, ****$p<0.0001$, ns: non-significant.

The expression of VCAN was significantly higher in VSMCs derived from ruptured compared to unstable lesions ($p=0.032$). Similarly, ruptured lesions displayed a higher expression of COL1A1 and COL3A1 than the non-ruptured lesions ($p=0.180$ and $p=0.233$, respectively); these results substantiate the hypothesis of active vascular reconstruction by VSMCs in ruptured lesions.

Additionally, the inflammatory marker LGALS3 was upregulated in unstable lesions vs ruptured lesions, yet not significantly ($p=0.197$). The expression of CD68 showed no significant differences between the groups.

Furthermore, the results indicated a 90-fold upregulation in the gene expression of α-SMA in stable compared to unstable lesions: representation of a contractile phase in early atherosclerosis. This result correlates with the increased expression of MYOCD in stable vs unstable lesions, as the transcription factor MYOCD is a driver of the contractile phenotype in VSMCs ($p=0.275$).

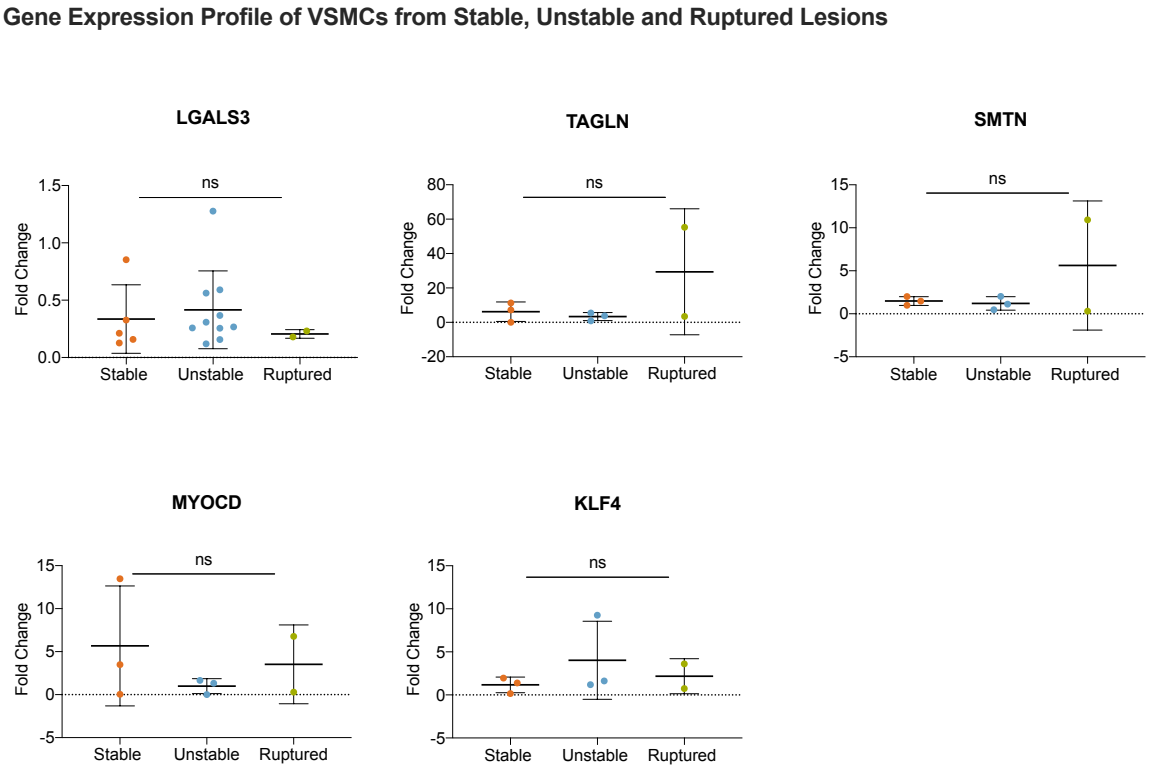

Figure 13: Gene expression panel of VSMCs derived from carotid lesions classified as stable, unstable or ruptured, normalised to RPLP0, and compared to healthy carotid VSMCs.

Galectin-3 (LGALS3); Transgelin (TAGLN); Smoothelin (SMTN); Myocardin (MYOCD); Kruppel-like factor 4 (KLF4). Expression data is represented as mean ±SD. *$p<0.05$, **$p<0.01$, ***$p<0.001$, ****$p<0.0001$, ns: non-significant.

8.7. Live-cell imaging analysis

8.7.1. Migration activity

Migratory behaviour in VSMCs was evaluated after implementing a standardised wound scratch. Using the IncuCyte® Zoom System, two images were captured every 2 hours from each well over 48 hours. In the data collected after 24 hours, solely the healthy human carotid VSMCs reached a relative wound confluence of 100%. After 48 hours, the VSMCs from stable and the healthy control reached a relative wound confluence of 100%. On the other hand, VSMCs from unstable and ruptured lesions demonstrated decreased migration activity, not reaching 100% wound confluency. Figure 14 represents sample images taken during the experiment with a computationally generated initial wound scratch mask.

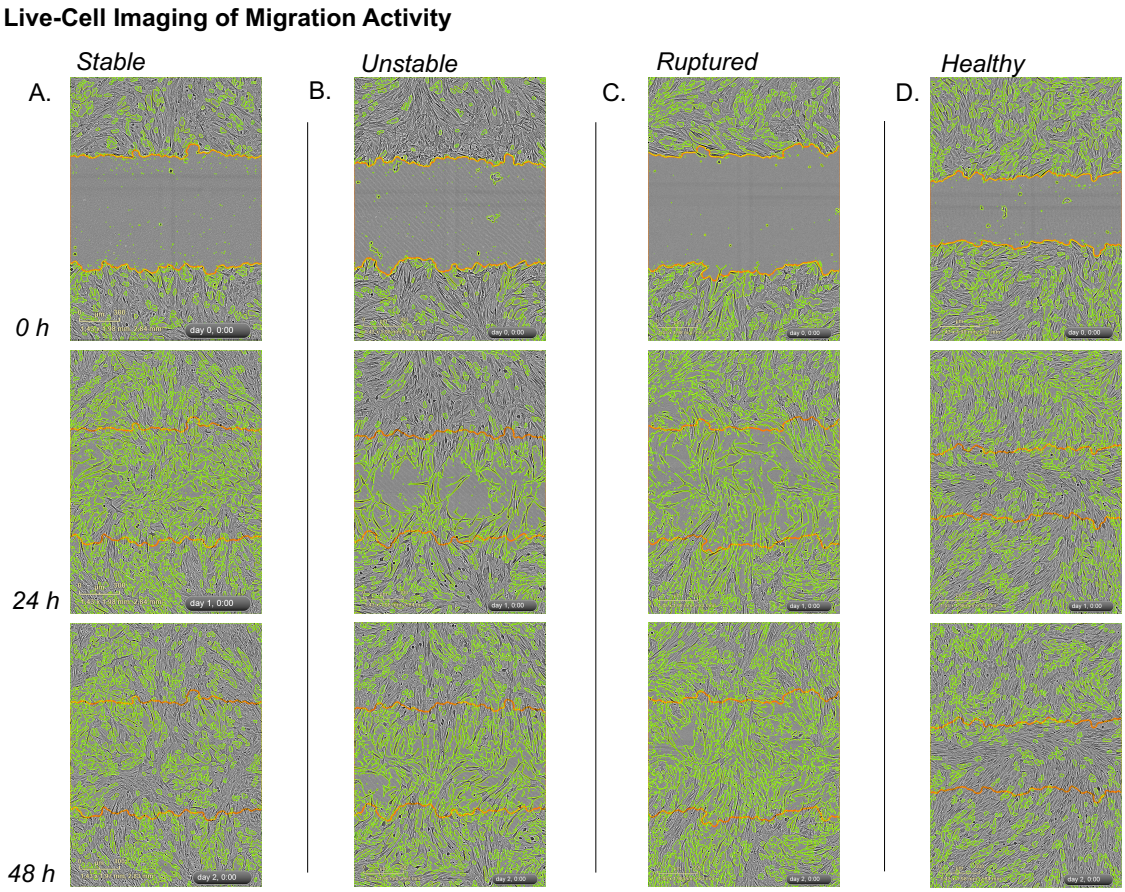

Figure 14: Migration live-cell imaging after wound scratch of patient-derived VSMCs captured with the IncuCyte Zoom System at 0, 24 and 48 hours.

VSMCs isolated from (A.) stable, (B.) unstable and (C.) ruptured carotid lesions, compared to (D.) healthy human carotid VSMCs, were examined over 48 hours. The orange line represents the initial wound scratch outline; the green colour outlines VSMCs for visibility.

The results of the IncuCyte® Scratch Wound Assay are presented in Figure 15, comparing the migratory behaviour of healthy carotid VSMCs to carotid lesion VSMCs (*n=4*). The statistical evaluation determined significant differences in the relative wound confluence of all samples. The p-values for healthy VSMCs vs stable, unstable and ruptured lesion-derived samples were *p=0,0382*, *p<0,0001* and *p=0.0004*, respectively.

Figure 16 depicts the results of the IncuCyte® Scratch Wound Assay measuring the migratory behaviour of VSMCs derived from stable, unstable and ruptured carotid lesions (*n=3*). The relative wound confluence digressed significantly between stable vs unstable lesions (*p<0.0001*), stable vs ruptured lesions (*p=0.0026*), and unstable vs ruptured lesions (*p=0.0026*).

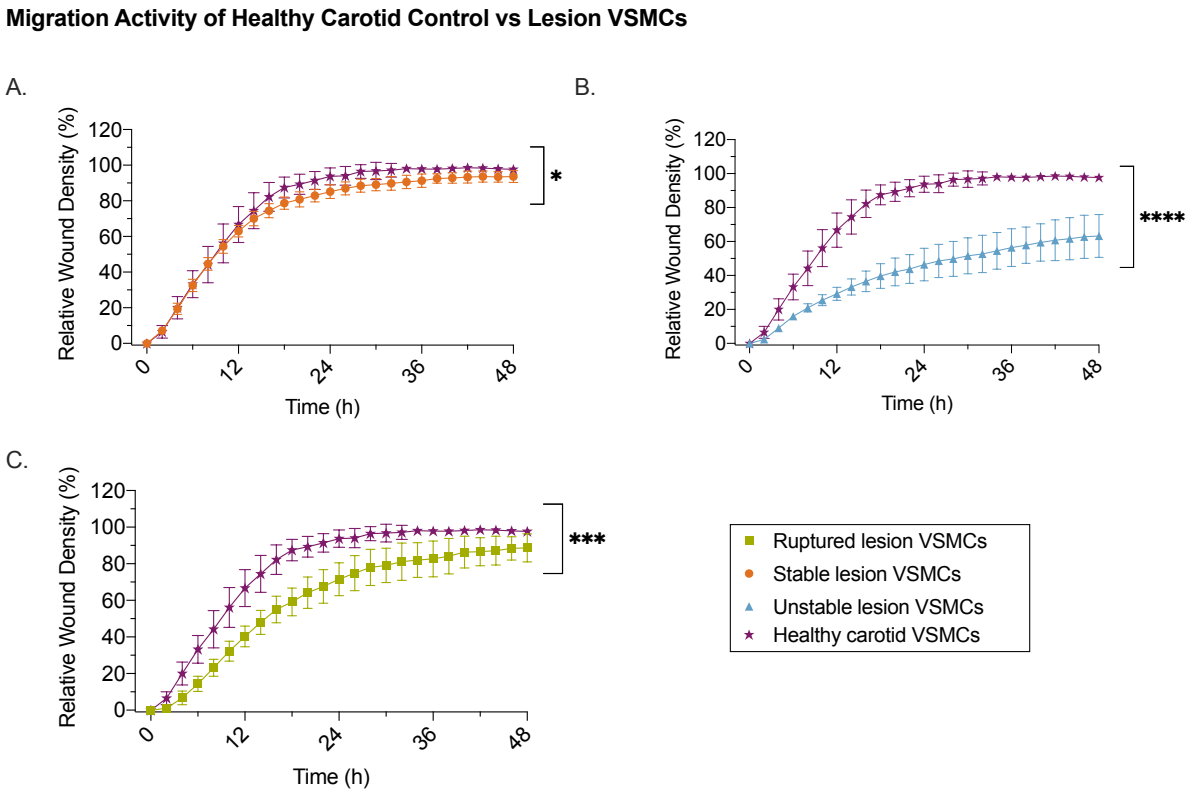

Figure 15: Migration behaviour comparison between healthy patient VSMCs and atherosclerotic VSMCs measured by the IncuCyte Zoom System every 2 hours.

★ (purple star): healthy carotid VSMCs; ● (orange dot): stable lesion VSMCs; ▲ (blue triangle): unstable lesion VSMCs; ■ (green square): ruptured lesion VSMCs. Statistical evaluation using Two-Way ANOVA in GraphPad Prism. The data is represented as mean ±SD. *$p<0.05$, **$p<0.01$, ***$p<0.001$, ****$p<0.0001$, ns: non-significant.

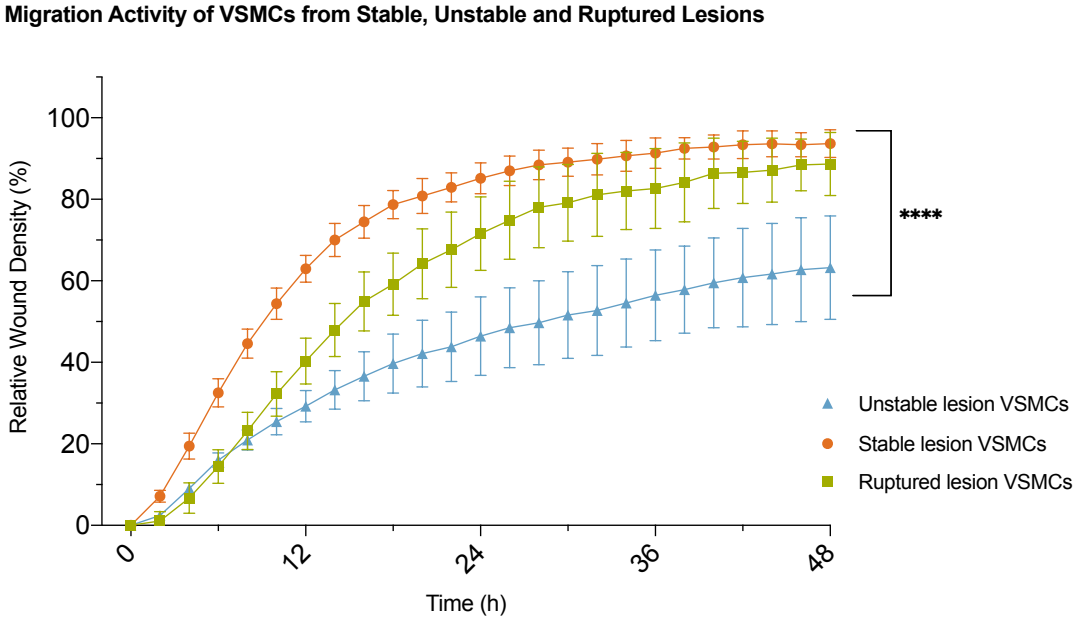

Figure 16: Migration behaviour comparison between stable, unstable and ruptured lesion-derived VSMCs measured by IncuCyte Zoom System every 2 hours.

● (orange dot): stable lesion VSMCs; ▲ (blue triangle): unstable lesion VSMCs; ■ (green square): ruptured lesion VSMCs. Statistical evaluation using Two-Way ANOVA in GraphPad Prism. The data is represented as mean ±SD. *$p<0.05$, **$p<0.01$, ***$p<0.001$, ****$p<0.0001$, ns: non-significant.

This investigation demonstrated a reduction in migratory effectiveness with the progression of CAD. Stable VSMC specimen displayed a migration behaviour similar to that of healthy donor cells. The unstable lesion cells exhibited the least migration ability, arriving at only 60% relative wound confluence after 48 hours. The ruptured sample behaved similarly to the stable example.

8.7.2. Proliferation activity

Proliferation behaviour was analysed using the IncuCyte® Zoom System after seeding the VSMCs at a 10-20% confluence ($n=4$). Two images were captured every 2 hours from each well over 48 hours, as displayed in Figure 17. VSMCs extracted from stable lesions attained a higher confluence after 48 hours than the other cells. Morphologically, the unstable and ruptured lesion-derived VSMCs displayed a loss in fusiform shape. Compared to the stable and healthy specimen, they acquired an epithelioid form and proliferated uncoordinatedly.

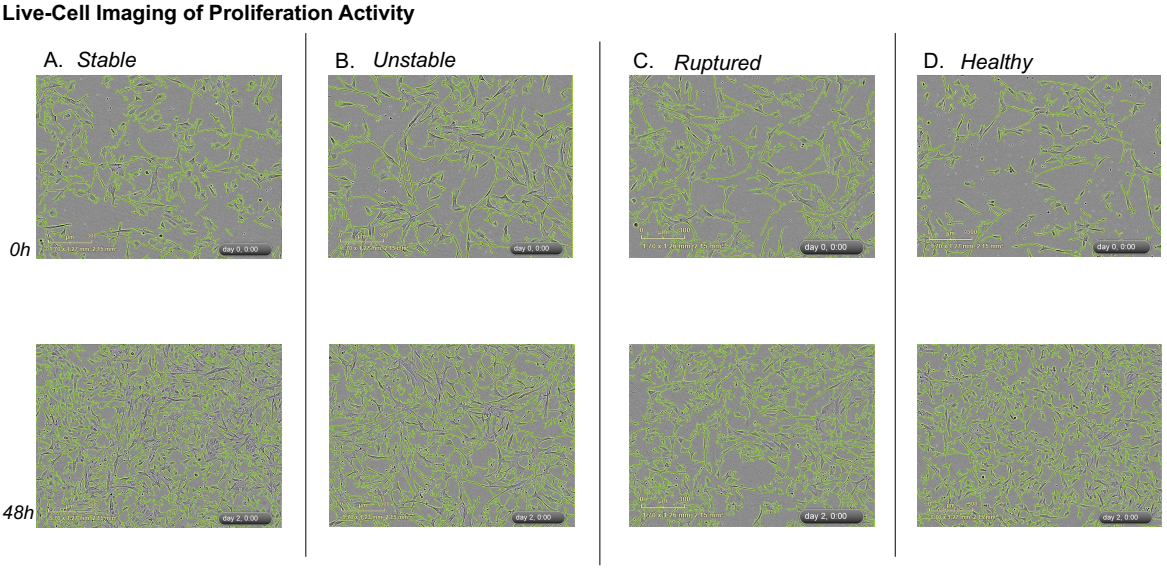

Figure 17: Proliferation live-cell imaging captured with the IncuCyte Zoom System of patient-derived VSMCs at 0 and 48 hours.

VSMCs derived from (A.) stable, (B.) unstable, and (C.) ruptured carotid lesions compared to (D.) healthy human carotid VSMCs, examined over 48 hrs. The green colour outlines VSMCs for visibility.

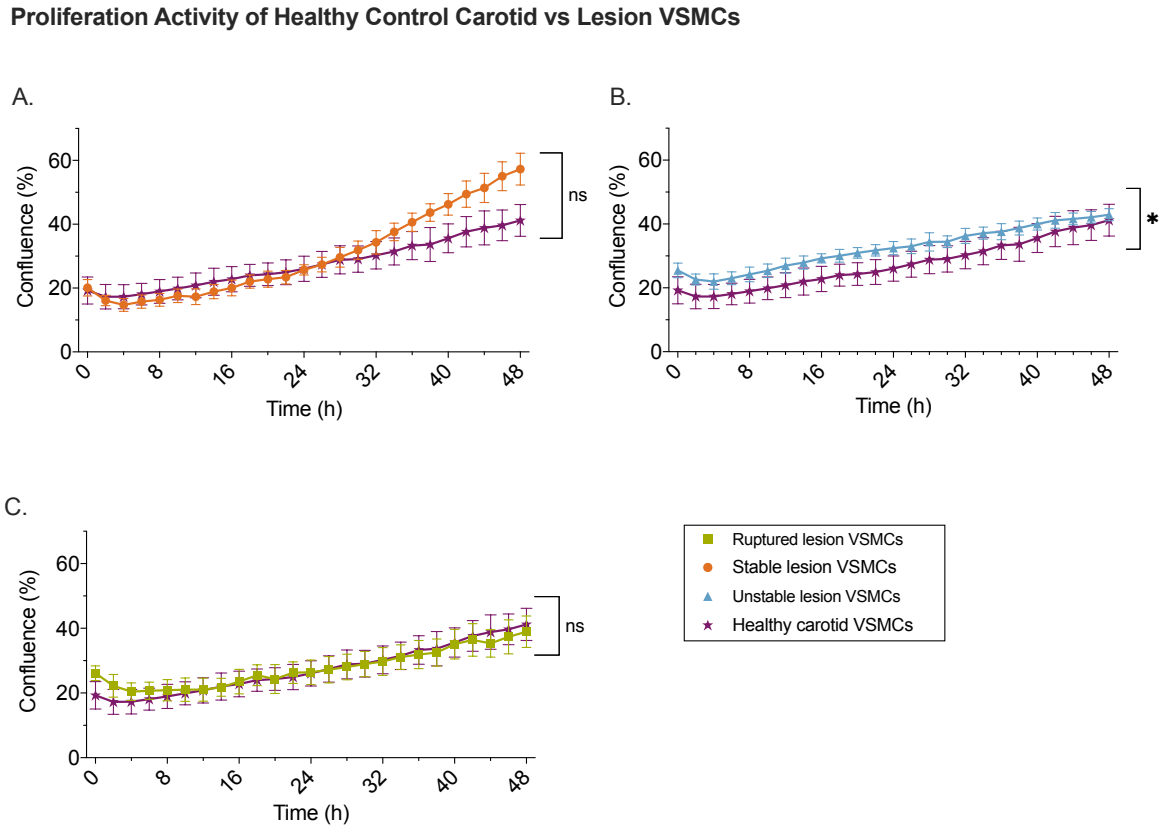

Figure 18: Proliferation behaviour comparison between healthy patient VSMCs and atherosclerotic VSMCs measured by the IncuCyte Zoom System every 2 hours.

★ (purple star): healthy carotid VSMCs; ● (orange dot): stable lesion VSMCs; ▲ (blue triangle): unstable lesion VSMCs; ■ (green square): ruptured lesion VSMCs. Statistical evaluation using Two-Way ANOVA in GraphPad Prism. The data is represented as mean ±SD. *$p<0.05$, **$p<0.01$, ***$p<0.001$, ****$p<0.0001$, ns: non-significant.

The results of the proliferation behaviour analysis are outlined in Figure 18 and 19. Healthy carotid VSMCs reached a maximum confluence of 46% after 48 hours. Stable lesion-derived VSMCs had higher proliferation rates and reached a maximum of 64%. VSMCs isolated from unstable and ruptured lesions reached a maximum confluence level of 45%, comparable to the healthy VSMCs. Significant differences in confluence percentage were evident between the healthy carotid VSMCs and those derived from unstable lesions ($p=0.0182$). Additionally, the investigation highlighted differences in the proliferation rate of stable and unstable VSMCs ($p=0.0991$). The statistical analysis also revealed a significant difference between VSMCs derived from ruptured vs unstable lesions ($p=0.0152$).

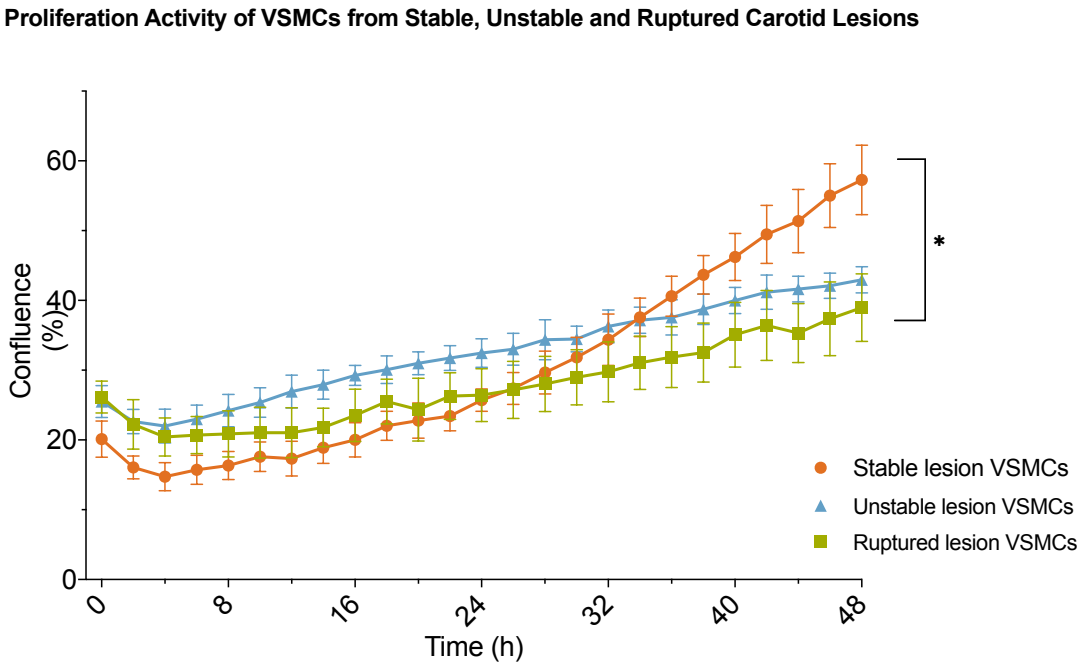

Figure 19: Proliferation behaviour comparison between stable, unstable and ruptured lesion-derived VSMCs measured by IncuCyte Zoom System.

● (orange dot): stable lesion VSMCs; ▲ (blue triangle): unstable lesion VSMCs; ■ (green square): ruptured lesion VSMCs. Statistical evaluation using Two-Way ANOVA in GraphPad Prism. The data is represented as mean ±SD. *$p<0.05$, **$p<0.01$, ***$p<0.001$, ****$p<0.0001$, ns: non-significant.

9. Discussion

9.1. Clinical relevance

CAD is a fatal disease and the most common cause of stroke worldwide. Recently, VSMCs have propelled to the forefront in atherosclerosis investigations; they are recognised as the most relevant players in the disease by retaining plasticity while fully differentiated (Basatemur et al., 2019).

9.2. Investigative results

9.2.1. Lesion classification interpretation

To examine VSMCs at different stages of the disease, carotid lesion samples were collected during CEA. According to Redgrave et al. (2008), plaque stability was determined by histological HE and EvG staining (Redgrave et al., 2008). Moreover, the plaques were categorised according to the AHA Classification (Stary et al., 1995). Most lesions were classified as type VII (*n=9*) (complex lesion with calcified tissues) and type VI (*n=6*) (complex lesions with thrombus formation or intraplaque haemorrhage). As expected, the carotid samples were mainly advanced atherosclerotic lesions, resulting from current ESC guidelines recommending interventional revascularisation in patients with stenosis ≥50% (Eckstein, 2018).

Immunohistochemistry anti-CD68 was performed on the carotid endarterectomy samples. IHC staining revealed the anticipated CD68+ cell infiltration in the shoulder region of the plaque. Lineage-tracing of atherosclerotic cells has highlighted CD68 expression in monocyte-derived macrophages and de-differentiated VSMCs (Albarran-Juarez et al., 2016; Andreeva et al., 1997b). Consequently, the marker CD68 only provides information about the present condition of the cell and not its origin (Albarran-Juarez et al., 2016; Feil et al., 2014; Vengrenyuk et al., 2015). Nevertheless, the presence of monocyte- and VSMC-derived-macrophages in the shoulder region substantiated evidence provided by previous studies, marking it as the plaque site most susceptible to rupture (Richardson et al., 1989; Virmani et al., 2000).

IHC staining accentuated α-SMA+ cells in the tunica intima and media of the ICA samples. The protein α-SMA is a significant component of the cytoskeletal constructional system and is highly expressed by VSMCs, myofibroblasts and myoepithelial cells (Frangogiannis et al., 2000; Skalli et al., 1986). Prior *in vitro* studies have suggested that macrophages and monocytes in atherosclerotic lesions are also capable of α-SMA expression, for instance, via thrombin stimulation (Martin et al., 2009; Stewart et al., 2009). However, endeavours to corroborate the phenomenon *in vivo* in mice or humans have been unsuccessful. These results further enhance the ambivalence concerning the ancestral origin of the cells active in atherosclerosis (Gomez et al., 2012). Hence, IHC α-SMA staining provided evidence of VSMCs or macrophage-derived VSMC-like cells in the intima; this affirms VSMC migration from the tunica media to the intima (Chappell et al., 2016; Shanahan et al., 1998).

9.2.2. Gene expression patterns

Gene expression differences of primary VSMCs from asymptomatic and symptomatic patients were investigated. Furthermore, the differences between VSMCs derived from stable, unstable and ruptured lesions were examined. The gene panel selected aimed to differentiate the possible phenotypical states of VSMCs presently validated (as highlighted in Figure 3). Preceding research has proven that VSMCs can express different phenotypes: contractile, inflammatory-like, synthetic and osteoblast-like (Andreeva et al., 1997a; Bobryshev, 2005; Chellan et al., 2018; Feil et al., 2014). These phenotypical switches are influenced by transcription factors, growth factors, environmental factors, extracellular lipoproteins and lipids, ECM components and haemodynamic influences (Holycross et al., 1992; Lee et al., 2001; Pidkovka et al., 2007; Pipes et al., 2006; Raines, 2000; Yoshida et al., 2013).

9.2.2.1. Synthetic gene expression patterns

In this investigation, VSMCs from symptomatic patients displayed a significant expression upregulation of VCAN compared to asymptomatic patients. Past studies have depicted versican as an atherogenic, lipid-retentive proteoglycan; versican's negatively charged side chain interacts with the positively charged LPs and thus facilitates the retention of LDL-LPs (Camejo et al., 1980; Chang et al., 2000).

Accordingly, a significant increase of COL1A1 expression in VSMCs of symptomatic patients was identified. RT-qPCR also highlighted an increased expression of COL3A1 in symptomatic patients, however non-significant. Collagen types I and III are the most common ECM elements of the fibrous cap (Shekhonin et al., 1987). The formation of the fibrous cap is a response of VSMCs to strengthen the intima as the necrotic core extends into the vessel lumen (Libby et al., 2011). Moreover, augmented collagen type I levels may be evidence of subclinical plaque ruptures (Mann et al., 1999). Burke et al. (2001) suggested that VSMCs regulate repair and reorganisation mechanisms in lesions with subclinical fissures (Burke et al., 2001). The results yielded indirect evidence that VSMCs synthesise a significantly greater quantity of ECM in symptomatic patients; this highlights the positive correlation between the grade of stenosis, advancement of vascular reconstruction and thus stroke occurrence (Clowes et al., 1982).

Furthermore, gene expression analysis distinguished variations in expression patterns between VSMCs derived from stable, unstable and ruptured plaques. A significantly increased expression of VCAN in ruptured compared to unstable lesions was demonstrated. Similarly, the comparison between unstable and ruptured lesions yielded an augmented expression rate of COL1A1 and COL3A1 in the latter. Consistent with the results in symptomatic patients, these results support the evidence of a significantly higher synthetic activity in ruptured lesions. As stated by Davies et al. (1992), the rupture of the fibrous cap is the most common precursor of the clinical sequelae of atherosclerosis, for example, stroke (M. J. Davies, 1992). The increased ECM synthesis of VSMCs contributes to our understanding of their role in late atherosclerosis: beneficial in preventing further rupture by vascular reconstruction. However, the remodelling may also be interpreted as a response to the advancing necrotic core and stenosis grade in the late stages.

9.2.2.2. Inflammatory gene expression patterns

Whilst examining inflammatory markers, this study outlined an increased expression of LGALS3 in stable and unstable lesions compared to ruptured lesions. These results indicate that, in early atherosclerosis, VSMCs adopt an inflammatory cell type state and thereby presumably employ a role in furthering plaque progression. The expression of CD68, unfortunately, showed no significant differences between the

three lesion groups. Nonetheless, the cells did demonstrate an increased CD68 fold change compared to healthy donor VSMCs, underlining the evidence of VSMC-derived macrophage-like cells in all atherosclerotic lesions (Allahverdian et al., 2014; Feil et al., 2014; Rong et al., 2003). The lack of expression differences between stable, unstable and ruptured lesion-derived VSMCs perhaps portrays a premature inflammatory activation already present in early-stage atherosclerosis.

9.2.2.3. Migration- and proliferation-related expression patterns

In this study, PDGF-β served as a marker for proliferation and migration activity (Sano et al., 2001). A significant increase in PDGF-β expression in asymptomatic compared to symptomatic patients was exhibited. The potent growth factor PDGF is a critical modulator in VSMC phenotypic switch regulation (Dandre et al., 2004). Prior research has further indicated a correlation between a high expression of PDGF-β and cardiovascular disease (Koyama et al., 1994). Various cell types express PDGF: VSMCs, ECs, monocyte-derived macrophages and activated platelets (DiCorleto et al., 1983; Kohler et al., 1974; Nilsson et al., 1985; Shimokado et al., 1985). Studies have affirmed its function in the augmentation of VSMC proliferation and migration rates and the repression of contractile marker genes (Dandre et al., 2004; Jawien et al., 1992; Ross et al., 1974). Likewise, Ferns et al. (1991) and Sano et al. (2001) conveyed a suppression of intimal lesion and fibrous cap formation by VSMCs following intraarterial balloon catheter injury in mice after PDGF inhibition (Ferns et al., 1991; Sano et al., 2001). The elevated PDGFB expression provides indirect evidence of increased migration and proliferation activity and decreased contractile behaviour in asymptomatic patients.

The transcription factor KLF4 was previously identified as a genetic marker for the phenotypical de-differentiation, considering it is not expressed in healthy carotid VSMCs (Yoshida et al., 2008b). Examined by McDonald et al. (2006), the overstimulation of PDGF generated an augmented expression of KLF4 in VSMCs, suggesting a link between the function of the two factors (McDonald et al., 2006). While this investigation did render the corresponding increased expression of KLF4 in asymptomatic patients, it was, however, non-significant.

9.2.3. Live-cell imaging analysis

9.2.3.1. Variations in migration activity

Given the difficulties of finding sufficient gene markers for proliferation and migration, VSMC behavioural changes were assessed directly *in vitro* via live-cell imaging. Migration of cells within the vessel is an indispensable feature of atherosclerosis, as it is necessary for the VSMC relocation from the media to the intima for fibrous cap formation (Newby et al., 1999). Preceding studies have rendered that medial VSMCs contribute to the most of the neointima formation (Herring et al., 2014).

The relative wound confluence was examined for migration analysis, resulting in significant differences between stable, unstable and ruptured lesions compared to healthy donor VSMCs. Thus, migration activity is prone to changes while the CAD progresses. As anticipated, the migratory activity of stable and healthy VSMCs showed similar effectiveness, resulting in the highest relative wound density. Correspondingly, it was observed that unstable and ruptured lesion VSMCs were the least effective. Surprisingly, the ruptured lesions demonstrated a partial recovery in efficacy, reaching a higher wound confluence than VSMCs derived from unstable lesions. The increased migration activity may represent vascular remodelling processes evident in subclinical ruptures (Burke et al., 2001). As previously stated, the transcription factor KLF4 may function as a marker for VSMC migration in unstable plaques resulting in increased fibrous cap stability to avert lesion rupture (Deaton et al., 2009; McDonald et al., 2006; Yoshida et al., 2013). Thus, KLF4 emerges as an attractive target in late atherosclerosis.

9.2.3.2. Variations in proliferation activity

The *in vitro* live-cell imaging results identified significant distinctions between the proliferation behaviour in unstable, stable and ruptured plaques. Prior investigations have outlined a low proliferation activity in healthy VSMCs (D. Gordon et al., 1990). As stated in the `response to injury´ hypothesis by Ross et al. (1977), VSMC proliferation is triggered by endothelial injury following platelet-dependent PDGF release (Ross, 1981; Ross et al., 1973; Ross et al., 1977).

Previous research has implicated replicative exhaustion and the resultant loss of VSMCs by apoptosis as contributing factors to fibrous cap thinning (Clarke et al., 2006). Additionally, the diminishing quantity of VSMCs is accountable for the reduction in collagen and matrix synthesis (Clarke et al., 2006). The relevance of proliferation also raises the question of monoclonality (Benditt et al., 1973). According to Chappell et al. (2016), lineage-tracing experiments in mice have indicated that the de-differentiated VSMCs at atherosclerotic sites arise from only a few ancestral cells (Chappell et al., 2016). Similar results in experiments with mice were concluded by Jacobsen et al. (2017) (Jacobsen et al., 2017). Attempts to address the uncertainty of monoclonality in human atherosclerotic VSMCs have been inconclusive.

In this investigation, the results indicated a surge in proliferation activity in the early phases of the disease, as stable lesions reached higher proliferation rates than healthy VSMCs. In agreement with the migration imaging results, VSMCs of unstable and ruptured lesions depicted reduced proliferation rates, whereby unstable and healthy VSMC proliferation differences were significant. It may prove beneficial to intervene and promote proliferation activity in late-stage atherosclerosis, to prevent fatal fibrous cap rupture. Ross et al. (1990) highlighted the importance of PDGF-β in VSMC proliferation regulation; thus, PDGF-β is evolving into a prospective therapeutic target to address reduced proliferation capabilities (Ross, 1990; Ross et al., 1973). Nevertheless, high proliferation indices also provoke adverse outcomes: the formation of complex lesions and in-stent stenosis (MacLeod et al., 1994; Rekhter et al., 1995).

9.3. Methods and limitations

9.3.1. Advantages and disadvantages of biobanking

To expand the Munich Vascular Biobank, which previously only contained FFPE tissues, fresh frozen tissues and serum samples, a method for isolating primary human VSMCs from CAD specimens was established. Biobanking is an imperative pre-clinical tool: to examine and perform experiments on human cells and corroborate results based on animal models (Pelisek et al., 2019). Managing a biobank involves the construction and maintenance of a complex workflow between a team of medical specialists, biologists, surgeons and technicians. In addition to the assertation of high-quality vascular tissue samples, patient-specific data was collected: a benefit of using

patient-derived cells as opposed to cell lines. With access to patient clinical information, it was possible to investigate the implications of symptomatic or asymptomatic presentation on gene expression patterns.

The collected samples were classified according to the method implemented by Stary et al. (1995) and Redgrave et al. (2008) (Redgrave et al., 2008; Stary et al., 1995). Although this framework is a widely administered method, it leaves a margin for error. As a result of surgical manipulation during specimen removal, the lesions may resemble differently histologically than *in vivo*. Even though lesion classification was performed by two investigators and one experienced senior pathologist, minor differences in assessments may have occurred within the process. Atherosclerotic plaques have a complex architecture; neighbouring segments of the same lesion often exhibit contrasting stability. Lesion classification was applied to the clinically most relevant part of the plaque, for example, the ruptured or unstable section. VSMC isolation occurred from a different region within the lesion, thus perhaps leading to inaccuracies within the classification approach.

9.3.2. Advantages and disadvantages of cell culture

Cell culture experiments in atherosclerosis research have many benefits; they are a scalable, robust and inexpensive method for performing investigations on human cells (Ronaldson-Bouchard et al., 2018). However, compared to animal models, cell culture investigations lack the biological functionality necessary to imitate multi-organ-level functions, diminishing their predictive capability (Ronaldson-Bouchard et al., 2018).

The drawbacks of animal models arise due to discrepancies with the human physiology. For example, atherosclerotic lesions do not form spontaneously in animal models; these models are founded on the accelerated lesion formation following (1) cholesterol gene manipulation, (2) a high-cholesterol diet or (3) the introduction of earlier discussed atherosclerosis risk factors (Emini Veseli et al., 2017). In addition, the animal model fibroatheromas vary in structure, with a less-developed fibrous cap and absence of plaque fissuring; further, they develop at other sites within the vasculature than observed in humans (Lusis, 2000; Ni et al., 2009; Schwartz et al., 2007; VanderLaan et al., 2004).

Organs-on-a-chip (OOC) are a possible outlook for future atherosclerosis research: a technological advancement merging the advantages of both approaches (Fernandez et al., 2016; Kurokawa et al., 2017). OOCs incorporate tissue-specific tri-dimensional cell culture with haemodynamic, mechanical and electrical forces *in vitro*: to mirror *in vivo* human subsystems of organs (Moya et al., 2013; Nunes et al., 2013; Wikswo et al., 2013).

The successful isolation of SMCs was morphologically validated by phalloidin immunofluorescence staining. While we could affirm that the experiments were not performed on immune cells, this method failed to exclude the isolation of myofibroblasts. This limitation may be remedied by using flow-cytometry to distinguish SMCs from myofibroblasts. The lack of identified markers presently limits researchers from discriminating between the two cell types.

Past researchers have communicated concerns about the impact of the *in vitro* culture environment, the lack of their local tissue environment and cell-to-cell interactions on the isolated cells (Chamley-Campbell et al., 1979). VSMCs in long-term *in vitro* culture modulate their cytoskeleton; they appear as fibroblast-like cells with a concurrent α-actin content reduction (Absher et al., 1988). Subsequently, *in vitro* cultivation may cause alterations in transcriptional and epigenetic programs, prompting a modification in gene expression (Absher et al., 1988). The primary cells used in this study were passaged a limited number of times (≤ passage 7) to minimise the effect of cultivation on the protein expression levels. To circumvent this argument in future investigations, new technological improvements like single-cell sequencing may provide insight into the VSMCs of atherosclerosis without employing cell culture (J. W. Williams et al., 2020).

9.3.3. Advantages and disadvantages of primary cells

Working with primary cells has its advantages and disadvantages. Primary cells mainly retain their origin tissue's morphological and functional characteristics (Alge et al., 2006; Pan et al., 2009). A benefit of working with primary cells is the access to patient clinical data. Examining the donor data is crucial, as age and genetic characteristics may generate distinctions in cell culture behaviour. Thus, primary cell culture is an approach to bridge the translational gap between experimental and

clinical medicine, for example, by investigating the effects of medical treatment, RNA or antibodies on a specific human cell type. With no interspecies variances in metabolism, anatomy or molecular pathways, primary cell culture may reduce or eliminate the need for animal model experiments in the future.

Nonetheless, studies have displayed subsequent changes in morphology and function as the cells are passaged in culture; a maximum of 7 passages is generally accepted in current research (Absher et al., 1988; Chamley-Campbell et al., 1979). In addition, Hayflick (1965) observed a limiting factor in primary cell investigations: the burden of senescence (Hayflick, 1965). Primary cells display a restricted ability for differentiation and self-renewal (Hayflick, 1965). Furthermore, isolated primary cells derive from human tissue samples often containing various cell types. Consequently, this increases the difficulty of isolating a pure cell population, further aggravating the potential of misidentifying cells.

On the other hand, cell lines are irreplaceable in modern science. Due to their simple expansion and manipulation, they are frequently used to establish new methods, test drug and vaccine efficacy, metabolism and cytotoxicity, and for the production of antibodies, artificial tissue and therapeutic proteins (Gomez-Lechon et al., 2003; MacDonald, 1990; Schurr et al., 2009). Additional benefits are cost-effectiveness and an unlimited supply (Kaur et al., 2012). A pure cell population further correlates with higher experimental consistency and reproducibility (Kaur et al., 2012).

However, cell lines are immortalised cells. The genetic modifications may cause transformations in phenotype, function and response to stimuli; thus, the investigative results cannot be fully translated to humans (Kaur et al., 2012). Furthermore, as cell lines can stay in culture for more extended periods than primary cells, the probability of alterations to phenotype and genotype rises in serial passages (Alge et al., 2006; Pan et al., 2009). This decreases their physiological relevance and forces researchers to periodically verify the characteristics of immortalised cells in culture (Alge et al., 2006; Pan et al., 2009). Another limitation is the chance of cell cross-contamination, first discovered in 1981 by Nelson-Rees et al., which presently remains a concern in cell line research (Capes-Davis et al., 2010; Nelson-Rees et al., 1981).

9.3.4. Limitations of the gene expression investigation

Unfortunately, gene expression analysis of α-SMA, TAGLN, SMTN and MYOCD showed no significant differences. The investigation was, presumably, limited by the number of patient samples collected in the Munich Vascular Biobank. To discover trends and advance the characterisation of VSMCs in different lesion stabilities, more patients should be involved in the *in vitro* study.

Gene expression analyses are restricted by providing only indirect evidence of the cell state at RNA level. Discussions regarding the absence or presence of a correlation between transcript levels and corresponding protein levels in human cells have dominated molecular research in recent years (Anderson et al., 1997; Gry et al., 2009; Maier et al., 2009). Several studies have reported an insufficient association between proteome and transcriptome levels (Payne, 2015; Vogel et al., 2012). Genome-scale investigations have challenged these suggestions by providing evidence of a link between the steady-state mRNA and protein quantity (Wilhelm et al., 2014). Therefore, the selected genes should be examined on a protein level, for instance, by western blotting, ELISA or immunohistochemistry, to validate the indirect expression analysis.

Comparing patient-derived cells and healthy donor cells is a frequently implemented method. Yet, less variance may be obtained by simultaneously isolating VSMCs from a diseased and non-diseased part of the same patient's carotid artery and comparing their gene expression patterns. This method is currently being established at the Laboratory for Vascular Biology and Experimental Vascular Medicine at Klinikum rechts der Isar of the Technical University Munich (TUM).

10. Summary and Outlook

Atherosclerosis is a complex disease involving the accumulation of lipoproteins, an interminable inflammation and vascular remodelling. Discussions regarding the behaviour of VSMCs in vascular reconstruction have dominated atherosclerosis research in recent years. Prior studies have highlighted that VSMCs play a valuable role throughout the disease. Nevertheless, they have neglected to identify the specific phases to target VSMC function to prevent lesion rupture and thereby clinical manifestation.

This study contributes to a better understanding of gene expression research on VSMCs derived from stable, unstable and ruptured carotid endarterectomy samples. Clinical data, histological stains on the corresponding tissue and *in vitro* experiments give insight into VSMCs and their migratory and proliferative behaviour in the intricate process of human atherosclerosis.

Future investigations of VSMCs from atherosclerotic lesions should focus on the gene expression patterns of diseased and healthy cells derived from the same patient using new scientific technologies like single-cell sequencing or OOCs to provide even more mechanistic insight into the phenotypical changes during disease progression. These technological advances reduce the limitations of cell culture and may, in the future, reduce or even replace ethically problematic animal model experiments.

A prospective application of biobanking includes minimising the translational gap between experimental research and the clinical appliance of new observations. Additionally, biobanking will be instrumental in health innovation: identifying genetic risk factors and biomarkers of disease progression and implementing personalised medicine.

11. Tables

12. Figures

13. Acknowledgments

Herrn Prof. Dr. med. Lars Mägdefessel danke ich für die Überlassung des Themas dieser Arbeit. Zudem bedanke ich mich für die stetige Begleitung und konstruktive Kritik während der Dissertation.

Weiterhin möchte ich mich bei allen Mitgliedern der Arbeitsgruppe bedanken, besonders bei Jessica Pauli, für die mühevolle und geduldige Einarbeitung, Betreuung und Unterstützung.

Außerdem möchte ich mich bei meinem Mitdoktoranden Max Vogelsang für die freundschaftliche Zusammenarbeit und den hilfreichen Austausch bedanken.

Zuletzt bedanke ich mich zutiefst bei Victoria Jurisch und meiner Familie für die kontinuierliche Unterstützung während meines Medizinstudiums und in allen Lebenslagen.

16. References

Abe, J., & Berk, B. C. (2014). Novel mechanisms of endothelial mechanotransduction. *Arterioscler Thromb Vasc Biol, 34*(11), 2378-2386.

Aboyans, V., Ricco, J. B., Bartelink, M. E. L., Bjorck, M., Brodmann, M., Cohnert, T., Collet, J. P., Czerny, M., De Carlo, M., Debus, S., Espinola-Klein, C., Kahan, T., Kownator, S., Mazzolai, L., Naylor, A. R., Roffi, M., Rother, J., Sprynger, M., Tendera, M., Tepe, G., Venermo, M., Vlachopoulos, C., Desormais, I., & Group, E. S. C. S. D. (2018). 2017 ESC Guidelines on the Diagnosis and Treatment of Peripheral Arterial Diseases, in collaboration with the European Society for Vascular Surgery (ESVS): Document covering atherosclerotic disease of extracranial carotid and vertebral, mesenteric, renal, upper and lower extremity arteriesEndorsed by: the European Stroke Organization (ESO)The Task Force for the Diagnosis and Treatment of Peripheral Arterial Diseases of the European Society of Cardiology (ESC) and of the European Society for Vascular Surgery (ESVS). *Eur Heart J, 39*(9), 763-816.

Absher, M., Woodcock-Mitchell, J., Mitchell, J., Baldor, L., Low, R., & Warshaw, D. (1988). Characterization of vascular smooth muscle cell phenotype in long-term culture. *In Vitro Cellular & Developmental Biology, 25*(2), 183-192.

Ackers-Johnson, M., Talasila, A., Sage, A. P., Long, X., Bot, I., Morrell, N. W., Bennett, M. R., Miano, J. M., & Sinha, S. (2015). Myocardin regulates vascular smooth muscle cell inflammatory activation and disease. *Arterioscler Thromb Vasc Biol, 35*(4), 817-828.

Aikawa, M., Sakomura, Y., Ueda, M., Kimura, K., Manabe, I., Ishiwata, S., Komiyama, N., Yamaguchi, H., Yazaki, Y., & Nagai, R. (1997). Redifferentiation of smooth muscle cells after coronary angioplasty determined via myosin heavy chain expression. *Circulation, 96*(1), 82-90.

Aikawa, M., Sivam, P. N., Kuro-o, M., Kimura, K., Nakahara, K., Takewaki, S., Ueda, M., Yamaguchi, H., Yazaki, Y., Periasamy, M., & et al. (1993). Human smooth muscle myosin heavy chain isoforms as molecular markers for vascular development and atherosclerosis. *Circ Res, 73*(6), 1000-1012.

Albarran-Juarez, J., Kaur, H., Grimm, M., Offermanns, S., & Wettschureck, N. (2016). Lineage tracing of cells involved in atherosclerosis. *Atherosclerosis, 251*, 445-453.

Alge, C. S., Hauck, S. M., Priglinger, S. G., Kampik, A., & Ueffing, M. (2006). Differential protein profiling of primary versus immortalized human RPE cells identifies expression patterns associated with cytoskeletal remodeling and cell survival. *J Proteome Res, 5*(4), 862-878.

Allahverdian, S., Chehroudi, A. C., McManus, B. M., Abraham, T., & Francis, G. A. (2014). Contribution of intimal smooth muscle cells to cholesterol accumulation and macrophage-like cells in human atherosclerosis. *Circulation, 129*(15), 1551-1559.

Amarenco, P., Kim, J. S., Labreuche, J., Charles, H., Abtan, J., Bejot, Y., Cabrejo, L., Cha, J. K., Ducrocq, G., & Giroud, M. (2020). Treat stroke to target investigators. A comparison of two LDL cholesterol targets after ischemic stroke. *N Engl J Med, 382*, 9-19.

Amarenco, P., Labreuche, J., Lavallee, P., & Touboul, P. J. (2004). Statins in stroke prevention and carotid atherosclerosis: systematic review and up-to-date meta-analysis. *Stroke, 35*(12), 2902-2909.

Amento, E. P., Ehsani, N., Palmer, H., & Libby, P. (1991). Cytokines and growth factors positively and negatively regulate interstitial collagen gene expression in human vascular smooth muscle cells. *Arterioscler Thromb, 11*(5), 1223-1230.

Andersen, K. K., Olsen, T. S., Dehlendorff, C., & Kammersgaard, L. P. (2009). Hemorrhagic and ischemic strokes compared: stroke severity, mortality, and risk factors. *Stroke, 40*(6), 2068-2072.

Anderson, L., & Seilhamer, J. (1997). A comparison of selected mRNA and protein abundances in human liver. *Electrophoresis, 18*(3-4), 533-537.

Andreeva, E. R., Pugach, I. M., & Orekhov, A. N. (1997a). Collagen-synthesizing cells in initial and advanced atherosclerotic lesions of human aorta. *Atherosclerosis, 130*(1-2), 133-142.

Andreeva, E. R., Pugach, I. M., & Orekhov, A. N. (1997b). Subendothelial smooth muscle cells of human aorta express macrophage antigen in situ and in vitro. *Atherosclerosis, 135*(1), 19-27.

Ang, A. H., Tachas, G., Campbell, J. H., Bateman, J. F., & Campbell, G. R. (1990). Collagen synthesis by cultured rabbit aortic smooth-muscle cells. Alteration with phenotype. *Biochem J, 265*(2), 461-469.

Assmann, G., Cullen, P., Jossa, F., Lewis, B., & Mancini, M. (1999). Coronary heart disease: reducing the risk: the scientific background to primary and secondary prevention of coronary heart disease. A worldwide view. International Task force for the Prevention of Coronary Heart disease. *Arterioscler Thromb Vasc Biol, 19*(8), 1819-1824.

Atkins, G. B., & Simon, D. I. (2013). Interplay between NF-kappaB and Kruppel-like factors in vascular inflammation and atherosclerosis: location, location, location. *J Am Heart Assoc, 2*(3), e000290.

Back, M., Yurdagul, A., Jr., Tabas, I., Oorni, K., & Kovanen, P. T. (2019). Inflammation and its resolution in atherosclerosis: mediators and therapeutic opportunities. *Nat Rev Cardiol, 16*(7), 389-406.

Baigent, C., Keech, A., Kearney, P. M., Blackwell, L., Buck, G., Pollicino, C., Kirby, A., Sourjina, T., Peto, R., Collins, R., Simes, R., & Cholesterol Treatment Trialists, C. (2005). Efficacy and safety of cholesterol-lowering treatment: prospective meta-analysis of data from 90,056 participants in 14 randomised trials of statins. *Lancet, 366*(9493), 1267-1278.

Balestrini, S., Perozzi, C., Altamura, C., Vernieri, F., Luzzi, S., Bartolini, M., Provinciali, L., & Silvestrini, M. (2013). Severe carotid stenosis and impaired cerebral hemodynamics can influence cognitive deterioration. *Neurology, 80*(23), 2145-2150.

Barnett, H. J., Taylor, D. W., Eliasziw, M., Fox, A. J., Ferguson, G. G., Haynes, R. B., Rankin, R. N., Clagett, G. P., Hachinski, V. C., Sackett, D. L., Thorpe, K. E., Meldrum, H. E., & Spence, J. D. (1998). Benefit of carotid endarterectomy in patients with symptomatic moderate or severe stenosis. North American Symptomatic Carotid Endarterectomy Trial Collaborators. *N Engl J Med, 339*(20), 1415-1425.

Barrett, T. B., & Benditt, E. P. (1988). Platelet-derived growth factor gene expression in human atherosclerotic plaques and normal artery wall. *Proc Natl Acad Sci U S A, 85*(8), 2810-2814.

Basatemur, G. L., Jorgensen, H. F., Clarke, M. C. H., Bennett, M. R., & Mallat, Z. (2019). Vascular smooth muscle cells in atherosclerosis. *Nat Rev Cardiol, 16*(12), 727-744.

Bauriedel, G., Hutter, R., Welsch, U., Bach, R., Sievert, H., & Luderitz, B. (1999). Role of smooth muscle cell death in advanced coronary primary lesions: implications for plaque instability. *Cardiovasc Res, 41*(2), 480-488.

Benditt, E. P., & Benditt, J. M. (1973). Evidence for a monoclonal origin of human atherosclerotic plaque. *Proc Natl Acad Sci, 70*(6).

Bennett, M. R., Sinha, S., & Owens, G. K. (2016). Vascular Smooth Muscle Cells in Atherosclerosis. *Circ Res, 118*(4), 692-702.

Berliner, J. A., Territo, M. C., Sevanian, A., Ramin, S., Kim, J. A., Bamshad, B., Esterson, M., & Fogelman, A. M. (1990). Minimally modified low density lipoprotein stimulates monocyte endothelial interactions. *J Clin Invest, 85*(4), 1260-1266.

Bobryshev, Y. V. (2005). Transdifferentiation of smooth muscle cells into chondrocytes in atherosclerotic arteries in situ: implications for diffuse intimal calcification. *J Pathol, 205*(5), 641-650.

Bonetti, P. O., Lerman, L. O., & Lerman, A. (2002). Endothelial dysfunction: a marker of atherosclerotic risk. *Arterioscler Thromb and Vasc Biol, 23*(2), 168-175.

Brenner, B. M., Troy, J. L., & Ballermann, B. J. (1989). Endothelium-dependent vascular responses. Mediators and mechanisms. *J Clin Invest, 84*(5), 1373-1378.

Brott, T. G., Adams, H. P., Jr., Olinger, C. P., Marler, J. R., Barsan, W. G., Biller, J., Spilker, J., Holleran, R., Eberle, R., & Hertzberg, V. (1989). Measurements of acute cerebral infarction: a clinical examination scale. *Stroke, 20*(7), 864-870.

Brott, T. G., Hobson, R. W., 2nd, Howard, G., Roubin, G. S., Clark, W. M., Brooks, W., Mackey, A., Hill, M. D., Leimgruber, P. P., Sheffet, A. J., Howard, V. J., Moore, W. S., Voeks, J. H., Hopkins, L. N., Cutlip, D. E., Cohen, D. J., Popma, J. J., Ferguson, R. D., Cohen, S. N., Blackshear, J. L., Silver, F. L., Mohr, J. P., Lal, B. K., & Meschia, J. F. (2010). Stenting versus endarterectomy for treatment of carotid-artery stenosis. *N Engl J Med, 363*(1), 11-23.

Brown, B. G., & Zhao, X. Q. (2008). Nicotinic acid, alone and in combinations, for reduction of cardiovascular risk. *Am J Cardiol, 101*(8A), 58B-62B.

Buratti, L., Balucani, C., Viticchi, G., Falsetti, L., Altamura, C., Avitabile, E., Provinciali, L., Vernieri, F., & Silvestrini, M. (2014). Cognitive deterioration in bilateral asymptomatic severe carotid stenosis. *Stroke, 45*(7), 2072-2077.

Burke, A. P., Kolodgie, F. D., Farb, A., Weber, D. K., Malcom, G. T., Smialek, J., & Virmani, R. (2001). Healed plaque ruptures and sudden coronary death - evidence that subclinical rupture has a role in plaque progression. *Circulation, 103*, 934-940.

Butcher, E. C. (1991). Leukocyte-endothelial cell recognition: three (or more) steps to specificity and diversity. *Cell, 67*(6), 1033-1036.

Camejo, G., Lalaguna, F., Lopez, F., & Starosta, R. (1980). Characterization and properties of a lipoprotein-complexing proteoglycan from human aorta. *Atherosclerosis, 35*(3), 307-320.

Campbell, J. H., Popadynec, L., Nestel, P. J., & Campbell, G. R. (1983). Lipid accumulation in arterial smooth muscle cells. Influence of phenotype. *Atherosclerosis, 47*(3), 279-295.

Campbell, J. H., Reardon, M. F., Campbell, G. R., & Nestel, P. J. (1985). Metabolism of atherogenic lipoproteins by smooth muscle cells of different phenotype in culture. *Arteriosclerosis, 5*(4), 318-328.

Cannon, C. P., Shah, S., Dansky, H. M., Davidson, M., Brinton, E. A., Gotto, A. M., Stepanavage, M., Liu, S. X., Gibbons, P., Ashraf, T. B., Zafarino, J., Mitchel, Y., Barter, P., Determining the, E., & Tolerability, I. (2010). Safety of anacetrapib in patients with or at high risk for coronary heart disease. *N Engl J Med, 363*(25), 2406-2415.

Capes-Davis, A., Theodosopoulos, G., Atkin, I., Drexler, H. G., Kohara, A., MacLeod, R. A., Masters, J. R., Nakamura, Y., Reid, Y. A., Reddel, R. R., & Freshney, R. I. (2010). Check your cultures! A list of cross-contaminated or misidentified cell lines. *Int J Cancer, 127*(1), 1-8.

Caro, C. G., Fitz-Gerald, J. M., & Schroter, R. C. (1971). Atheroma and arterial wall shear. Observation, correlation and proposal of a shear dependent mass transfer mechanism for atherogenesis. *Proc R Soc Lond B Biol Sci, 177*(1046), 109-159.

Carr, S., Farb, A., Pearce, W. H., Virmani, R., & Yao, J. S. (1996). Atherosclerotic plaque rupture in symptomatic carotid artery stenosis. *J Vasc Surg, 23*(5), 755-765; discussion 765-756.

Chamley-Campbell, J., Campbell, G. R., & Ross, R. (1979). The smooth muscle cell in culture. *Physiol Rev, 59*(1), 1-61.

Chang, M. Y., Potter-Perigo, S., Tsoi, C., Chait, A., & Wight, T. N. (2000). Oxidized low density lipoproteins regulate synthesis of monkey aortic smooth muscle cell proteoglycans that have enhanced native low density lipoprotein binding properties. *J Biol Chem, 275*, 4766-4773.

Chappell, J., Harman, J. L., Narasimhan, V. M., Yu, H., Foote, K., Simons, B. D., Bennett, M. R., & Jorgensen, H. F. (2016). Extensive Proliferation of a Subset of Differentiated, yet Plastic, Medial Vascular Smooth Muscle Cells Contributes to Neointimal Formation in Mouse Injury and Atherosclerosis Models. *Circ Res, 119*(12), 1313-1323.

Chatzizisis, Y. S., Coskun, A. U., Jonas, M., Edelman, E. R., Feldman, C. L., & Stone, P. H. (2007). Role of endothelial shear stress in the natural history of coronary atherosclerosis and vascular remodeling: molecular, cellular, and vascular behavior. *J Am Coll Cardiol, 49*(25), 2379-2393.

Chellan, B., Rojas, E., Zhang, C., & Hofmann Bowman, M. A. (2018). Enzyme-modified non-oxidized LDL (ELDL) induces human coronary artery smooth muscle cell transformation to a migratory and osteoblast-like phenotype. *Sci Rep, 8*(1), 11954.

Chen, S., & Lechleider, R. J. (2004). Transforming growth factor-β-induced differentiation of smooth muscle from a neural crest stem cell line. *Circ Res, 94*, 1195-1202.

Cheng, C., Tempel, D., van Haperen, R., van der Baan, A., Grosveld, F., Daemen, M. J., Krams, R., & de Crom, R. (2006). Atherosclerotic lesion size and vulnerability are determined by patterns of fluid shear stress. *Circulation, 113*(23), 2744-2753.

Cheng, G. C., Loree, H. M., Kamm, R. D., Fishbein, M. C., & Lee, R. T. (1993). Distribution of circumferential stress in ruptured and stable atherosclerotic lesions. A structural analysis with histopathological correlation. *Circulation, 87*(4), 1179-1187.

Clarke, M. C., Figg, N., Maguire, J. J., Davenport, A. P., Goddard, M., Littlewood, T. D., & Bennett, M. R. (2006). Apoptosis of vascular smooth muscle cells induces features of plaque vulnerability in atherosclerosis. *Nat Med, 12*(9), 1075-1080.

Clarke, M. C., Littlewood, T. D., Figg, N., Maguire, J. J., Davenport, A. P., Goddard, M., & Bennett, M. R. (2008). Chronic apoptosis of vascular smooth muscle cells accelerates atherosclerosis and promotes calcification and medial degeneration. *Circ Res, 102*(12), 1529-1538.

Clarke, M. C., Talib, S., Figg, N. L., & Bennett, M. R. (2010). Vascular smooth muscle cell apoptosis induces interleukin-1-directed inflammation: effects of hyperlipidemia-mediated inhibition of phagocytosis. *Circ Res, 106*(2), 363-372.

Clowes, A. W., Reidy, M. A., & Clowes, A. W. (1982). Mechanisms of stenosis after arterial injury. *Lab Invest, 49*(2), 208-215.

Constantinides, P. (1966). Plaque fissuring in human coronary thrombosis. *J Atheroscler Res, 6*, 1-17.

Cornhill, J. F., & Roach, M. R. (1976). A quantitative study of the localization of atherosclerotic lesions in the rabbit aorta. *Atherosclerosis, 23*(3), 489-501.

Cunningham, K. S., & Gotlieb, A. I. (2005). The role of shear stress in the pathogenesis of atherosclerosis. *Lab Invest, 85*(1), 9-23.

Cushing, S. D., Berliner, J. A., Valente, A. J., Territo, M. C., Navab, M., Parhami, F., Gerrity, R., Schwartz, C. J., & Fogelman, A. M. (1990). Minimally modified low density lipoprotein induces

monocyte chemotactic protein 1 in human endothelial cells and smooth muscle cells. *Proc Natl Acad Sci U S A, 87*(13), 5134-5138.

Cybulsky, M. I., & Gimbrone, M. A., Jr. (1991). Endothelial expression of a mononuclear leukocyte adhesion molecule during atherogenesis. *Science, 251*(4995), 788-791.

Dai, G., Kaazempur-Mofrad, M. R., Natarajan, S., Zhang, Y., Vaughn, S., Blackman, B. R., Kamm, R. D., Garcia-Cardena, G., & Gimbrone, M. A., Jr. (2004). Distinct endothelial phenotypes evoked by arterial waveforms derived from atherosclerosis-susceptible and -resistant regions of human vasculature. *Proc Natl Acad Sci U S A, 101*(41), 14871-14876.

Dandre, F., & Owens, G. K. (2004). Platelet-derived growth factor-BB and Ets-1 transcription factor negatively regulate transcription of multiple smooth muscle cell differentiation marker genes. *Am J Physiol Heart Circ Physiol, 286*(6), H2042-2051.

Dardik, A., Yamashita, A., Aziz, F., Asada, H., & Sumpio, B. E. (2005). Shear stress-stimulated endothelial cells induce smooth muscle cell chemotaxis via platelet-derived growth factor-BB and IL-1alpha. *J Vasc Surg, 41*, 321-331.

Davies, M. J. (1992). Anatomic features in victims of sudden coronary death. Coronary artery pathology. *Circulation, 85*(1 Suppl), I19-24.

Davies, M. J., Richardson, P. D., Woolf, N., Katz, D. R., & Mann, J. (1993). Risk of thrombosis in human atherosclerotic plaques: role of extracellular lipid, macrophage, and smooth muscle cell content. *Br Heart J, 69*(5), 377-381.

Davies, M. J., & Thomas, A. (1984). Thrombosis and acute coronary-artery lesions in sudden cardiac ischemic death. *N Engl J Med, 310*(18), 1137-1140.

Davies, P. F. (2009). Hemodynamic shear stress and the endothelium in cardiovascular pathophysiology. *Nat Clin Pract Cardiovasc Med, 6*(1), 16-26.

Davies, P. F., Civelek, M., Fang, Y., & Fleming, I. (2013). The atherosusceptible endothelium: endothelial phenotypes in complex haemodynamic shear stress regions in vivo. *Cardiovasc Res, 99*(2), 315-327.

de Weerd, M., Greving, J. P., de Jong, A. W. F., Buskens, E., & Bots, M. L. (2009). Prevalence of asymptomatic carotid artery stenosis according to age and sex: systematic review and metaregression analysis. *Stroke, 40*(4), 1105-1113.

de Weerd, M., Greving, J. P., Hedblad, B., Lorenz, M. W., Mathiesen, E. B., O'Leary, D. H., Rosvall, M., Sitzer, M., Buskens, E., & Bots, M. L. (2010). Prevalence of asymptomatic carotid artery stenosis in the general population: an individual participant data meta-analysis. *Stroke, 41*(6), 1294-1297.

Deaton, R. A., Gan, Q., & Owens, G. K. (2009). Sp1-dependent activation of KLF4 is required for PDGF-BB-induced phenotypic modulation of smooth muscle. *Am J Physiol Heart Circ Physiol, 296*(4), H1027-1037.

DiCorleto, P. E., & Bowen-Pope, D. F. (1983). Cultured endothelial cells produce a platelet-derived growth factor-like protein. *Proc Natl Acad Sci U S A, 80*(7), 1919-1923.

Durham, A. L., Speer, M. Y., Scatena, M., Giachelli, C. M., & Shanahan, C. M. (2018). Role of smooth muscle cells in vascular calcification: implications in atherosclerosis and arterial stiffness. *Cardiovasc Res, 114*(4), 590-600.

Dutrochet, H. (1824). *Recherches anatomiques et physiologiques sur la structure intime des animaux et des végetaux, et sur leur motilité*. Paris: Bailliere et fils.

Eckstein, H. H. (2018). European Society for Vascular Surgery Guidelines on the Management of Atherosclerotic Carotid and Vertebral Artery Disease. *Eur J Vasc Endovasc Surg, 55*(1), 1-2.

Eckstein, H. H., Kühnl, A., Berkefeld, J., Dörfler, A., Kopp, I., Langhoff, R., Lawall, H., Ringleb, P. A., Sander, D., Storck, M., Czerny, M., Engelhard, K., Fraedrich, G., Fründ, A., George, S., Görtz, H., Gross-Fengels, W., Hanl, J., Hörstgen, A., Huppert, P., Litz, R., Lüdeking, C., Mudra, H., Navabi, D. G., Ploenes, C., Rantner, B., Rittig, K., Schamberger, R., Schnell, O., Schulte, S., Schwerdtfeger, K., Steinbauer, M., Stingele, R., & Zeller, T. (2020). S3-Leitlinie zur Diagnostik, Therapie und Nachsorge der extracraniellen Carotisstenose. 2. Retrieved from https://www.awmf.org/uploads/tx_szleitlinien/004-028k_extracranielle-Carotisstenose-Diagnostik-Therapie-Nachsorge_2020-02_1.pdf

Emini Veseli, B., Perrotta, P., De Meyer, G. R. A., Roth, L., Van der Donckt, C., Martinet, W., & De Meyer, G. R. Y. (2017). Animal models of atherosclerosis. *Eur J Pharmacol, 816*, 3-13.

Falk, E. (1983). Plaque rupture with severe pre-existing stenosis precipitating coronary thrombosis. Characteristics of coronary atherosclerotic plaques underlying fatal occlusive thrombi. *Br Heart J, 50*(2), 127-134.

Falk, E. (1989). Morphologic features of unstable atherothrombotic plaques underlying acute coronary syndromes. *Am J Cardiol, 63*, 114E-120E.

Feil, S., Fehrenbacher, B., Lukowski, R., Essmann, F., Schulze-Osthoff, K., Schaller, M., & Feil, R. (2014). Transdifferentiation of vascular smooth muscle cells to macrophage-like cells during atherogenesis. *Circ Res, 115*(7), 662-667.

Fernandez, C. E., Yen, R. W., Perez, S. M., Bedell, H. W., Povsic, T. J., Reichert, W. M., & Truskey, G. A. (2016). Human Vascular Microphysiological System for in vitro Drug Screening. *Sci Rep, 6*, 21579.

Ferns, G. A., Raines, E. W., Sprugel, K. H., Motani, A. S., Reidy, M. A., & Ross, R. (1991). Inhibition of neointimal smooth muscle accumulation after angioplasty by an antibody to PDGF. *Science, 253*(5024), 1129-1132.

Forstermann, U., Mugge, A., Alheid, U., Bode, S. M., & Frolich, J. C. (1989). Endothelium-derived relaxing factor (EDRF): a defence mechanism against platelet aggregation and vasospasm in human coronary arteries. *Eur Heart J, 10 Suppl F*, 36-43.

Frangogiannis, N. G., Michael, L. H., & Entman, M. L. (2000). Myofibroblasts in reperfused myocardial infarcts express the embryonic form of smooth muscle myosin heavy chain (SMemb). *Cardiovasc Res, 48*(1), 89-100.

Frick, M. H., Elo, O., Haapa, K., Heinonen, O. P., Heinsalmi, P., Helo, P., Huttunen, J. K., Kaitaniemi, P., Koskinen, P., Manninen, V., & et al. (1987). Helsinki Heart Study: primary-prevention trial with gemfibrozil in middle-aged men with dyslipidemia. Safety of treatment, changes in risk factors, and incidence of coronary heart disease. *N Engl J Med, 317*(20), 1237-1245.

Furchgott, R. F., & Zawadzki, J. V. (1980). The obligatory role of endothelial cells in the relaxation of arterial smooth muscle by acetylcholine. *Nature, 288*(5789), 373-376.

Galis, Z. S., Muszynski, M., Sukhova, G. K., Simon-Morrissey, E., Unemori, E. N., Lark, M. W., Amento, E., & Libby, P. (1994a). Cytokine-stimulated human vascular smooth muscle cells synthesize a complement of enzymes required for extracellular matrix digestion. *Circ Res, 75*(1), 181-189.

Galis, Z. S., Sukhova, G. K., Kranzhofer, R., Clark, S., & Libby, P. (1995). Macrophage foam cells from experimental atheroma constitutively produce matrix-degrading proteinases. *Proc Natl Acad Sci U S A, 92*(2), 402-406.

Galis, Z. S., Sukhova, G. K., Lark, M. W., & Libby, P. (1994b). Increased expression of matrix metalloproteinases and matrix degrading activity in vulnerable regions of human atherosclerotic plaques. *J Clin Invest, 94*(6), 2493-2503.

Gerhard, G. T., & Duell, P. B. (1999). Homocysteine and atherosclerosis. *Curr Opin Lipidol, 10*(5), 417-428.

Ghaleb, A. M., & Yang, V. W. (2017). Kruppel-like factor 4 (KLF4): What we currently know. *Gene, 611*(611), 27-37.

Gimbrone, M. A., Jr. (1987). Vascular endothelium: nature's blood-compatible container. *Ann N Y Acad Sci, 516*, 5-11.

Gimbrone, M. A., Jr., & Garcia-Cardena, G. (2013). Vascular endothelium, hemodynamics, and the pathobiology of atherosclerosis. *Cardiovasc Pathol, 22*(1), 9-15.

Goldbourt, U., & Neufeld, H. N. (1986). Genetic aspects of arteriosclerosis. *Arteriosclerosis, 6*(4), 357-377.

Goldstein, L. B., Adams, R., Alberts, M. J., Appel, L. J., Brass, L. M., Bushnell, C. D., Culebras, A., DeGraba, T. J., Gorelick, P. B., Guyton, J. R., Hart, R. G., Howard, G., Kelly-Hayes, M., Nixon, J. V., & Sacco, R. L. (2006). Primary Prevention of Ischemic Stroke. *Stroke, 37*(6), 1583-1633.

Gomez, D., & Owens, G. K. (2012). Smooth muscle cell phenotypic switching in atherosclerosis. *Cardiovasc Res, 95*(2), 156-164.

Gomez-Lechon, M. J., Donato, M. T., Castell, J. V., & Jover, R. (2003). Human hepatocytes as a tool for studying toxicity and drug metabolism. *Curr Drug Metab, 4*(4), 292-312.

Gordon, D., Reidy, M. A., Benditt, E. P., & Schwartz, S. M. (1990). Cell proliferation in human coronary arteries. *Proc Natl Acad Sci U S A, 87*(12), 4600-4604.

Gordon, D. J., & Rifkind, B. M. (1989). High-density lipoprotein--the clinical implications of recent studies. *N Engl J Med, 321*(19), 1311-1316.

Grant, E. G., Benson, C. B., Moneta, G. L., Alexandrov, A. V., Baker, J. D., Bluth, E. I., Carroll, B. A., Eliasziw, M., Gocke, J., Hertzberg, B. S., Katanick, S., Needleman, L., Pellerito, J., Polak, J. F., Rholl, K. S., Wooster, D. L., & Zierler, R. E. (2003). Carotid artery stenosis: gray-scale and Doppler US diagnosis--Society of Radiologists in Ultrasound Consensus Conference. *Radiology, 229*(2), 340-346.

Group, E. C. S. T. C. (1998). Randomised trial of endarterectomy for recently symptomatic carotid stenosis: final results of the MRC European Carotid Surgery Trial (ECST). *The Lancet, 351*(9113), 1379-1387.

Gry, M., Rimini, R., Strömberg, S., Asplund, A., Ponten, F., Uhlen, M., & Nilsson, P. (2009). Correlations between RNA and protein expression profiles in 23 human cell lines. *BMC Genomics, 10*, 365.

Gupta, A., Baradaran, H., Schweitzer, A. D., Kamel, H., Pandya, A., Delgado, D., Dunning, A., Mushlin, A. I., & Sanelli, P. C. (2013). Carotid plaque MRI and stroke risk: a systematic review and meta-analysis. *Stroke, 44*(11), 3071-3077.

Gupta, A., Kesavabhotla, K., Baradaran, H., Kamel, H., Pandya, A., Giambrone, A. E., Wright, D., Pain, K. J., Mtui, E. E., Suri, J. S., Sanelli, P. C., & Mushlin, A. I. (2015). Plaque echolucency and stroke risk in asymptomatic carotid stenosis: a systematic review and meta-analysis. *Stroke, 46*(1), 91-97.

Hackett, D., Davies, G., & Maseri, A. (1988). Pre-existing coronary stenoses in patients with first myocardial infarction are not necessarily severe. *Eur Heart J, 9*(12), 1317-1323.

Hajra, L., Evans, A. I., Chen, M., Hyduk, S. J., Collins, T., & Cybulsky, M. I. (2000). The NF-kappa B signal transduction pathway in aortic endothelial cells is primed for activation in regions predisposed to atherosclerotic lesion formation. *Proc Natl Acad Sci U S A, 97*(16), 9052-9057.

Hautmann, M. B., Madsen, C. S., & Owens, G. K. (1997). A transforming growth factor β (TGFβ) control element drives TGFβ-induced stimulation of smooth muscle α-Actin gene expression in concert with two CArG elements. *The Journal of Biological Chemistry, 272*(16), 10948-10956.

Hayden, M. R., & Tyagi, S. C. (2004). Vasa vasorum in plaque angiogenesis, metabolic syndrome, type 2 diabetes mellitus, and atheroscleropathy: a malignant transformation. *Cardiovasc Diabetol, 3*, 1.

Hayflick, L. (1965). The limited in vitro lifetime of human diploid cell strains. *Exp Cell Res, 37*(3), 614-636.

Heery, J. M., Kozak, M., Stafforini, D. M., Jones, A., Zimmerman, G. A., McIntyre, T. M., & Prescott, S. M. (1995). Oxidatively modified LDL contains phospholipids with platelet-activity factor-like activity and stimulates the growth of smooth muscle cells. *J Clin Invest, 96*, 2322-2330.

Herring, B. P., Hoggatt, A. M., Burlak, C., & Offermanns, S. (2014). Previously differentiated medial vascular smooth muscle cells contribute to neointima formation following vascular injury. *Vasc Cell, 6*(21), 21.

Herrmann, J., Lerman, L. O., Rodriguez-Porcel, M., Holmes, D. R., Jr., Richardson, D. M., Ritman, E. L., & Lerman, A. (2001). Coronary vasa vasorum neovascularization precedes epicardial endothelial dysfunction in experimental hypercholesterolemia. *Cardiovasc Res, 51*(4), 762-766.

Hickey, M. J., & Kubes, P. (1997). Role of nitric oxide in regulation of leukocyte-endothelial cell interactions. *Exp Physiol, 82*(2), 339-348.

Holness, C. L., & Simmons, D. L. (1993). Molecular cloning of CD68, a human macrophage marker related to lysosomal glycoproteins. *Blood 81*(6), 1607-1613.

Holycross, B. J., Blank, R. S., Thompson, M. M., Peach, M. J., & Owens, G. K. (1992). Platelet-derived growth factor-BB-induced suppression of smooth muscle cell differentiation. *Circ Res, 71*(6), 1525-1532.

Howard, G., Roubin, G. S., Jansen, O., Hendrikse, J., Halliday, A., Fraedrich, G., Eckstein, H. H., Calvet, D., Bulbulia, R., Bonati, L. H., Becqemin, J.-P., Algra, A., Brown, M. M., Ringleb, P. A., Brott, T., & Mas, J.-L. (2016). Association between age and risk of stroke or death from carotid endarterectomy and carotid stenting: a meta-analysis of pooled patient data from four randomised trials. *Lancet, 387*(10025), 1305-1311.

Iverius, P. H. (1972). The interaction between human plasma lipoproteins and connective tissue glycosaminoglycans. *J Biol Chem, 247*(8), 2607-2613.

Jacobsen, K., Lund, M. B., Shim, J., Gunnersen, S., Fuchtbauer, E. M., Kjolby, M., Carramolino, L., & Bentzon, J. F. (2017). Diverse cellular architecture of atherosclerotic plaque derives from clonal expansion of a few medial SMCs. *JCI Insight, 2*(19), 1-13.

Jawien, A., Bowen-Pope, D. F., Lindner, V., Schwartz, S. M., & Clowes, A. W. (1992). Platelet-derived growth factor promotes smooth muscle migration and intimal thickening in a rat model of balloon angioplasty. *J Clin Invest, 89*(2), 507-511.

Jayasooriya, G., Thapar, A., Shalhoub, J., & Davies, A. H. (2011). Silent cerebral events in asymptomatic carotid stenosis. *J Vasc Surg, 54*(1), 227-236.

Jeziorska, M., & Woolley, D. E. (1999). Local neovascularization and cellular composition within vulnerable regions of atherosclerotic plaques of human carotid arteries. *J Pathol, 188*, 189-196.

Jonasson, L., Holm, J., Skalli, O., Bondjers, G., & Hansson, G. K. (1986). Regional accumulations of T cells, macrophages, and smooth muscle cells in the human atherosclerotic plaque. *Arteriosclerosis, 6*(2), 131-138.

Kakkos, S. K., Nicolaides, A. N., Charalambous, I., Thomas, D., Giannopoulos, A., Naylor, A. R., Geroulakos, G., & Abbott, A. L. (2014). Predictors and clinical significance of progression or regression of asymptomatic carotid stenosis. *J Vasc Surg, 59*(4), 956-967 e951.

Kakkos, S. K., Sabetai, M., Tegos, T., Stevens, J., Thomas, D., Griffin, M., Geroulakos, G., & Nicolaides, A. N. (2009). Silent embolic infarcts on computed tomography brain scans and risk of ipsilateral hemispheric events in patients with asymptomatic internal carotid artery stenosis. *J Vasc Surg, 49*(4), 902-909.

Kamat, B. R., Galli, S. J., Barger, A. C., Lainey, L. L., & Silverman, K. J. (1987). Neovascularization and coronary atherosclerotic plaque: cinematographic localization and quantitative histologic analysis. *Hum Pathol, 18*(10), 1036-1042.

Karnovsky, M. J. (1967). The ultrastructural basis of capillary permeability studied witch peroxidase as a tracer. *J Cell Biol, 35*(1), 213-236.

Katsuda, S., Boyd, H. C., Fligner, C., Ross, R., & Gown, A. M. (1992). Human atherosclerosis. III. Immunocytochemical analysis of the cell composition of lesions of young adults. *Am J Pathol, 140*(4), 907-914.

Kaur, G., & Dufour, J. M. (2012). Cell lines: Valuable tools or useless artifacts. *Spermatogenesis, 2*(1), 1-5.

Kim, D. N., Imai, H., Schmee, J., Lee, K. T., & Thomas, W. A. (1985). Intimal cell mass-derived atherosclerotic lesions in the abdominal aorta of hyperlipidemic swine. Part 1. Cell of origin, cell divisions and cell losses in first 90 days on diet. *Atherosclerosis, 56*(2), 169-188.

Klouche, M., Rose-John, S., Schmiedt, W., & Bhakdi, S. (2000). Enzymatically degraded, nonoxidized LDL induces human vascular smooth muscle cell activation, foam cell transformation, and proliferation. *Circulation, 101*(15), 1799-1805.

Kockx, M. M., De Meyer, G. R., Muhring, J., Jacob, W., Bult, H., & Herman, A. G. (1998). Apoptosis and related proteins in different stages of human atherosclerotic plaques. *Circulation, 97*(23), 2307-2315.

Kohler, N., & Lipton, A. (1974). Platelets as a source of fibroblast growth-promoting activity. *Exp Cell Res, 87*, 297-301.

Kolodgie, F. D., Burke, A. P., Nakazawa, G., & Virmani, R. (2007). Is pathologic intimal thickening the key to understanding early plaque progression in human atherosclerotic disease? *Arterioscler Thromb Vasc Biol, 27*(5), 986-989.

Kolodgie, F. D., Gold, H. K., Burke, A. P., Fowler, D. R., Kruth, H. S., Weber, D. K., Farb, A., Guerrero, L. J., Hayase, M., Kutys, R., Narula, J., Finn, A. V., & Virmani, R. (2003). Intraplaque hemorrhage and progression of coronary atheroma. *N Engl J Med, 349*(24), 2316-2325.

Koyama, N., Hart, C. E., & Clowes, A. W. (1994). Different functions of the platelet-derived growth factor-alpha and -beta receptors for the migration and proliferation of cultured baboon smooth muscle cells. *Circ Res, 75*(4), 682-691.

Kronenberg, F., Kronenberg, M. F., Kiechl, S., Trenkwalder, E., Santer, P., Oberhollenzer, F., Egger, G., Utermann, G., & Willeit, J. (1999). Role of lipoprotein(a) and apolipoprotein(a) phenotype in atherogenesis: prospective results from the Bruneck study. *Circulation, 100*(11), 1154-1160.

Kubes, P., Kanwar, S., Niu, X.-F., & Gaboury, J. (1993). Nitric oxide synthesis inhibition induces leukocyte adhesion via superoxide and mast cells. *FASEB J, 7*, 1293-1299.

Kubes, P., Suzuki, M., & Granger, D. N. (1991). Nitric oxide: an endogenous modulator of leukocyte adhesion. *Proc Natl Acad Sci USA, 88*, 4651-4655.

Kugiyama, K., Ota, Y., Takazoe, K., Moriyama, Y., Kawano, H., Miyao, Y., Sakamoto, T., Soejima, H., Ogawa, H., Doi, H., Sugiyama, S., & Yasue, H. (1999). Circulating levels of secretory type II phospholipase A(2) predict coronary events in patients with coronary artery disease. *Circulation, 100*(12), 1280-1284.

Kumamoto, M., Nakashima, Y., & Sueishi, K. (1995). Intimal neovascularization in human coronary atherosclerosis: its origin and pathophysiological significance. *Hum Pathol, 26*(4), 450-456.

Kume, N., Cybulsky, M. I., & Gimbrone, M. A., Jr. (1992). Lysophosphatidylcholine, a component of atherogenic lipoproteins, induces mononuclear leukocyte adhesion molecules in cultured human and rabbit arterial endothelial cells. *J Clin Invest, 90*(3), 1138-1144.

Kurokawa, Y. K., Yin, R. T., Shang, M. R., Shirure, V. S., Moya, M. L., & George, S. C. (2017). Human Induced Pluripotent Stem Cell-Derived Endothelial Cells for Three-Dimensional Microphysiological Systems. *Tissue Eng Part C Methods, 23*(8), 474-484.

Langheinrich, A. C., Michniewicz, A., Sedding, D. G., Walker, G., Beighley, P. E., Rau, W. S., Bohle, R. M., & Ritman, E. L. (2006). Correlation of vasa vasorum neovascularization and plaque progression in aortas of apolipoprotein E(-/-)/low-density lipoprotein(-/-) double knockout mice. *Arterioscler Thromb Vasc Biol, 26*(2), 347-352.

Lawes, C. M., Bennett, D. A., Feigin, V. L., & Rodgers, A. (2004). Blood pressure and stroke: an overview of published reviews. *Stroke, 35*(3), 776-785.

Lee, R. T., Yamamoto, C., Feng, Y., Potter-Perigo, S., Briggs, W. H., Landschulz, K. T., Turi, T. G., Thompson, J. F., Libby, P., & Wight, T. N. (2001). Mechanical strain induces specific changes in the synthesis and organization of proteoglycans by vascular smooth muscle cells. *J Biol Chem, 276*(17), 13847-13851.

Lerman, A., & Burnett, J. C., Jr. (1992). Intact and altered endothelium in regulation of vasomotion. *Circulation, 86*(6 Suppl), III12-19.

Li, Z. Y., Howarth, S. P., Tang, T., & Gillard, J. H. (2006). How critical is fibrous cap thickness to carotid plaque stability? A flow-plaque interaction model. *Stroke, 37*(5), 1195-1199.

Libby, P. (2000). Changing concepts of atherogenesis. *J Intern Med, 247*(3), 349-358.

Libby, P. (2008). The molecular mechanisms of the thrombotic complications of atherosclerosis. *J Intern Med, 263*(5), 517-527.

Libby, P., DiCarli, M., & Weissleder, R. (2010). The vascular biology of atherosclerosis and imaging targets. *J Nucl Med, 51 Suppl 1*, 33S-37S.

Libby, P., Ridker, P. M., & Hansson, G. K. (2011). Progress and challenges in translating the biology of atherosclerosis. *Nature, 473*(7347), 317-325.

Little, P. J., Tannock, L., Olin, K. L., Chait, A., & Wight, T. N. (2002). Proteoglycans synthesized by arterial smooth muscle cells in the presence of transforming growth factor-beta1 exhibit increased binding to LDLs. *Arterioscler Thromb Vasc Biol, 22*(1), 55-60.

Liu, Y., Sinha, S., McDonald, O. G., Shang, Y., Hoofnagle, M. H., & Owens, G. K. (2005). Kruppel-like factor 4 abrogates myocardin-induced activation of smooth muscle gene expression. *J Biol Chem, 280*(10), 9719-9727.

Loftus, I. M., Naylor, A. R., Goodall, S., Crowther, M., Jones, L., Bell, P. R., & Thompson, M. M. (2000). Increased matrix metalloproteinase-9 activity in unstable carotid plaques. A potential role in acute plaque disruption. *Stroke, 31*(1), 40-47.

Luft, F. C. (1998). Molecular genetics of human hypertension. *J Hypertens, 16*(12 Pt 2), 1871-1878.

Lusis, A. J. (2000). Atherosclerosis. *Nature, 407*(6801), 233-241.

MacDonald, C. (1990). Development of new cell lines for animal cell biotechnology. *Crit Rev Biotechnol, 10*(2), 155-178.

MacLeod, D. C., Strauss, B. H., de Jong, M., Escaned, J., Umans, V. A., van Suylen, R. J., Verkerk, A., de Feyter, P. J., & Serruys, P. W. (1994). Proliferation and extracellular matrix synthesis of smooth muscle cells cultured from human coronary atherosclerotic and restenotic lesions. *J Am Coll Cardiol, 23*(1), 59-65.

Maier, T., Guell, M., & Serrano, L. (2009). Correlation of mRNA and protein in complex biological samples. *FEBS Lett, 583*(24), 3966-3973.

Mallat, Z., Gojova, A., Marchiol-Fournigault, C., Esposito, B., Kamate, C., Merval, R., Fradelizi, D., & Tedgui, A. (2001). Inhibition of transforming growth factor-beta signalling accelerates atherosclerosis and induces an unstable plaque phenotype in mice. *Circ Res, 89*(10), 930-934.

Mann, J. M., & Davies, M. J. (1996). Vulnerable plaque. Relation of characteristics to degree of stenosis in human coronary arteries. *Circulation, 94*(5), 928-931.

Mann, J. M., & Davies, M. J. (1999). Mechanisms of progression in native coronary artery disease: role of healed plaque disruption. *Heart, 82*(3), 265-268.

Mantese, V. A., Timaran, C. H., Chiu, D., Begg, R. J., & Brott, T. G. (2010). The Carotid Revascularization Endarterectomy versus Stenting Trial (CREST): stenting versus carotid endarterectomy for carotid disease. *Stroke, 41*(10 Suppl), S31-34.

Martin, K., Weiss, S., Metharom, P., Schmeckpeper, J., Hynes, B., O'Sullivan, J., & Caplice, N. (2009). Thrombin stimulates smooth muscle cell differentiation from peripheral blood mononuclear cells via protease-activated receptor-1, RhoA, and myocardin. *Circ Res, 105*(3), 214-218.

Mattsson, E. J., Kohler, T. R., Vergel, S. M., & Clowes, A. W. (1997). Increased blood flow induces regression of intimal hyperplasia. *Arterioscler Thromb Vasc Biol, 17*(10), 2245-2249.

McCarthy, M. J., Loftus, I. M., Thompson, M. M., Jones, L., London, N. J., Bell, P. R., Naylor, A. R., & Brindle, N. P. (1999). Angiogenesis and the atherosclerotic carotid plaque: an association between symptomatology and plaque morphology. *J Vasc Surg, 30*(2), 261-268.

McDonald, O. G., Wamhoff, B. R., Hoofnagle, M. H., & Owens, G. K. (2006). Control of SRF binding to CArG box chromatin regulates smooth muscle gene expression in vivo. *J Clin Invest, 116*(1), 36-48.

McGill, H. C., Jr., Geer, J. C., & Holman, R. L. (1957). Sites of vascular vulnerability in dogs demonstrated by Evans blue. *AMA Arch Pathol, 64*(3), 303-311.

Meschia, J. F., Klaas, J. P., Brown, R. D., Jr., & Brott, T. G. (2017). Evaluation and Management of Atherosclerotic Carotid Stenosis. *Mayo Clin Proc, 92*(7), 1144-1157.

Mietus-Snyder, M., Gowri, M. S., & Pitas, R. E. (2000). Class A scavenger receptor up-regulation in smooth muscle cells by oxidized low density lipoprotein. Enhancement by calcium flux and concurrent cyclooxygenase-2 up-regulation. *J Biol Chem, 275*(23), 17661-17670.

Minick, C. R., Stemerman, M. G., & Insull, W. J. (1977). Effect of regenerated endothelium on lipid accumulation in the arterial wall. *Proc Natl Acad Sci U S A, 74*(4), 1724-1728.

Mofidi, R., Crotty, T. B., McCarthy, P., Sheehan, S. J., Mehigan, D., & Keaveny, T. V. (2001). Association between plaque instability, angiogenesis and symptomatic carotid occlusive disease. *Br J Surg, 88*(7), 945-950.

Molloy, K. J., Thompson, M. M., Jones, J. L., Schwalbe, E. C., Bell, P. R., Naylor, A. R., & Loftus, I. M. (2004). Unstable carotid plaques exhibit raised matrix metalloproteinase-8 activity. *Circulation, 110*(3), 337-343.

Moreno, P. R., Purushothaman, K. R., Fuster, V., Echeverri, D., Truszczynska, H., Sharma, S. K., Badimon, J. J., & O'Connor, W. N. (2004). Plaque neovascularization is increased in ruptured atherosclerotic lesions of human aorta: implications for plaque vulnerability. *Circulation, 110*(14), 2032-2038.

Mosse, P. R., Campbell, G. R., Wang, Z. L., & Campbell, J. H. (1985). Smooth muscle phenotypic expression in human carotid arteries. I. Comparison of cells from diffuse intimal thickenings adjacent to atheromatous plaques with those of the media. . *Lab Invest, 53*(5), 556-562.

Moya, M. L., Hsu, Y. H., Lee, A. P., Hughes, C. C., & George, S. C. (2013). In vitro perfused human capillary networks. *Tissue Eng Part C Methods, 19*(9), 730-737.

Muller, W. A. (2002). Leukocyte-endothelial cell interactions in the inflammatory response. *Lab Invest, 82*(5), 521-533.

Nagao, S., Murao, K., Imachi, H., Cao, W. M., Yu, X., Li, J., Matsumoto, K., Nishiuchi, T., Ahmed, R. A., Wong, N. C., Ueda, K., & Ishida, T. (2006). Platelet derived growth factor regulates ABCA1 expression in vascular smooth muscle cells. *FEBS Lett, 580*(18), 4371-4376.

Nakashima, Y., Chen, Y. X., Kinukawa, N., & Sueishi, K. (2002). Distributions of diffuse intimal thickening in human arteries: preferential expression in atherosclerosis-prone arteries from an early age. *Virchows Arch, 441*(3), 279-288.

Nakashima, Y., Wight, T. N., & Sueishi, K. (2008). Early atherosclerosis in humans: role of diffuse intimal thickening and extracellular matrix proteoglycans. *Cardiovasc Res, 79*(1), 14-23.

Nathan, L., & Chaudhuri, G. (1997). Estrogens and atherosclerosis. *Annu Rev Pharmacol Toxicol, 37*, 477-515.

Naylor, A. R., Ricco, J. B., de Borst, G. J., Debus, S., de Haro, J., Halliday, A., Hamilton, G., Kakisis, J., Kakkos, S., Lepidi, S., Markus, H. S., McCabe, D. J., Roy, J., Sillesen, H., van den Berg, J. C., Vermassen, F., Esvs Guidelines, C., Kolh, P., Chakfe, N., Hinchliffe, R. J., Koncar, I., Lindholt, J. S., Vega de Ceniga, M., Verzini, F., Esvs Guideline, R., Archie, J., Bellmunt, S., Chaudhuri, A., Koelemay, M., Lindahl, A. K., Padberg, F., & Venermo, M. (2018). Editor's Choice - Management of Atherosclerotic Carotid and Vertebral Artery Disease: 2017 Clinical Practice Guidelines of the European Society for Vascular Surgery (ESVS). *Eur J Vasc Endovasc Surg, 55*(1), 3-81.

Nelson-Rees, W. A., Daniels, D. W., & Flandermeyer, R. R. (1981). Cross-contamination of cells in culture. *Science, 212*(4493), 446-452.

Newby, A. C., & Zaltsman, A. B. (1999). Fibrous cap formation or destruction--the critical importance of vascular smooth muscle cell proliferation, migration and matrix formation. *Cardiovasc Res, 41*(2), 345-360.

Ni, M., Chen, W. Q., & Zhang, Y. (2009). Animal models and potential mechanisms of plaque destabilisation and disruption. *Heart, 95*(17), 1393-1398.

Nicolaides, A. N., Kakkos, S. K., Griffin, M., Sabetai, M., Dhanjil, S., Tegos, T., Thomas, D. J., Giannoukas, A., Geroulakos, G., Georgiou, N., Francis, S., Ioannidou, E., & Dore, C. J. (2005). Severity of asymptomatic carotid stenosis and risk of ipsilateral hemispheric ischaemic events: results from the ACSRS study. *Eur J Vasc Endovasc Surg, 30*(3), 275-284.

Nicolaides, A. N., Kakkos, S. K., Kyriacou, E., Griffin, M., Sabetai, M., Thomas, D. J., Tegos, T., Geroulakos, G., Labropoulos, N., Dore, C. J., Morris, T. P., Naylor, R., & Abbott, A. L. (2010). Asymptomatic internal carotid artery stenosis and cerebrovascular risk stratification. *J Vasc Surg, 52*(6), 1486-1496 e1481-1485.

Nicoll, R., & Henein, M. Y. (2014). The predictive value of arterial and valvular calcification for mortality and cardiovascular events. *Int J Cardiol Heart Vessel, 3*(3), 1-5.

Nigro, P., Abe, J., & Berk, B. C. (2011). Flow shear stress and atherosclerosis: a matter of site specificity. *Antioxid Redox Signal, 15*(5), 1405-1414.

Nilsson, J., Sjolund, M., Palmberg, L., Thyberg, J., & Heldin, C. H. (1985). Arterial smooth muscle cells in primary culture produce a platelet-derived growth factor-like protein. *Proc Natl Acad Sci U S A, 82*(13), 4418-4422.

Nunes, S. S., Miklas, J. W., Liu, J., Aschar-Sobbi, R., Xiao, Y., Zhang, B., Jiang, J., Masse, S., Gagliardi, M., Hsieh, A., Thavandiran, N., Laflamme, M. A., Nanthakumar, K., Gross, G. J., Backx, P. H., Keller, G., & Radisic, M. (2013). Biowire: a platform for maturation of human pluripotent stem cell-derived cardiomyocytes. *Nat Methods, 10*(8), 781-787.

O'Leary, D. H., Polak, J. F., Kronmal, R. A., Savage, P. J., Borhani, N. O., Kittner, S. J., Tracy, R., Gardin, J. M., Price, T. R., & Furberg, C. D. (1996). Thickening of the carotid wall. A marker for atherosclerosis in the elderly? Cardiovascular Health Study Collaborative Research Group. *Stroke, 27*(2), 224-231.

Oates, C. P., Naylor, A. R., Hartshorne, T., Charles, S. M., Fail, T., Humphries, K., Aslam, M., & Khodabakhsh, P. (2009). Joint recommendations for reporting carotid ultrasound investigations in the United Kingdom. *Eur J Vasc Endovasc Surg, 37*(3), 251-261.

Okura, Y., Brink, M., Itabe, H., Scheidegger, K. J., Kalangos, A., & Delafontaine, P. (2000). Oxidized low-density lipoprotein is associated with apoptosis of vascular smooth muscle cells in human atherosclerotic plaques. *Circulation, 102*, 2680-2686.

Ooi, Y. C., & Gonzalez, N. R. (2015). Management of extracranial carotid artery disease. *Cardiol Clin, 33*(1), 1-35.

Opitz, F., Schenke-Layland, K., Cohnert, T. U., & Stock, U. A. (2007). Phenotypical plasticity of vascular smooth muscle cells-effect of in vitro and in vivo shear stress for tissue engineering of blood vessels. *Tissue Eng, 13*(10), 2505-2514.

Organisation, W. H. (2020). The top 10 causes of death. Retrieved from https://www.who.int/news-room/fact-sheets/detail/the-top-10-causes-of-death

Palade, G. E. (1953). Fine structure of blood capillaries. *Journal of Applied Physics, 24*.

Palmer, R. M., Ashton, D. S., & Moncada, S. (1988). Vascular endothelial cells synthesize nitric oxide from L-arginine. *Nature, 333*(6174), 664-666.

Pan, C., Kumar, C., Bohl, S., Klingmueller, U., & Mann, M. (2009). Comparative proteomic phenotyping of cell lines and primary cells to assess preservation of cell type-specific functions. *Mol Cell Proteomics, 8*(3), 443-450.

Parmacek, M. S. (2008). Myocardin: dominant driver of the smooth muscle cell contractile phenotype. *Arterioscler Thromb Vasc Biol, 28*(8), 1416-1417.

Payne, S. H. (2015). The utility of protein and mRNA correlation. *Trends Biochem Sci, 40*(1), 1-3.

Pelisek, J., Hegenloh, R., Bauer, S., Metschl, S., Pauli, J., Glukha, N., Busch, A., Reutersberg, B., Kallmayer, M., Trenner, M., Wendorff, H., Tsantilas, P., Schmid, S., Knappich, C., Schaeffer, C., Stadlbauer, T., Biro, G., Wertern, U., Meisner, F., Stoklasa, K., Menges, A. L., Radu, O.,

Dallmann-Sieber, S., Karlas, A., Knipfer, E., Reeps, C., Zimmermann, A., Maegdefessel, L., & Eckstein, H. H. (2019). Biobanking: Objectives, Requirements, and Future Challenges-Experiences from the Munich Vascular Biobank. *J Clin Med, 8*(2), 1-15.

Petty, G. W., Brown, R. D., Jr., Whisnant, J. P., Sicks, J. D., O'Fallon, W. M., & Wiebers, D. O. (1999). Ischemic stroke subtypes: a population-based study of incidence and risk factors. *Stroke, 30*(12), 2513-2516.

Pidkovka, N. A., Cherepanova, O. A., Yoshida, T., Alexander, M. R., Deaton, R. A., Thomas, J. A., Leitinger, N., & Owens, G. K. (2007). Oxidized phospholipids induce phenotypic switching of vascular smooth muscle cells in vivo and in vitro. *Circ Res, 101*(8), 792-801.

Pipes, G. C., Creemers, E. E., & Olson, E. N. (2006). The myocardin family of transcriptional coactivators: versatile regulators of cell growth, migration, and myogenesis. *Genes Dev, 20*(12), 1545-1556.

Proudfoot, D., Skepper, J. N., Hegyi, L., Bennett, M. R., Shanahan, C. M., & Weissberg, P. L. (2000). Apoptosis regulates human vascular calcification in vitro: evidence for initiation of vascular calcification by apoptotic bodies. *Circ Res, 87*(11), 1055-1062.

Quinn, M. T., Parthasarathy, S., Fong, L. G., & Steinberg, D. (1987). Oxidatively modified low density lipoproteins: a potential role in recruitment and retention of monocyte/ macrophages during atherogenesis. *Proc Natl Acad Sci, 84*, 2995-2998.

Quyyumi, A. A., Dakak, N., Andrews, N. P., Gilligan, D. M., Panza, J. A., & Cannon, R. O., 3rd. (1995). Contribution of nitric oxide to metabolic coronary vasodilation in the human heart. *Circulation, 92*(3), 320-326.

Raines, E. W. (2000). The extracellular matrix can regulate vascular cell migration, proliferation, and survival: relationships to vascular disease. *Int J Exp Path, 81*, 173-182.

Rajavashisth, T. B., Andalibi, A., Territo, M. C., Berliner, J. A., Navab, M., Fogelman, A. M., & Lusis, A. J. (1990). Induction of endothelial cell expression of granulocyte and macrophage colony-stimulating factors by modified low-density lipoproteins. *Nature, 344*(6263), 254-257.

Rantner, B., Kollerits, B., Roubin, G. S., Ringleb, P. A., Jansen, O., Howard, G., Hendrikse, J., Halliday, A., Gregson, J., & Eckstein, H. H. (2017). Carotid stenosis trialists' collaboration. Early endarterectomy carries a lower procedural risk than early stenting in patients with symptomatic stenosis of the internal carotid artery: results from 4 randomized controlled trials. *Stroke, 48*, 1580-1587.

Redgrave, J. N., Gallagher, P., Lovett, J. K., & Rothwell, P. M. (2008). Critical cap thickness and rupture in symptomatic carotid plaques: the oxford plaque study. *Stroke, 39*(6), 1722-1729.

Rekhter, M. D., & Gordon, D. (1995). Active proliferation of different cell types, including lymphocytes, in human atherosclerotic plaques. *Am J Pathol, 147*(3), 668-677.

Rekhter, M. D., Zhang, K., Narayanan, A. S., Phan, S., Schork, M. A., & Gordon, D. (1993). Type I collagen gene expression in human atherosclerosis. Localization to specific plaque regions. *Am J Pathol, 143*(6), 1634-1648.

Rensen, S. S., Doevendans, P. A., & van Eys, G. J. (2007). Regulation and characteristics of vascular smooth muscle cell phenotypic diversity. *Neth Heart J, 15*(3), 100-108.

Richardson, P. D., Davies, M. J., & Born, G. V. (1989). Influence of plaque configuration and stress distribution on fissuring of coronary atherosclerotic plaques. *Lancet, 2*(8669), 941-944.

Robins, S. J., Collins, D., Wittes, J. T., Papademetriou, V., Deedwania, P. C., Schaefer, E. J., McNamara, J. R., Kashyap, M. L., Hershman, J. M., Wexler, L. F., & Rubins, H. B. (2001).

Relation of gemfibrozil treatment and lipid levels with major coronary events: VA-HIT: a randomized controlled trial. *JAMA, 285*(12), 1585-1591.

Ronaldson-Bouchard, K., & Vunjak-Novakovic, G. (2018). Organs-on-a-Chip: A Fast Track for Engineered Human Tissues in Drug Development. *Cell Stem Cell, 22*(3), 310-324.

Rong, J. X., Shapiro, M., Trogan, E., & Fisher, E. A. (2003). Transdifferentiation of mouse aortic smooth muscle cells to a macrophage-like state after cholesterol loading. *Proc Natl Acad Sci U S A, 100*(23), 13531-13536.

Ross, R. (1981). Atherosclerosis: A problem of the biology of arterial wall cells and their interactions with blood components. *Arteriosclerosis, 1*, 293-311.

Ross, R. (1990). Localization of PDGF-B protein in macrophages in all phases of atherogenesis. *Science, 248*, 1009-1012.

Ross, R. (1999). Atherosclerosis - an inflammatory disease. *N Engl J Med, 340*(2), 115-126.

Ross, R., & Glomset, J. A. (1973). Atherosclerosis and the arterial smooth muscle cell: Proliferation of smooth muscle is a key event in the genesis of the lesions of atherosclerosis. *Science, 180*(4093), 1332-1339.

Ross, R., & Glomset, J. A. (1976). The pathogenesis of atherosclerosis. *N Engl J Med, 295*, 420-425.

Ross, R., Glomset, J. A., & Harker, L. (1977). Response to injury and atherogenesis. *Am J Pathol, 86*(3), 675-684.

Ross, R., Glomset, J. A., Kariya, B., & Harker, L. (1974). A platelet-dependent serum factor that stimulates the proliferation of arterial smooth muscle cells in vitro. *Proc Natl Acad Sci U S A, 71*(4), 1207-1210.

Rothwell, P. M., Eliasziw, M., Gutnikov, S. A., Fox, A. J., Taylor, D. W., Mayberg, M. R., Warlow, C. P., Barnett, H. J., & Carotid Endarterectomy Trialists, C. (2003a). Analysis of pooled data from the randomised controlled trials of endarterectomy for symptomatic carotid stenosis. *Lancet, 361*(9352), 107-116.

Rothwell, P. M., Gibson, R., & Warlow, C. P. (2000). Interrelation between plaque surface morphology and degree of stenosis on carotid angiograms and the risk of ischemic stroke in patients with symptomatic carotid stenosis. *Stroke, 31*(3), 615-621.

Rothwell, P. M., Gutnikov, S. A., Warlow, C. P., & European Carotid Surgery Trialist's, C. (2003b). Reanalysis of the final results of the European Carotid Surgery Trial. *Stroke, 34*(2), 514-523.

Rubanyi, G. M. (1991). Endothelium-derived relaxing and contracting factors. *J Cell Biochem, 46*(1), 27-36.

Sacco, R. L., Gan, R., Boden-Albala, B., Lin, I. F., Kargman, D. E., Hauser, W. A., Shea, S., & Paik, M. C. (1998). Leisure-time physical activity and ischemic stroke risk: the Northern Manhattan Stroke Study. *Stroke, 29*(2), 380-387.

Sano, H., Sudo, T., Yokode, M., Murayama, T., Kataoka, H., Takakura, N., Nishikawa, S., Nishikawa, S. I., & Kita, T. (2001). Functional blockade of platelet-derived growth factor receptor-beta but not of receptor-alpha prevents vascular smooth muscle cell accumulation in fibrous cap lesions in apolipoprotein E-deficient mice. *Circulation, 103*(24), 2955-2960.

Sarwar, N., Danesh, J., Eiriksdottir, G., Sigurdsson, G., Wareham, N., Bingham, S., Boekholdt, S. M., Khaw, K. T., & Gudnason, V. (2007). Triglycerides and the risk of coronary heart disease: 10,158 incident cases among 262,525 participants in 29 Western prospective studies. *Circulation, 115*(4), 450-458.

Schenkel, A. R., Mamdouh, Z., & Muller, W. A. (2004). Locomotion of monocytes on endothelium is a critical step during extravasation. *Nat Immunol, 5*(4), 393-400.

Schrijvers, D. M., De Meyer, G. R., Kockx, M. M., Herman, A. G., & Martinet, W. (2005). Phagocytosis of apoptotic cells by macrophages is impaired in atherosclerosis. *Arterioscler Thromb Vasc Biol, 25*(6), 1256-1261.

Schurr, M. J., Foster, K. N., Centanni, J. M., Comer, A. R., Wicks, A., Gibson, A. L., Thomas-Virnig, C. L., Schlosser, S. J., Faucher, L. D., Lokuta, M. A., & Allen-Hoffmann, B. L. (2009). Phase I/II clinical evaluation of StrataGraft: a consistent, pathogen-free human skin substitute. *J Trauma, 66*(3), 866-873; discussion 873-864.

Schwartz, S. M., Galis, Z. S., Rosenfeld, M. E., & Falk, E. (2007). Plaque rupture in humans and mice. *Arterioscler Thromb Vasc Biol, 27*(4), 705-713.

Schwenke, D. C., & Carew, T. E. (1989a). Initiation of atherosclerotic lesions in cholesterol-fed rabbits. I. Focal increases in arterial LDL concentration precede development of fatty streak lesions. *Arteriosclerosis, 9*(6), 895-907.

Schwenke, D. C., & Carew, T. E. (1989b). Initiation of atherosclerotic lesions in cholesterol-fed rabbits. II. Selective retention of LDL vs. selective increases in LDL permeability in susceptible sites of arteries. *Arteriosclerosis, 9*(6), 908-918.

Shah, N. M., Groves, A. K., & Anderson, D. J. (1996). Alternative neural crest cell fates are instructively promoted by TGF-β superfamily members. *Cell, 85*, 331-343.

Shah, P. K., Falk, E., Badimon, J. J., Fernandez-Ortiz, A., Mailhac, A., Villareal-Levy, G., Fallon, J. T., Regnstrom, J., & Fuster, V. (1995). Human monocyte-derived macrophages induce collagen breakdown in fibrous caps of atherosclerotic plaques. Potential role of matrix-degrading metalloproteinases and implications for plaque rupture. *Circulation, 92*(6), 1565-1569.

Shanahan, C. M., & Weissberg, P. L. (1998). Smooth muscle cell heterogeneity: patterns of gene expression in vascular smooth muscle cells in vitro and in vivo. *Arterioscler Thromb Vasc Biol, 18*(3), 333-338.

Shankman, L. S., Gomez, D., Cherepanova, O. A., Salmon, M., Alencar, G. F., Haskins, R. M., Swiatlowska, P., Newman, A. A., Greene, E. S., Straub, A. C., Isakson, B., Randolph, G. J., & Owens, G. K. (2015). KLF4-dependent phenotypic modulation of smooth muscle cells has a key role in atherosclerotic plaque pathogenesis. *Nat Med, 21*(6), 628-637.

Sharrett, A. R., Patsch, W., Sorlie, P. D., Heiss, G., Bond, M. G., & Davis, C. E. (1994). Associations of lipoprotein cholesterols, apolipoproteins A-I and B, and triglycerides with carotid atherosclerosis and coronary heart disease. The Atherosclerosis Risk in Communities (ARIC) Study. *Arterioscler Thromb, 14*(7), 1098-1104.

Shekhonin, B. V., Domogatsky, S. P., Idelson, G. L., Koteliansky, V. E., & Rukosuev, V. S. (1987). Relative distribution of fibronectin and type I, III, IV, V collagens in normal and atherosclerotic intima of human arteries. *Atherosclerosis, 67*(1), 9-16.

Shimokado, K., Raines, E. W., Madtes, D. K., Barrett, T. B., Benditt, E. P., & Ross, R. (1985). A significant part of macrophage-derived growth factor consists of at least two forms of PDGF. *Cell, 43*(1), 277-286.

Skalen, K., Gustafsson, M., Rydberg, E. K., Hulten, L. M., Wiklund, O., Innerarity, T. L., & Boren, J. (2002). Subendothelial retention of atherogenic lipoproteins in early atherosclerosis. *Nature, 417*(6890), 750-754.

Skalli, O., Ropraz, P., Trzeciak, A., Benzonana, G., Gillessen, D., & Gabbiani, G. (1986). A monoclonal antibody against alpha-smooth muscle actin: a new probe for smooth muscle differentiation. *J Cell Biol, 103*(6), 2787-2796.

Sobieszczyk, P., & Beckman, J. (2006). Carotid artery disease. *Circulation, 114*(7), e244-247.

Spring, P. M., & Hoff, H. F. (1989). LDL accumulation in the grossly normal human iliac bifurcation and common iliac arteries. *Exp Mol Pathol, 51*(2), 179-185.

Stary, H. C. (2000). Natural history and histological classification of atherosclerotic lesions: an update. *Arterioscler Thromb Vasc Biol, 20*(5), 1177-1178.

Stary, H. C., Blankenhorn, D. H., Chandler, A. B., Glagov, S., Insull, W., Richardson, M., Rosenfeld, M. E., Schaffer, S. A., Schwartz, C. J., Wagner, W. D., & Wissler, R. W. (1992). A definition of the intima of human arteries and of its atherosclerosis-prone regions. *Circulation, 85*(1), 391-405.

Stary, H. C., Chandler, A. B., Dinsmore, R. E., Fuster, V., Glagov, S., Insull, W., Rosenfeld, M. E., Schwartz, M. A., Wagner, W. D., & Wissler, R. W. (1995). A definition of advanced types of atherosclerotic lesions and a histological classification of atherosclerosis. *Circulation, 92*(5), 1355-1374.

Stary, H. C., Chandler, A. B., Glagov, S., Guyton, J. R., Insull, W., Rosenfeld, M. E., Schaffer, S. A., Schwartz, C. J., Wagner, W. D., & Wissler, R. W. (1994). A definition of initial, fatty streak, and intermediate lesions of atherosclerosis. *Circulation, 89*(5), 2462-2478.

Steinberg, D. (2009). The LDL modification hypothesis of atherogenesis: an update. *J Lipid Res, 50 Suppl*, S376-381.

Stewart, H. J., Guildford, A. J., Lawrence-Watt, D. J., & Santin, M. (2009). Substrate-induced phenotypical change of monocytes/ macrophages into myofibroblast-like cells: a new insight into the mechanism of in-stent restenosis. *J Biomed Mater Res A, 90*(2), 465-471.

Sudhop, T., Lutjohann, D., Kodal, A., Igel, M., Tribble, D. L., Shah, S., Perevozskaya, I., & von Bergmann, K. (2002). Inhibition of intestinal cholesterol absorption by ezetimibe in humans. *Circulation, 106*(15), 1943-1948.

Tabas, I. (2010). Macrophage death and defective inflammation resolution in atherosclerosis. *Nat Rev Immunol, 10*(1), 36-46.

Tabas, I., Garcia-Cardena, G., & Owens, G. K. (2015). Recent insights into the cellular biology of atherosclerosis. *J Cell Biol, 209*(1), 13-22.

Tabas, I., Williams, K. J., & Boren, J. (2007). Subendothelial lipoprotein retention as the initiating process in atherosclerosis: update and therapeutic implications. *Circulation, 116*(16), 1832-1844.

Tran-Lundmark, K., Tran, P. K., Paulsson-Berne, G., Friden, V., Soininen, R., Tryggvason, K., Wight, T. N., Kinsella, M. G., Boren, J., & Hedin, U. (2008). Heparan sulfate in perlecan promotes mouse atherosclerosis: roles in lipid permeability, lipid retention, and smooth muscle cell proliferation. *Circ Res, 103*(1), 43-52.

van der Loop, F. T., Schaart, G., Timmer, E. D., Ramaekers, F. C., & van Eys, G. J. (1996). Smoothelin, a novel cytoskeletal protein specific for smooth muscle cells. *J Cell Biol, 134*(2), 401-411.

van der Wal, A. C., Becker, A. E., van der Loos, C. M., & Das, P. K. (1993). Site of intimal rupture or erosion of thrombosed coronary atherosclerotic plaques is characterized by an inflammatory process irrespective of the dominant plaque morphology. *Circulation, 89*(1), 36-44.

VanderLaan, P. A., Reardon, C. A., & Getz, G. S. (2004). Site specificity of atherosclerosis: site-selective responses to atherosclerotic modulators. *Arterioscler Thromb Vasc Biol, 24*(1), 12-22.

Varnava, A. M., Mills, P. G., & Davies, M. J. (2002). Relationship between coronary artery remodeling and plaque vulnerability. *Circulation, 105*(8), 939-943.

Velican, C. (1981). A dissecting view on the role of the fatty streak in the pathogenesis of human atherosclerosis: culprit or bystander? *Med Interne, 19*(4), 321-337.

Velican, C., & Velican, D. (1975). Intimal thickening in developing coronary arteries and its relevance to atherosclerotic involvement. *Atherosclerosis, 23*, 345-355.

Velican, C., & Velican, D. (1984). Study of coronary intimal thickening. *Atherosclerosis, 56*, 331-344.

Vengrenyuk, Y., Nishi, H., Long, X., Ouimet, M., Savji, N., Martinez, F. O., Cassella, C. P., Moore, K. J., Ramsey, S. A., Miano, J. M., & Fisher, E. A. (2015). Cholesterol loading reprograms the microRNA-143/145-myocardin axis to convert aortic smooth muscle cells to a dysfunctional macrophage-like phenotype. *Arterioscler Thromb Vasc Biol, 35*(3), 535-546.

Virchow, R. (1989). Cellular pathology. As based upon physiological and pathological histology. Lecture XVI--Atheromatous affection of arteries. 1858. *Nutr Rev, 47*(1), 23-25.

Virmani, R., Kolodgie, F. D., Burke, A. P., Farb, A., & Schwartz, S. M. (2000). Lessons from sudden coronary death: a comprehensive morphological classification scheme for atherosclerotic lesions. *Arterioscler Thromb Vasc Biol, 20*(5), 1262-1275.

Vogel, C., & Marcotte, E. M. (2012). Insights into the regulation of protein abundance from proteomic and transcriptomic analyses. *Nat Rev Genet, 13*(4), 227-232.

Wafa, H. A., Wolfe, C. D. A., Emmett, E., Roth, G. A., Johnson, C. O., & Wang, Y. (2020). Burden of Stroke in Europe: Thirty-Year Projections of Incidence, Prevalence, Deaths, and Disability-Adjusted Life Years. *Stroke, 51*(8), 2418-2427.

Wang, D., Chang, P. S., Wang, Z., Sutherland, L., Richardson, J. A., Small, E., Krieg, P. A., & Olson, E. N. (2001). Activation of cardiac gene expression by myocardin, a transcriptional cofactor for serum response factor. *Cell, 105*(7), 851-862.

Weissberg, P. L., Cary, N. R., & Shanahan, C. M. (1995). Gene expression and vascular smooth muscle cell phenotype. *Blood Press Suppl, 2*, 68-73.

Wendorff, C., Wendorff, H., Pelisek, J., Tsantilas, P., Zimmermann, A., Zernecke, A., Kuehnl, A., & Eckstein, H. H. (2015). Carotid Plaque Morphology Is Significantly Associated With Sex, Age, and History of Neurological Symptoms. *Stroke, 46*(11), 3213-3219.

Wikswo, J. P., Curtis, E. L., Eagleton, Z. E., Evans, B. C., Kole, A., Hofmeister, L. H., & Matloff, W. J. (2013). Scaling and systems biology for integrating multiple organs-on-a-chip. *Lab Chip, 13*(18), 3496-3511.

Wilcox, J. N., Smith, K. M., Schwartz, S. M., & Gordon, D. (1989). Localization of tissue factor in the normal vessel wall and in the atherosclerotic plaque. *Proc Natl Acad Sci U S A, 86*(8), 2839-2843.

Wilhelm, M., Schlegl, J., Hahne, H., Gholami, A. M., Lieberenz, M., Savitski, M. M., Ziegler, E., Butzmann, L., Gessulat, S., Marx, H., Mathieson, T., Lemeer, S., Schnatbaum, K., Reimer, U., Wenschuh, H., Mollenhauer, M., Slotta-Huspenina, J., Boese, J. H., Bantscheff, M., Gerstmair, A., Faerber, F., & Kuster, B. (2014). Mass-spectrometry-based draft of the human proteome. *Nature, 509*(7502), 582-587.

Williams, J. W., Winkels, H., Durant, C. P., Zaitsev, K., Ghosheh, Y., & Ley, K. (2020). Single Cell RNA Sequencing in Atherosclerosis Research. *Circ Res, 126*(9), 1112-1126.

Williams, K. J., & Tabas, I. (1995). The response-to-retention hypothesis of early atherogenesis. *Arterioscler Thromb Vasc Biol, 15*(5), 551-561.

Williams, K. J., & Tabas, I. (2005). Lipoprotein retention--and clues for atheroma regression. *Arterioscler Thromb Vasc Biol, 25*(8), 1536-1540.

Winter, Y., Rohrmann, S., Linseisen, J., Lanczik, O., Ringleb, P. A., Hebebrand, J., & Back, T. (2008). Contribution of obesity and abdominal fat mass to risk of stroke and transient ischemic attacks. *Stroke, 39*(12), 3145-3151.

Wolf, P. A., D'Agostino, R. B., Kannel, W. B., Bonita, R., & Belanger, A. J. (1988). Cigarette smoking as a risk factor for stroke. The Framingham Study. *JAMA, 259*(7), 1025-1029.

Yan, P., Xia, C., Duan, C., Li, S., & Mei, Z. (2011). Biological characteristics of foam cell formation in smooth muscle cells derived from bone marrow stem cells. *Int J Biol Sci, 7*(7), 937-946.

Yanagisawa, M., Kurihara, H., Kimura, S., Goto, K., & Masaki, T. (1988). A novel peptide vasoconstrictor, endothelin, is produced by vascular endothelium and modulates smooth muscle Ca2+ channels. *J Hypertens Suppl, 129*, 407-413.

Yao, S. K., Ober, J. C., Krishnaswami, A., Ferguson, J. J., Anderson, H. V., Golino, P., Buja, L. M., & Willerson, J. T. (1992). Endogenous nitric oxide protects against platelet aggregation and cyclic flow variations in stenosed and endothelium-injured arteries. *Circulation, 86*(4), 1302-1309.

Yoshida, T., Gan, Q., & Owens, G. K. (2008a). Kruppel-like factor 4, Elk-1, and histone deacetylases cooperatively suppress smooth muscle cell differentiation markers in response to oxidized phospholipids. *Am J Physiol Cell Physiol, 295*(5), C1175-1182.

Yoshida, T., Kaestner, K. H., & Owens, G. K. (2008b). Conditional deletion of Kruppel-like factor 4 delays downregulation of smooth muscle cell differentiation markers but accelerates neointimal formation following vascular injury. *Circ Res, 102*(12), 1548-1557.

Yoshida, T., Yamashita, M., Horimai, C., & Hayashi, M. (2013). Smooth muscle-selective inhibition of nuclear factor-kappaB attenuates smooth muscle phenotypic switching and neointima formation following vascular injury. *J Am Heart Assoc, 2*(3), e000230.

Yurdagul, A., Jr., Doran, A. C., Cai, B., Fredman, G., & Tabas, I. A. (2017). Mechanisms and Consequences of Defective Efferocytosis in Atherosclerosis. *Front Cardiovasc Med, 4*(86), 86.

Zeiher, A. M., Drexler, H., Wollschlager, H., & Just, H. (1991). Modulation of coronary vasomotor tone in humans. Progressive endothelial dysfunction with different early stages of coronary atherosclerosis. *Circulation, 83*(2), 391-401.